Regulation of Neural Stem Cell Reactivation from Quiescence by Maternal Lipids and the Microtubule Binding Protein Toucan

Md Ausrafuggaman Nahid
Dhaka, Bangladesh

M.S University of Dhaka, Bangladesh, 2013
B.Sc. University of Dhaka, Bangladesh, 2011

A Dissertation presented to the Graduate Faculty of the University of Virginia
in Candidacy for the Degree of Doctor of Philosophy

Department of Biology

University of Virginia

July 10, 2024

Sarah Siegrist (Advisor) _____ _____

Sarah Kucenas (First Reader) _____ _____

Barry Condron _____ _____

Christopher Deppmann _____ _____

Michelle Bland (Dean's Representative) _____ _____

Project summary

Controlled proliferation of neural stem and progenitor cells (NSPCs) produces various types of neuron and glial cells which eventually form neural circuits and a functional brain. Both cell extrinsic and intrinsic factors are known to play key roles in controlling NSPCs proliferation throughout development. In this thesis, I will investigate how lipid droplets availability and lipid metabolism as cell extrinsic factors affect NSPCs proliferation in the *Drosophila* freshly hatched larval brain. Next, I will show how a microtubule binding protein affects asymmetric cell division in the mushroom body neuroblasts (MB NBs) during early stages of *Drosophila* larval brain development.

Here I show that lipid metabolism plays an important role during neuroblasts (NBs) reactivation from quiescence. *Drosophila* females deposit a large number of lipid droplets in the egg during oogenesis which become depleted at the end of the embryonic stage. Recent studies have shown that these LDs in the embryonic core are distributed to the peripheral tissues during the very early embryonic developmental stages and interference with this process leads to developmental delay or embryonic lethality. We have discovered that the maternally deposited lipids droplets are required for the timely reactivation of the *Drosophila* neural stem cells. Either knockdown of the Brummer lipase in the NBs or mutation in the genes that are involved in maternal lipid droplets homeostasis in the freshly hatched brain leads to a significant delay in the NBs reactivation from quiescence. We have also identified that the evolutionarily conserved growth signaling PI3K pathway is attenuated when the NBs either lack or fail to break down maternally deposited lipid droplets. Freshly hatched *Drosophila* larvae start feeding

immediately once they hatch out of the embryo and have access to food. They can access lipids from the food and use carbohydrates to synthesize lipids through the *de novo* lipogenesis. We have determined that dietary lipids are not essential for the quiescent NBs timely reactivation. However, lipids produced via *de novo* lipogenesis plays a role in the quiescent NBs reactivation. Overall, our data indicate that lipid metabolism plays an important role in the quiescent NBs reactivation.

I also show that a microtubule associated protein (MAP), called Toucan (Toc), regulates NBs asymmetric cell division. The function of MAPs in cell division is evolutionarily conserved across a wide range of species. MAPs play critical roles in the organization, stabilization, and regulation of microtubules during cell division, ensuring proper chromosome alignment, segregation, and cytokinesis. Earlier studies showed that Toc is provided maternally in the *Drosophila* embryo and plays a critical role in nuclear division during the syncytial blastoderm stage. The maternal pool of Toc is depleted by the end of the embryonic stage. We have discovered that Toc is also expressed in the *Drosophila* larval brain, presumably another isoform of Toc as there are ten unique polypeptides of Toc in *Drosophila*. In Toc mutant larval brains, quiescent NBs fail to reactivate, and the proliferating MB NBs exit cell cycle by 24 hours after larval hatching (ALH). Further studies revealed that Toc mutant MB NBs had defects in their microtubule network and most of them underwent cytokinesis failure. We have also found that Toc mutant MB NBs have defects in asymmetric segregation of the basal polarity proteins. By 40 hours ALH, MB NBs were terminally differentiated due to nuclear accumulation of

Prospero. Our findings strongly suggest that Toc is a microtubule associated protein required for the asymmetric cell division of the NBs in the *Drosophila* brain.

Acknowledgments

It has been a long journey, and I would like to thank everyone who helped and supported me along the way. First, I would like to express my deepest gratitude to my advisor, Sarah Siegrist, for accepting me as a graduate student and offering me the incredible opportunity to explore genetic mechanisms involved in *Drosophila* brain development. I cherished the freedom to ask my own research questions and test them in the lab. Her kindness, patience, and constant support have been invaluable throughout my time in the lab. I particularly appreciate her guidance in helping me wrap up my projects over the last two years of my thesis. I would also like to thank my committee members, Drs. Sarah Kucenas, Barry Condron, Michelle Bland, and Christopher Deppmann for their valuable feedback. A special thanks to Michelle Bland for her assistance with my experiments.

I have been fortunate to meet a group of passionate and considerate individuals in the Siegrist lab. I would like to thank everyone I met during my time there: Conor Sipe, Susan Doyle, Matthew Pahl, Xin Yuan, Chhavi Sood, Taylor Nystrom, Kendal Branham, Cami Keliinui, Sagar Kasar, Omina Nazarzoda, Gary Teeters, and Bharath Sunchu. I would especially like to thank Susan Doyle for her support over the years. Her passion for science is exemplary, and I could always count on her whenever I needed anything.

I extend my heartfelt gratitude to my friends and family for their support over the years. First and foremost, I am thankful to the Almighty for blessing me with such wonderful parents. Their unconditional support and unwavering faith have shaped me into

who I am today. I am deeply grateful to my beloved wife, Martina Mondol, for her constant support and belief in me. Since the birth of our son, she has managed everything at home almost single-handedly, allowing me to dedicate time to the lab and complete my thesis work. Lastly, I cannot express how fortunate I feel to have Nahiyan B. Zaman as my son; his presence inspires me to keep going, no matter what.

List of abbreviations

NSC: Neural stem cell
NSPC: Neural stem and progenitor cell
ASH: Achaete Scute family
ATO: Atonal family
NEC: Neuroepithelial cells
aRG: Apical radial glial cells
BP: Basal progenitor cells
bIP: Basal intermediate progenitor
SVZ: Sub ventricular zone
SGZ: Subgranular zone
NB: Neuroblasts
MB NB:Mushroom body neuroblasts
GMC: Ganglion mother cell
INP: Intermediate progenitor cell
VNC: Ventral nerve cord
Hb: Hunchback
Kr: Kruppel
Cas: Castor
Grh: Grainyhead
Antp: Antennapedia
abd-A: Abdominal-A
Msh: Muscle segment homeobox
Dap: Dacapo
Pros: Prospero
Dpn: deadpan
Ase: Asense
Chro: Chromator
Pon: Partner of Numb
Mira: Miranda
Brat: Brain tumor
Insc: Inscuteable
Pins: Partner of Inscuteable
Mud: Mushroom body defect
Pav: Pavarotti
Tum: Tumbleweed
Pbl: Pebble
Dia: Diaphanous
Chic: Chickadee
Tsr: twinstar
FRAP: Fluorescence Recovery after Photobleaching
BBB: Blood brain barrier
Ana: Anachronism
dILP: Drosophila insulin like peptide
SPG: Sub perineurial glia

IPC: Insulin producing cells
Trol: Terribly reduced optic lobes
CRL-4: Cullin4-ring ligase
Hh: Hedgehog
Wts: Warts
Yki: Yorkie
NWM: Nutrient withdrawal media
ACC: Acetyl-CoA carboxylase
FASN: Fatty acid synthase
SREBP: Sterol Regulatory Element Binding Protein
FAO: Fatty acid beta oxidation
MPC: Mitochondrial pyruvate carrier
LD: Lipid droplets
LDD: Lipid depleted diet
Lsd1: Lipid storage droplet 1
Lsd2: Lipid storage droplet 2
Sik3: Salt-inducible kinase 3
Mdy: Midway
Akh: Adipokinetic hormone
Bmm: Brummer
HSL: Hormone sensitive lipase
DAG: Diacylglycerol
TAG: Triacylglycerol
G-3-P: Glycerol-3 phosphate
FA: Fatty acid
ROS: Reactive oxygen species
HSC: Hematopoietic stem cells
ISC: Intestinal stem cells
CSC: Cancer stem cells
FDS: Fat body derived signal
SREBP: Sterol regulatory element binding protein
Lkb1: Liver kinase B1
Lpp: Lipophorin
Ltp: Lipid transfer particle
Lpr: lipoprotein receptors
BDSC: Bloomington Drosophila stocks center

Table of contents

Chapter 1

Introduction

Neurogenesis gives rise to many neurons and glia of various types from a relatively small pool of neural stem cells (NSCs) during brain development. Precise regulation of this process is critical for forming appropriate neural circuits and ensuring the overall functioning of the brain. Neurogenesis follows a predefined genetic program in which both cell-intrinsic and extrinsic factors coordinate to ensure proper development. Failure to regulate NSC proliferation can result in neurodevelopmental disorders, including cortical malformations such as microcephaly and macrocephaly, as well as the development of abnormal neural circuits such as those associated with autism spectrum disorders[1–5].

In this thesis, I will use the *Drosophila* brain as a model system to study how cell extrinsic and intrinsic factors affect NSCs, known as neuroblasts (NBs), proliferation during early stages of larval brain development. I will discuss how maternally deposited lipid droplets as a cell extrinsic factor regulate quiescent NBs reactivation. Next, I will focus on the microtubule binding protein Toucan and show how it is required in a cell intrinsic manner for the NBs asymmetric cell division.

1.1 General mechanism of neurogenesis

The process of neurogenesis begins at a very early embryonic stage with the selection of neural progenitor cells in the ectodermal layer during gastrulation. In some animals the entire ectoderm might have neurogenic potential, in which case it gives rise to a nerve plexus [6,7]. Otherwise, neurogenesis becomes restricted to a part of the ectoderm, called neuroectoderm, and gives rise to a central nervous system [8,9]. Neural progenitors in the

neuroectoderm might reside as individual cells or a group of contiguous cells. They might remain integrated in the surface neuroepithelium layer throughout development or be internalized by means of dislocalization such as delamination, invagination or ingression [10]. In some instances, cells in the neuroectoderm become neural precursors and directly differentiate into neurons [10]. However, most of the time the neural progenitors proliferate by means of asymmetric cell division in which they mitotically divide to self-renew the stem cell pool and at the same time give rise to neural progenitor cells with limited proliferation capacities that produce neurons or glial cells [11–13].

Genetic factors that regulate the selection and maintenance of the neural progenitor cells in the neuroectoderm are conserved across the animal kingdom. The expression of SoxB family transcription factors in the ectoderm is crucial for the selection of neural progenitor cells [14–16]. Signaling pathways, such as BMP and Wnt, play critical roles in maintaining SoxB expression, thereby stabilizing the selected neural progenitor pools [17,18]. Notch is another signaling pathway that controls selection of neural progenitor cells by a lateral inhibition mechanism [9,19]. Within the proneural cluster, cells that receive high levels of Notch signaling activity turn off proneural genes (Achaete Scute family (ASH) and Atonal family (ATO) of transcription factors) and turn on a E(Spl)/HES family of genes that prevents differentiation of the neural progenitor cells and maintains their stemness [20,21].

Once established, controlled proliferation of the neural progenitors produces diverse neuronal and glial cells which ultimately form neural circuits and a functional brain. The nature of the genetic mechanisms underlying the variation in neuronal cell population

number and diversity observed among species is currently a topic of intense investigation. It is presumably dependent on the types of neural progenitor cells present in the brain and their mode of proliferation [22–25]. Neurogenesis is most intense during embryonic and early stages of development and is usually restricted to parts of the brain in adult animals such as in rats and mice [3,12]. In some animals, for example *Drosophila*, neurogenesis is completely absent in the adult brain[12].

Vertebrate neurogenesis

Neurogenesis in higher vertebrate animals (including rats, mice, monkeys and humans) begins with the symmetric division of the neuroepithelial cells (NEC) which increases the neural progenitor pool rapidly and shortly thereafter they become apical radial glial cells (aRG) [26,27]. aRG cells at the ventricular surface divide asymmetrically and produce basal progenitor cells (BP) that make the sub ventricular zone (SVZ) [26]. The bulk of the neurons in the mammalian neocortex are produced by these BP cells. There are two types of BP cells: basal intermediate progenitor (bIP) and outer radial glia (oRG) cells [28–30]. The relative abundance and proliferative capacity of basal intermediate progenitors (bIP) and outer radial glia (oRG) cells are decisive factors in interspecies differences in brain size as they play key roles in the expansion of the cerebral cortex during development. In mice, basal intermediate progenitors (bIP) differentiate terminally to produce neurons [23,23,31]. In contrast, bIPs in the primate brain have the capacity to divide up to five times [32]. Additionally, the presence of outer radial glia (oRG) cells in the mouse brain during embryonic corticogenesis is very scarce (less than 0.5 percent) compared to the primate brain (more than 75 percent) [24,32–34].

In adult animals, neurogenesis declines and becomes restricted to certain regions of the brain. For example, in adult mice neurogenesis is restricted to the ventricular/subventricular (V/SVZ) region of the lateral ventricles and subgranular zone (SGZ) of the hippocampus [35–37]. Most of the neural stem cells remain in a quiescent state in the adult brain presumably to reactivate later in response to certain stimuli such as hypoxia, brain injury and exercise [38–40]. There is clear evidence of adult neurogenesis in animals such as rodents, zebrafish, songbirds and lizards [41,42]. However, the evidence for adult neurogenesis in humans remains controversial to date [43,44].

1.2 The *Drosophila* brain as a model system to study neurogenesis

Neural stem cells in the *Drosophila* brain, known as neuroblasts (NBs), follow a mechanism of neurogenesis remarkably similar to that in vertebrate brains [12]. This similarity makes the *Drosophila* brain an excellent model system for studying neurogenesis *in vivo*. NBs in the *Drosophila* brain originate from the ventrolateral neuroepithelium layer during embryonic stages 9-11 [45–47]. Notch signaling pathway plays a crucial role in this process [9,48]. NBs delaminate from the neural epithelium in several waves during embryogenesis and they express a combination of positional factors that confer spatial identity [45,47]. NBs gain their dorsal-ventral identity by expressing columnar genes, which are homeodomain containing transcription factors such as *vnd*, *ind* and *msh*, in response to their interactions with a morphogen gradient, whereas the anterior-posterior axis is determined by their expression of gap and segment polarity genes as well as homeotic transcription factors [49–52]. NBs also express temporal factors that ensure neuronal diversity over time and determine when to exit the cell cycle. Expression of

temporal factors has been most extensively studied in the embryonic ventral nerve cord (VNC) where a cascade of transcription factors are expressed sequentially to generate neuronal diversity. Sequential expression of *Hunchback (Hb) - Kruppel (Kr) - Pdm2 - Castor (Cas) - Grainyhead (Grh)* confers temporal identity to the NBs and their progeny [53–55]. Most of the embryonic NBs in the brain follow the expression of same temporal transcriptional factors with a few exceptions where a new temporal window might be added or skipped [56].

NBs proliferate throughout the embryonic stage and produce about ten percent of the neurons found in the adult brain [57,58]. Most of the NBs exit the cell cycle at the end of the embryonic stage and they either enter quiescence or are eliminated by apoptosis [57]**(Fig. 1.2)**. NBs at the gnathal and VNC segments undergo apoptosis whereas thoracic VNC and central brain NBs enter quiescence [57,59–61]. A small subset of central brain lobe neuroblasts, known as Mushroom body neuroblasts (MB NBs), do not enter quiescence at the end of the embryonic stage [60,62]. Embryonic NBs enter into quiescence following the depletion of maternally deposited resources, and these quiescent NBs resume proliferation in response to larval feeding [60,62,63]. This suggests that the NBs entry into quiescence at the end of the embryonic stage is a strategy for the fly brain to preserve its NB pool when resources are unavailable. The metabolic and transcriptional changes associated with NB entry and exit from quiescence are not completely understood.

Neuroblast entry into quiescence

Spatial and temporal factors that control NB cell lineage progression are also involved in NB entry into quiescence [61]. Temporal factor Cas inhibits Pdm2 which induces the expression of the transcriptional cofactor Nab which binds with another transcription factor squeeze (Sqz) to induce NBs quiescence [61]. *Antennapedia (Antp)* and *abdominal-A (abd-A)* are two of the segment polarity genes of the Hox family and are required for timely NB entry into quiescence. NB3-3T lineage NBs mutant for *AntP* proliferate for extended periods of time in the embryonic brain whereas overexpression of *abd-A* also prolongs the NB3-3T proliferation [61]. NBs located dorsally in the VNC enter quiescence by the action of homeobox protein muscle segment homeobox (Msh) which induces expression of *dacapo (Dap)*. NBs located at the ventral surface of the VNC express another transcription factor Vnd which promotes their quiescence [64]. The homeodomain transcription factor Prospero (Pros) plays a crucial role in NBs entering quiescence in a dose-dependent manner [65]. NBs lacking Pros fail to enter quiescence, NBs with high amounts of Pros become terminally differentiated, and NBs with moderate levels of Pros successfully enter quiescence [65]. Once embryonic NBs exit the cell cycle, their quiescence is maintained by the Hippo signaling pathway [66]. Blood brain barrier (BBB) glia express intracellular transmembrane proteins Echnoid and Crumbs which activate evolutionarily conserved Hippo signaling pathways that induce and maintain quiescence in the NBs [66,67]. The glial niche is also known to secrete the glycoprotein anachronism (Ana) in the postembryonic larval brain to maintain quiescence [68].

Neuroblast exit from quiescence

NBs reactivation from developmental quiescence is regulated by a direct interplay between NB intrinsic and extrinsic factors. One of the earlier studies suggested that dietary amino acids are the critical extrinsic cues necessary for the reactivation [62,63]. Later it was proposed that dietary amino acids activate TOR signaling in the fat body which in turn produces a yet unknown fat body derived signal (FDS) necessary for insulin-like peptide (dILP) secretion in the larval brain [69]. There are eight dILPs (1-8) in *Drosophila* and presumably they play tissue specific roles in controlling cell growth and proliferation. In the VNC, sub perineurial glia (SPG) produce dILP6 which is required for the NBs reactivation [70]. In contrast, dILP2 is produced in the neurosecretory insulin producing cells (IPCs) and regulates reactivation from quiescence in the central brain NBs. dILP2 drives PI3K-mediated growth in both NBs and their surrounding cortex glial niche, which are both critical for the reactivation of the NBs [62,71]. NBs fail to reactivate from quiescence when cortex glial membrane niche development is inhibited by the reduction of the PI3K signaling pathway or when cortex glial cells are ablated by inducing apoptotic cell death [71]. The formation and maintenance of the cortex glial niche are essential for the proliferation of neuroblasts (NBs) in the central brain [71]. However, beyond providing a physical niche, the specific ways in which NBs and cortex glia support each other through the sharing of metabolic resources and signaling molecules remain understudied. Surface glia specific DE-cadherin expression plays a role in the NBs reactivation [72]. A subset of dorsal midline glial cells expresses a heparan sulfate proteoglycan named terribly reduced optic lobes (Trol) which promotes NBs reactivation, presumably by antagonizing

the glycoprotein Ana and modulating FGF and Hedgehog signaling pathway [73–75]. dILP2 mediated activation of PI3K reactivates quiescent NBs by inhibiting transcription factor FOXO [76–78]. Inhibition of Pros is also necessary for the NBs reactivation which is mediated by Chromator (Chro), a spindle matrix protein which functions downstream of InR/PI3K/Akt signaling pathway [79]. Maintenance of NB quiescence is dependent on the Hippo signaling pathway and two recent studies have shown that Cullin4-ring ligase (CRL-4) and STRIPAK complex proteins promote NB reactivation by repressing the Hippo signaling pathway. CRL4 is an evolutionary conserved E3 ligase protein that degrades Warts (Wts) and the STRIPAK complex protein components inhibit Hippo kinase activity thus inhibiting Hippo signaling pathway and promoting Yorkie (Yki) mediated NB growth and proliferation [80,81]. Notch signaling pathway also plays a role in a subset of central brain NBs decision to enter and exit quiescence. A high level of Notch activity in the NBs during late embryonic stages promotes their quiescence entry and a low level of Notch activity in the freshly hatched larvae brain is required for the NBs to enter cell cycle in response to extrinsic nutrient cues. Notch signaling mediates its function by regulating Dacapo (Dap) activity [82].

Overall, recent studies have identified several NB intrinsic and extrinsic factors as critical for the quiescent NBs reactivation. However, it is still not clear how exactly the interaction between NB intrinsic and extrinsic factors lead to their exit from quiescence.

Asymmetric cell division in the *Drosophila* neuroblasts

Neuroblasts (NBs) proliferate through asymmetric cell division, producing one self-renewing progeny that maintains the NB pool and one differentiating ganglion mother cell

(GMC). The GMC terminally differentiates into either a neuron, a glial cell, or both [3,83]. There are two types of NBs in the *Drosophila* brain, type I and type II **(Fig. 1.1)**. Most of the NBs are type I and they are identified based on their expression of the transcription factors deadpan (Dpn) and Asense (Ase). During each round of asymmetric division, type I NBs produce one self-renewing NB progeny and one GMC. Type II NBs are Dpn positive but Ase negative. Compared with the type I NBs, type II NBs produce an intermediate progenitor cell (INP) in place of a GMC. INPs can divide several more times (3-6 rounds) before terminal differentiation [47,84–86].

Asymmetric cell division in the NBs begins with the establishment of an intrinsic polarity axis by localizing polarity proteins to the apical cortex. Next, the microtubule spindle aligns itself with the apical axis and the basal cell fate determinants become localized to the basal NB cortex. The process concludes with the unequal segregation of the cell fate determinants into the daughter cells [12,83].

Establishment of apical basal polarity

NB apical polarity is established by the Par complex. The Par complex is composed of Par-6, aPKC and Lgl during interphase [83]. During mitosis, Aurora A kinase activates aPKC by phosphorylating Par-6 which in turn causes Lgl to dissociate and allows Baz to enter the complex [87]. Par complex plays an important role in localization of the basal fate determinants and in the correct orientation of the mitotic spindle. aPKC/Par-6/Baz forms a tight apical crescent during metaphase [83]**(Fig 1.3).**

Basal cell fate determinants include Numb, Partner of Numb (Pon), the adaptor protein Miranda (Mira) and its cargo proteins Prospero (Pros) and Brain tumor (Brat) [88–91]. Mira is basally localized during metaphase and ultimately partitioned into the GMC [89]. The exact mechanism controlling basal localization of Mira remains unclear. Initially it was suggested that Mira was sent to the basal cortex by active transport mediated by non-muscle Myosin ll and unconventional Myosin Vl. This model was rejected later due to experimental limitations [83]. One recent study using Fluorescence Recovery after Photobleaching (FRAP) experiments has suggested that Mira is transported to the basal cortex by passive diffusion [92]. Phosphorylation status of Mira plays a key role in determining Mira cortical versus cytoplasmic localization. Unphosphorylated Mira is usually localized to the cortex and prior to the onset of metaphase it gets phosphorylated by aPKC which dislodges Mira from the cortex [93]. Therefore, the current model of Mira basal localization proposes that Mira is excluded from the apical cortex by aPKC-mediated phosphorylation and then settles at the basal cortex by passive diffusion. Another basal cell fate determinant Numb also requires phosphorylation by aPKC for its localization at the basal cell cortex during metaphase [94]. Numb forms a complex with Pon, however Pon is not required for the correct localization of Numb [95]. One study has suggested that the mitotic kinase Polo directly phosphorylates Pon which facilitates Numb localization [96]. Basal cell fate determinants form a tight crescent at the basal cortex during mitosis and are eventually segregated into the smaller GMC at the end of cytokinesis. Shortly after cell division, Mira dissociates from the GMC cortex and releases Pros. Pros enters the GMC nucleus and cause the GMC to differentiate into neurons [83].

Proper microtubule spindle orientation plays an important role in the appropriate segregation of the cell fate determinants and overall NB homeostasis [97]. NBs with an orthogonal (in relation to the apical-basal axis) microtubule spindle divide symmetrically due to their failure to segregate cell fate determinants [98]. Apical polarity proteins important for the spindle orientation are heterotrimeric G-protein alpha subunit (Gai), Inscuteable (Insc), Partner of Inscuteable (Pins) and Mushroom body defect (Mud). Pins mutant NBs lose their cell apical polarity and proper spindle orientation. In Mud mutants, NBs only lose their mitotic spindle orientation but not the apical-basal polarity [99–102]. There is an alternative spindle orientation pathway, called astral microtubule/Khc-73 pathway, that can induce cortical polarity in the absence of Insc and orient the mitotic spindle properly with its apical-basal domain [103].

Cytokinesis

Cytokinesis is the process by which dividing cells physically separate to produce two daughter cells. This process involves several distinct steps: first, a cleavage furrow forms at the cell cortex. Then, a contractile ring assembles at the cleavage furrow site and constricts, causing the cleavage furrow to ingress. Finally, an abscission event occurs, physically separating the sibling cells [104].

In *Drosophila*, earlier studies on cytokinesis were done mainly using symmetrically dividing spermatocytes and S2 cell lines [105–107]. According to a current model, cleavage furrow positioning is achieved by the activation of RhoA kinase by central spindle complex proteins. This model requires a stable population of central spindle microtubules and the

components of the central spindle complex, Pavarotti (Pav) and Tumbleweed (Tum, also known as RacGAP50C), to travel along the plus end of the microtubules to the cell cortex where they activate RhoGEF Pebble (Pbl) which in turn activates Rho A. Genetic and physical interaction studies have shown that mutations in either *pav*, *tum*, *pbl*, or *rho1* lead to very early cytokinesis defects [104,108–112]. Live imaging in spermatocytes has shown that a population of peripheral microtubules contacts the cell cortex before the emergence of the cleavage furrow which also supports this model [113].

Drosophila NBs divide asymmetrically and produce siblings of different sizes. As it is common in metazoans to position cleavage furrows using cues from the mitotic spindle, it would be plausible for the mitotic spindle asymmetry to position the cleavage furrow in an asymmetric manner in the NBs. However, it has been observed that markers for the cleavage furrow (e.g. Myosin) appear earlier than the establishment of spindle asymmetry in the NBs [98]. This suggests that in the NBs cleavage furrow positioning is determined by signals independent of the mitotic spindle. Experiments in which the mitotic spindle in the NBs was completely ablated using a chemical method still retained the capacity to distribute Myosin asymmetrically [98,114]. Additionally, mutants in which the mitotic spindle was misplaced orthogonal to the NB intrinsic apical-basal polarity axis were still able to form a cleavage furrow that leads to asymmetric cell division [97,102,115]. These findings strongly suggest the presence of polarity cues that determine the NBs cleavage furrow positioning. Genetic studies have identified Dlg and Pins to be required for the asymmetric distribution of Myosin. Mutants in which both Dlg and Pins are mutated divide symmetrically due to their failure in asymmetric distribution of Myosin [104,116]. Recent

findings suggest that the level of cortical Myosin is inversely correlated with cortical expansion. In the wild type NBs, the apical cortex extends much more than the basal cortex which directly correlates with the level of Myosin present during the cortical expansion event [117,118]. The mechanisms involved in the NBs polarity mediated asymmetric cleavage furrow positioning are still poorly understood and need further investigation.

Once RhoA signaling determines the site of the cleavage furrow, an actomyosin contractile ring assembles at the site. F-actin assembly is mainly regulated by the genes *diaphanous (dia), chickadee (chic) and twinstar (tsr)*, and myosin activation is regulated by the kinases Rok and Sti [119]. Myosin plays a critical role in cytokinesis, however, the exact mechanism of Myosin localization at the cleavage furrow remains unknown. Anillin and Septins play key roles in tethering the contractile ring to the cell membrane and overall completion of the cytokinesis process [120–122].

1.3 Lipid metabolism and NSC proliferation

The role of lipid metabolism in neural stem cell proliferation and maintenance has been best studied in the adult mouse brain. It has been shown that fatty acid synthase (FASN), a key enzyme in de-novo lipogenesis, is enriched in the SVZ and DG of adult mouse brains. Conditional knockdown of FASN greatly reduced the proliferation of neural stem and progenitor cells (NSPCs) in the SVZ and DG region [123]. FASN converts malonyl-CoA into free fatty acids. It has been reported that quiescent NSPCs in the adult mouse brain express Spot14, a thyroid hormone responsive protein that reduces FASN activity

by restricting its access to its substrate malonyl-CoA. Knockdown of Spot14 in the SGZ of adult mice increased NSPC proliferation [124]. The importance of FASN in brain development is further highlighted by the fact that human individuals with a faulty variant of FASN (FASN-R1819W) in their NSPCs show cognitive impairment [125]. Radioactive tracing of the lipids generated by FASN dependent lipogenesis in the NSPCs showed that these lipids are almost exclusively used for cell membrane synthesis [123]. This makes sense because NSPC proliferation requires membrane synthesis for generation of new progeny.

Mitochondrial fatty acid beta oxidation (FAO) is also important for NSPC proliferation and maintenance of quiescence. Disruption of FAO in the embryonic mouse brain led to reduced NSPC proliferation at the apical surface of the ventricle and an overall disorganization of the ventricular/subventricular zone. Inhibition of FAO in the adult brain also leads to reduced NSPC proliferation in the SVZ region [126,127]. FAO plays an even more important role in quiescence versus proliferation decisions in the NSPCs. Quiescent NSPCs have a higher level of FAO compared with the proliferating NSPCs [127,128]. Inhibition of FAO and enhancement of *de-novo* lipogenesis by increasing malonyl-CoA levels are sufficient to induce the proliferation of quiescent NSPCs [127]. A recent study has demonstrated that quiescent NSPCs in the mice dentate gyrus (DG) prefer FAO over glycolysis. A disruption in this balance causes NSPCs to exit quiescence. This same study also showed that quiescent NSPCs highly express mitochondrial pyruvate carrier (MPC) which carries pyruvate, the end product of glycolysis, inside the mitochondrion.

Pharmacological and genetic inhibition of MPC triggered quiescent NSPCs reactivation which again highlights the importance of FAO for quiescence maintenance [129].

Lipid droplets (LDs) are ubiquitous organelles composed of a neutral lipid core enclosed in a phospholipid monolayer. They are well-known for their role in maintaining organismal energy homeostasis. Recent studies have highlighted the role of lipid droplets (LDs) in normal animal development across multiple tissues. These studies also show how disruptions in LD homeostasis can lead to various diseases [130–132]. However, very little is known about the role of LDs in NSPCs proliferation and overall brain development. *In vitro* studies with adult mouse SVZ derived NSPCs have shown that LD availability directly correlates with their proliferative capacity [133]. It remains to be shown whether this holds true for the NSPCs *in vivo*. So far, we know that the NSPC niche cells contain lipid LDs [134]. In *Drosophila*, LDs in the glial niche cells play roles in protecting NBs against stress stimuli such as hypoxia and reactive oxygen species (ROS) [135,136]. The exact role played by LDs in ependymal niche cells in the mouse brain is not yet known. Investigations with a mouse model of Alzheimer's showed that ependymal cells had an increase in LD accumulation and the NSPCs proliferation was reduced [134].

Besides NSPCs, lipid metabolism is also known to play an important role in the homeostasis of other stem cell populations such as hematopoietic stem cells (HSC), intestinal stem cells (ISC), cancer stem cells (CSC), and others [128,137–141]. Recent work in mice has shown that FAO is important for HSC homeostasis: inhibition of FAO leads to the exhaustion of the HSC pool whereas an increase in FAO improves their proliferation

[142]. In *Drosophila* hemocytes, functionally equivalent to mammalian blood macrophages, proper FAO is important for the production of differentiated progeny. Upregulation of FAO in *Drosophila* hemocytes increases the progenitor pool [143]. Similar to HSCs, FAO in mice also plays a crucial role in maintaining the ISC pool [128]. CSCs also have been reported to upregulate their FAO. Upregulation of FAO most likely helps CSCs to remain in a quiescent state which likely helps them maintain a CSC pool and even be resistant to treatments. Pharmacological inhibition of FASN seems to decrease CSC viability thus it is likely that de-novo lipogenesis plays a role in CSC homeostasis [137,144,145].

Lipid metabolism in *Drosophila*

The core cellular machinery required for the synthesis and breakdown of lipids is conserved in the animal kingdom. Here I will focus my discussion on the metabolism of the neutral lipid triacylglycerol (TAG) in *Drosophila,* because TAG represents the most abundant form of stored energy in the *Drosophila* embryo and its role remains understudied during early stages of brain development. *Drosophila* can access triacylglycerol (TAG) in three ways during their life cycle. First, they can synthesize free fatty acids (FAs) through *de-novo* lipogenesis using carbohydrates as precursors **(Fig. 1.5)**. Second, diet is another major source of TAG in flies which they digest and either use immediately or store in the fat body as LDs for future use. Third, maternally deposited LDs in the egg supply TAG essential for embryonic development [146,147]. These three mechanisms for acquiring TAG will be described below.

De-novo lipogenesis

De-novo lipogenesis begins with the conversion of acetyl-CoA into malonyl-CoA by the enzyme acetyl-CoA carboxylase (ACC). In the next step, fatty acid synthase (FASN) sequentially condenses malonyl-CoA units with acetyl-CoA and produces long chain FAs. The *Drosophila* genome encodes a single *ACC* and three *FASN (FASN1, FASN2 and FASN3)* genes [148]. Both ACC and FASN are very important for *Drosophila* development which is evident by the fact that loss of ACC or FASN causes lethality during the embryonic or larval stage respectively [149,150]. Transcriptional activity of *ACC* and *FASN* along with many other genes involved in lipogenesis and membrane synthesis are controlled by the transcription factor Sterol Regulatory Element Binding Protein (SREBP). SREBP remains localized to the ER membrane in its inactive form. It is activated by proteolytic cleavage at specific sites which cause its bHLH-Zip domains to translocate to the nucleus and drive lipogenic gene expression [151–153]. SREBP activity is controlled by membrane lipid compositions [151]. It is also controlled by hormonal cues especially through the evolutionary conserved InR/PI3K/Akt pathway [154–156]. There are several pathways that compete for the free FAs such as beta-oxidation, membrane phospholipid biosynthesis and TAG synthesis.

Dietary TAG

Diet is another source for neutral lipids in flies. Dietary TAG is digested by lipases into simpler lipid molecules such as fatty acids, glycerol and acylglycerols before they can be transported and used by different tissues. The *Drosophila* genome encodes about a dozen putative digestive lipase; however, they still remain uncharacterized [148,157,158].

Digested lipids, from both diet and *de-novo* synthesis, are transported through the hemolymph by lipoproteins. Lipophorin (Lpp) is the major lipoprotein in *Drosophila,* and it is responsible for more than 95 percent of the lipid transport in hemolymph. Diacylglycerol (DAG) is the main Lpp bound lipid in the hemolymph although it carries trace amounts of other lipids such as PC, PE, sphingolipids, free sterols and hydrocarbons [159,160]. Lipid transfer particle (Ltp) proteins are responsible for loading Lpp with lipids [159,161]. In addition to Ltp, tissue specific lipid transfer depends on lipoprotein receptors (Lpr). There are seven Lpr encoded by the *Drosophila* genome and presumably they are expressed in a tissue specific manner. Lpp is mainly expressed in the fat body of *Drosophila* and plays a critical role in development. Lpp mutant flies arrest their development as L3 larvae and eventually die [159,161,162].

Maternal LD

The early stages of *Drosophila* development are fueled by maternally deposited lipid droplets (LDs). These LDs are also packed with histone proteins that provide for the rapid nuclear division during the early embryonic stage. LDs in the egg are deposited by the nurse cells during oogenesis, and there could be a pool of *de-novo* synthesized lipids too [146,147,163]. Female flies that are mutant for the *midway* gene, which converts DAG to TAG, face degeneration of egg chambers and their progeny dies during embryonic stage [164,165]. During the very early stages of embryonic development, maternal LDs are distributed from the core of the embryonic sac to the newly formed peripheral cells. Mutations in genes that interfere with this LD distribution process (*Jabba, Klar*) or their subsequent breakdown (*Brummer*) have negative consequences in development [147]. It is

currently unknown whether embryonic LDs are distributed evenly or preferentially to certain cell types.

TAG homeostasis

TAG is the main stored form of energy in *Drosophila*, and its turnover plays a crucial role in maintaining energy homeostasis, as well as providing structural and signaling lipids. TAG is produced by the actions of several enzymes **(Fig 1.5)** where free fatty acid (FA) moieties are sequentially added to the glycerol-3 phosphate (G-3-P) backbone. The last and only committed step in TAG synthesis is mediated by the enzyme Midway (Mdy) which converts DAG to TAG [148]. Adipokinetic hormone (Akh) signaling and increased cellular Ca2+ levels are known to suppress *Mdy* expression levels [166,167]. However, the molecular mechanisms connecting Akh/Ca2+ signaling to *Mdy* expression levels remain unknown.

The fat body is the primary organ for TAG synthesis and storage in *Drosophila*. However, other cell types, including the midgut, ovaries, imaginal discs, salivary glands, and brain also express the enzymes needed to synthesize their own lipids [136,159,162,168,169]. LDs are lipid storage organelles with a core of neutral lipids (TAG and sterol ester) inside a phospholipid monolayer. They originate from the ER and contain a specific set of surface proteins that maintain their homeostasis [170,171].

TAG is mobilized from the LDs during periods of increased energy demands or starvation. During this process, ester bonds in the TAG are hydrolysed by lipases. Brummer (Bmm) is the main TAG lipase in *Drosophila* **(Fig.1.4)** Bmm mutant adult flies accumulate excessive TAG and their TAG breakdown is significantly slowed down during periods of starvation. Interestingly, due to this excess fat storage and its slow breakdown, Bmm mutant flies live much longer when subjected to starvation [172]. This observation also implies that there is an alternative pathway for the breakdown of TAG in *Drosophila*. Studies have suggested alternative Akh-dependent lipolytic pathways in *Drosophila*, however, the lipases involved in this pathway remain uncharacterized [172]. Bmm breaks down TAG into DAG and free fatty acids, but it lacks the capacity to break down DAG any further. Hormone sensitive lipase (HSL) is the candidate DAG lipase in *Drosophila*. In mammals, HSL is known to function as a DAG lipase in multiple tissue types. However, the enzymatic properties and tissue specificity of HSL remains uncharacterized in *Drosophila* [172–174].

Lipase access to the LD surface is regulated by an evolutionarily conserved family of proteins known as perilipins [175]. Perilipins are well known for their function in regulating basal level of lipase access to the LDs and also in promoting lipase activity in response to hormonal signaling. There are two perilipins in *Drosophila* known as Lipid storage droplet 1 (Lsd1) and Lipid storage droplet 2 (Lsd2). Lsd2 inhibits lipolysis by limiting Bmm access to the LDs. Lsd2 mutant flies are lean and starvation sensitive whereas overexpression of Lsd2 in transgenic flies causes obesity and starvation resistance. In contrast, Lsd1 has a dual role: it functions as a docking interface for HSL during starvation

and simultaneously limits the activity of Bmm [172,176]. On a transcriptional level, *bmm* expression is controlled by the transcription factor Foxo. The insulin signaling pathway negatively regulates Foxo activity through Akt1 and Salt-inducible kinase 3 (Sik3) mediated phosphorylation [77,177,178]. Foxo activity could also be regulated by an insulin signaling independent mechanism such as through phosphorylation by Liver kinase B1 (Lkb1) [178].

Lipid Droplet availability and NB proliferation

Recent studies have reported the presence of LDs in the cortex glial niche of late-stage *Drosophila* larval brains [179]. LDs in the cortex glial niche harbor Hedgehog (Hh) signaling molecules that cell autonomously control glial niche formation. Disruption in LD homeostasis causes loss of Hh signaling which negatively affects cortex glial niche formation and also NB proliferation [180]. LDs in the cortex glial niche are formed in response to elevated levels of reactive oxygen species (ROS) in the neuron. Glial LDs protect the niche from oxidative damage caused by ROS mediated peroxidation by sequestering polyunsaturated fatty acids (PUFA), which is important for the NBs to be able to maintain their proliferation [135,136,181,182].

While evidence has emerged regarding the crucial role of LDs in late-stage larval brain development and maintaining adult brain homeostasis, the specific role of maternally deposited LDs in early brain development in *Drosophila* remains unknown.

Figures:

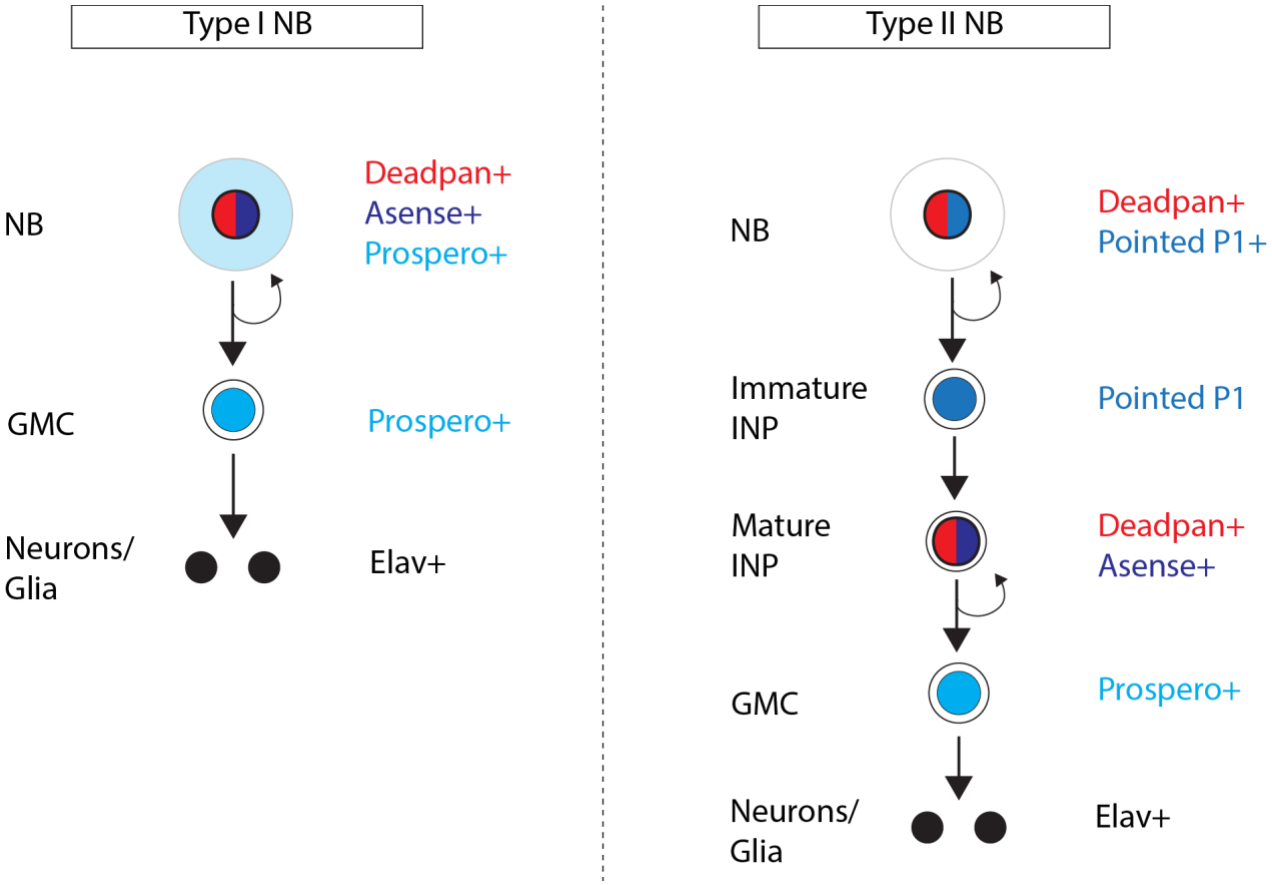

Fig 1.1: There are two types of NBs in the *Drosophila* brain- type I and type II. *Drosophila* central brain and ventral nerve cord NBs are mostly type I and they are identified based on their nuclear expression of bHLH transcription factors Deadpan and Asense. Type I NBs also contain low levels of cytoplasmic Prospero. In contrast, type II NBs do not contain cytoplasmic Prospero and they express transcription factors Deadpan and Pointed P1 in their nucleus. Type I NBs divide asymmetrically in which they self-renew the stem cell pool and produce a daughter ganglion mother cell (GMC). The GMC

divides symmetrically and produces either neurons or glia. In contrast, type II NBs produce an immature intermediate progenitor cell (ImINP) in place of a GMC. ImINPs express high levels of Pointed P1 in their nucleus and become mature INP (mINP). mINPs are identified by their expression of nuclear Deadpan and Asense. mINPs have the capacity to divide asymmetrically for a limited number of times (3-6 times) before their terminal differentiation.

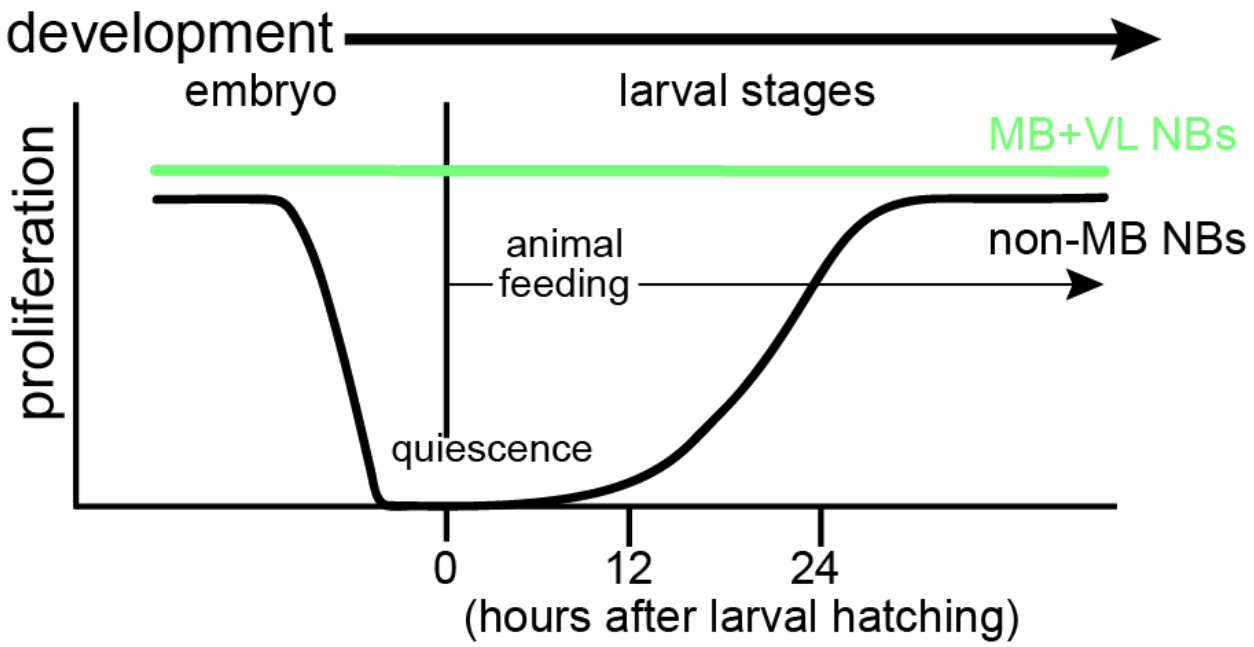

Fig 1.2: *Drosophila* central brain NBs proliferation pattern during early stages of larval development. Most of the NBs in the *Drosophila* brain enter quiescence at the end of the embryonic stage except for the four Mushroom body neuroblasts (MB NBs) and a ventrolateral (VL) NB in each brain hemisphere. All non-MB NBs exit quiescence in response to larvae feeding on a complete diet. By 24 hours ALH, almost sixty percent of the quiescent NBs enter cell cycle and by 48 hours ALH they are fully reactivated.

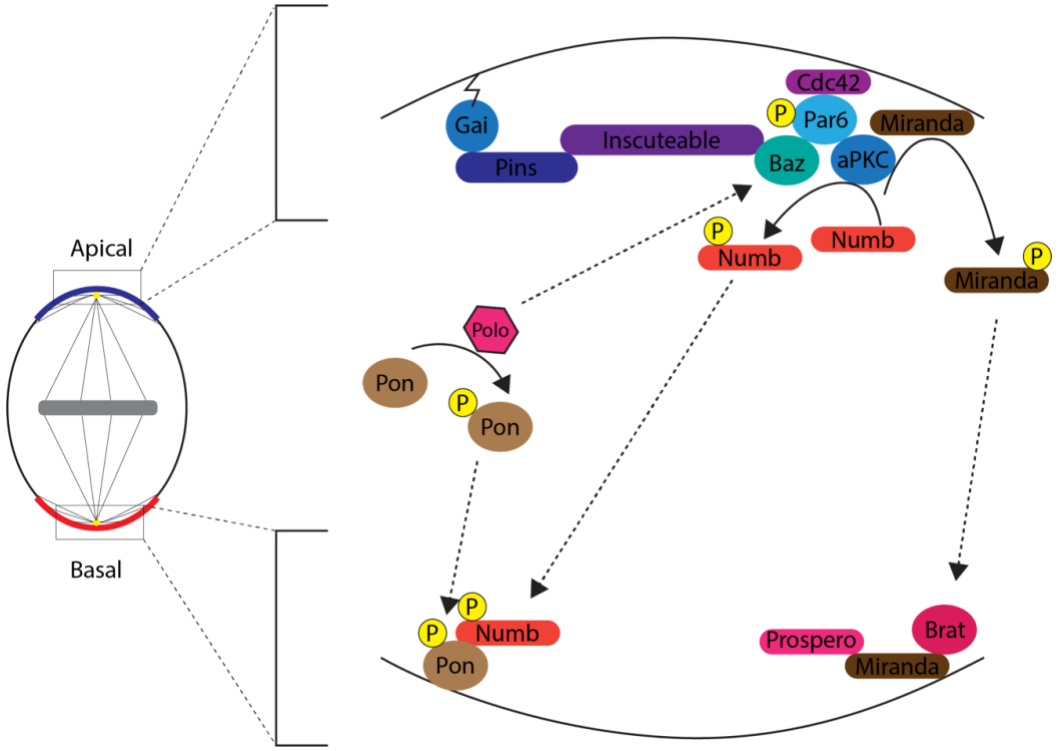

Fig 1.3: Apical-basal polarity axis in metaphase NBs. During metaphase, apical and basal polarity proteins form a tight crescent at the apical and basal cortex of the NBs respectively. GTP bound Gαi binds with Pins which is important for its localization. Pins binds with Inscuteable which keeps the apical Par complex in place. During mitosis, the apical core Par complex is made of Par-6, Bazooka (Baz) and aPKC proteins. Cdc42 binding with Par-6 keeps Par-6 and aPKC apical. Polo kinase phosphorylates Baz which is required for proper apical Par complex localization. Polo also phosphorylates Partner of numb (Pon) and sends it to the basal cortex. aPKC mediated phosphorylation of Miranda (Mira) is critical for Mira delocalization from the NB cortex which eventually settles at the basal cortex during metaphase. aPKC also phosphorylates Numb and sends it to the basal cortex.

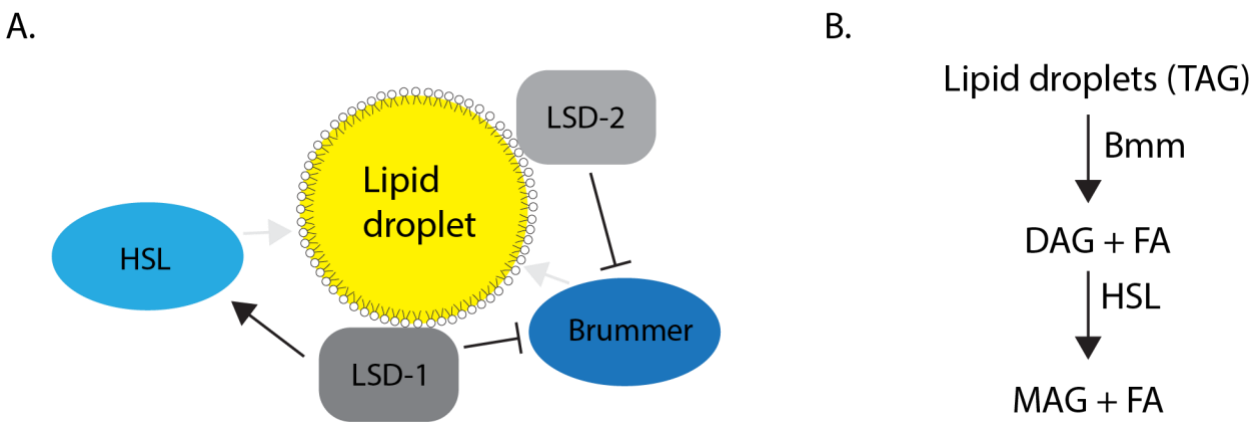

Fig 1.4: Lipid droplet homeostasis in *Drosophila*. (A) In homeostatic conditions, lipid droplet (LD) surface proteins, Lipid storage droplets 1 (LSD-1) and Lipid storage droplets 2 (LSD-2), control Brummer and Hormone sensitive lipase (HSL) enzymes access to the LD. LSD-2 inhibits Bmm access to the LD surface thus protecting LD breakdown. LSD-1 acts as a docking interface for HSL during starvation and simultaneously limits the activity of Bmm. (B) Once Bmm has access to the LDs, it breaks down TAG into DAG and free fatty acids (FAs). DAG is further broken down into monoacylglycerol (MAG) and more free FAs by HSL.

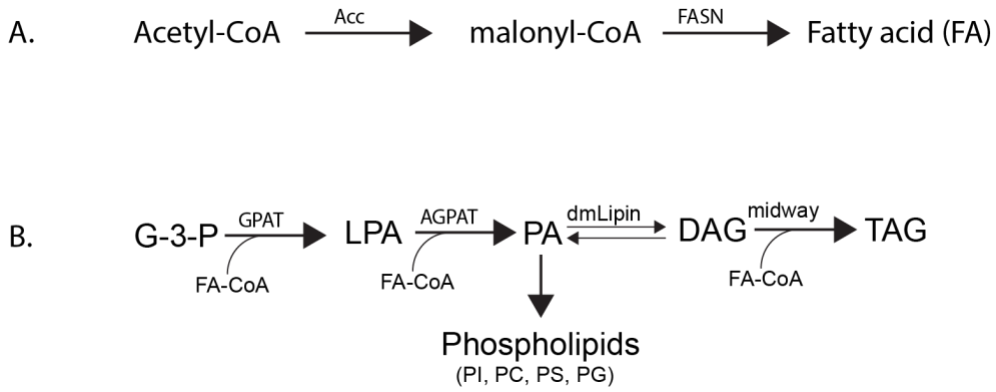

Fig 1.5: Free fatty acid (FA) and triacylglycerol (TAG) synthesis in *Drosophila*. (A) Acetyl-CoA from the mitochondrial TCA cycle is transported to the cytoplasm where it is converted into free fatty acids by *de-novo* lipogenesis. In *de-novo* lipogenesis, acetyl-CoA is converted into malonyl-CoA by the enzyme acetyl-CoA carboxylase (ACC). In the next step, fatty acid synthase (FASN) sequentially condenses malonyl-CoA units with acetyl-CoA and produces long chain FAs. (B) FAs are stored as TAG and this process takes place in the endoplasmic reticulum. FAs are added to the glycerol-3 phosphate backbone by the enzyme Glycerol-3-phosphate acyltransferase (GPAT) to produce lysophosphatidic acid (LPA). LPA gets converted into phosphatidic acid (PA) by the enzyme Acylglycerol phosphate acyltransferase (AGPAT). PA can be used as a precursor molecule to synthesize several cell membrane phospholipids such as Phosphatidylinositol (PI), Phosphatidylcholine (PC), Phosphatidylserine (PS) and Phosphatidylglycerol (PG). Next, *Drosophila* Lipins convert PA into diacylglycerol (DAG) which is ultimately converted into TAG by the Midway (Mdy) enzyme.

Chapter 2

Maternal lipid sources prime neural stem cells to switch from quiescence to proliferation in response to dietary nutrient availability

Md Ausrafuggaman Nahid, Susan E. Doyle, and Sarah E. Siegrist*

Department of Biology, University of Virginia, Charlottesville, VA 22904, USA

*Correspondence: ses4gr@virginia.edu

Summary

Stem cell quiescence--a state of mitotic and metabolic dormancy--is essential for tissue homeostasis and for coordinating growth with nutrient availability. Switching between quiescence and proliferation is controlled through stem cell intrinsic and extrinsic cues, with diet being key as diet provides macro- and micro-nutrients needed for synthesizing new membrane, protein, and nucleic acids. Yet, it remains unclear what nutrients control the stem cell switch and whether nutrient sources other than diet are required. Here, we report that lipids deposited maternally in the embryo regulate reactivation of *Drosophila* neural stem cells (neuroblasts) from quiescence. This maternal nutrient source is in addition to the known dietary amino acid requirement acquired during larval feeding. Moms fed reduced lipid diets or carrying mutations in genes essential for lipid deposition and metabolism produce larvae with fewer stored lipids in neural tissues. Reduced neural lipid stores result in glial growth and neuroblast reactivation delays due to the inability of neuroblasts to activate PI3-kinase signaling in response to dietary-induced expression of insulin-like peptides. Thus, neuroblasts, and potentially other stem cells, rely on two nutrient sources for switching between quiescence and proliferation, those that are stored maternally and those that are acquired through diet.

Introduction

Maternal deposition of mRNA, protein, lipid droplets, and glycogen is essential for supporting development of the fertilized egg [1]. Once eggs implant into the uterus in mammals or hatch in other species, continued growth and development relies on the acquisition of outside nutrients. A relatively simple yet functional CNS is present at

hatching in many animal species including fish, amphibians and insect larvae, containing both neural circuits that control feeding behavior and a diverse array of neural stem cell and progenitor cell types [2–5]. The transition from non-feeding to feeding stages marks a critical period in an organism's life cycle as egg supplied nutrients become depleted. Importantly, during this transition, most cell divisions are halted organism-wide and resume only after outside nutrients are acquired [6–8]. At the organism level, dietary nutrients are processed in the gut and delivered to cells in peripheral tissues providing the macromolecules needed to support synthesis of new nucleic acids, proteins, lipids, and essential metabolites. In the CNS, once nutrients are sensed and received, neural stem cells and progenitors reinitiate cell divisions, generating new progeny to support the ongoing expansion and diversification of the CNS [9–12].

In *Drosophila* larvae, the current model posits that peripheral tissues send a triggering mitogen to the brain in response to animal feeding. This leads to the synthesis and release of Dilp-2 from a group of neurosecretory neurons in the brain and possibly other Dilps from other sources including glia [13–15]. Dilp-2, one of eight *Drosophila* insulin-like peptides, is regulated by nutrient availability and during favorable conditions (presence of amino acids) is released systemically into the hemolymph and locally into the brain. Dilp-2 binds the Insulin-like tyrosine-kinase receptor in both neuroblasts and surrounding glia, leading to downstream activation of PI3-kinase (Phosphoinositide 3-kinase), Akt and TOR [15–17]. This leads to cellular uptake of glucose, synthesis of new protein and lipid, and changes in cell cycle gene expression. Remarkably, many stem cells found in other tissue types in other species across the animal kingdom control the

switch from quiescence to proliferation using the same growth signaling pathways, including intestinal and neural stem cells and even the blastocyst itself [18,19].

Results

Lipid droplet consumption correlates with neuroblast reactivation

Using *Drosophila* neuroblasts as a model, we set out to better understand how nutrients control the stem cell switch from quiescence to proliferation. We investigated the role of lipids and started by assaying lipid droplets (LDs). LDs are organelles that store neutral lipids in the form of triacylglycerol and sterol esters and in non-lipogenic tissues are associated with disease states [20–22]. However, LDs also accumulate in the Dauer *C. elegans* and in quiescent mammalian neural stem cells where they play a role in controlling stem cell behavior [23,24]. At freshly hatched (FH) larval stages (0 hours ALH), we found a more than 2 fold increase in the number of brain LDs compared to 24 hours later after feeding on a BL diet (Fig. 1A-C). This initial increase followed by a reduction in LD number was also observed in animals fed PBS only, suggesting that LDs are processed independent of dietary nutrient acquisition (Fig. 1A-C). LDs were found throughout the brain, in glia, neurons, quiescent neuroblasts, and in particular mushroom body (MB) neuroblasts (SF1A-F). MB neuroblasts are a neuroblast subset that divide continuously independent of dietary nutrient conditions [25]. Next, we examined LDs in brains of two types of mutants, those that deposit less lipid maternally and those that have defects in LD breakdown. Moms homozygous mutant for *Jabba*, *Lsd2* (*Lipid storage droplet-2*), or *klar* (*klarsicht*) produce embryos with fewer maternally deposited LDs and/or have lipid partitioning defects. Likewise, fewer LDs were found in brains at the FH larval

stage in each of these mutants and zygotic contribution played no role (Fig. 1D-E,H, SF1G,L). Next, we assayed LDs in animals homozygous mutant for the *hormone-sensitive lipase (hsl)* and *brummer* (*bmm*, ATGL in mammals), both encode lipases that breakdown LDs into free fatty acids and diacylglycerol. We found significantly more LDs in both *hsl* and *bmm* mutants compared to wildtype at both FH stages and 24 hours later (Fig. 1F-H, SF1I,J). Next, we assayed neuroblast reactivation from quiescence in each of the mutants. In wildtype animals, at FH stages, only the four mushroom body (MB) neuroblasts and one lateral neuroblast are dividing in each of the brain hemispheres as shown previously (Fig. 1I,O). After 24 hours of feeding on a complete BL diet, approximately sixty percent of quiescent neuroblasts (non-MB NBs) in Oregon R animals, identified based on expression of the Dpn transcription factor, reactivated and re-entered cell cycle, based on their incorporation of the thymidine analogue, EdU (Fig. 1J,O,P). In contrast, all animals carrying mutations in genes important for maternal lipid deposition or LD breakdown resulted in fewer neuroblasts reactivated from quiescence and zygotic contribution played no role (Fig. 1K-N,P, SF1H,K,M). After 48 hours of larval feeding, most neuroblasts in the mutants had reactivated (SF1N-T). We conclude that LDs stored in brains at freshly hatched stages are consumed rapidly and that LD consumption correlates with neuroblast reactivation from quiescence. Importantly, maternal deposition of lipids regulates timing of neuroblast reactivation.

LDs are utilized locally for promoting early neural growth

To test whether LDs are consumed locally in a cell intrinsic manner to support neuroblast reactivation, we carried out two experiments. First, we expressed *UAS-bmmRNAi* to knock down *bmm* in different cell types. Neuroblast reactivation was reduced in animals expressing *bmmRNAi* in neuroblasts (*worGAl4)* or glia (*repoGAL4*), including cortex glia (*NP0577GAL4*), but not in fat body (*r4GAL4*), a peripheral tissue that stores lipid and functions in an endocrine, liver-like manner (Fig. 2A-G). We also re-expressed *bmm* in a cell type specific manner in *bmm* mutants. We found reductions in brain LD numbers when *bmm* was reintroduced in neuroblasts (*worGAl4)* or ubiquitously (*actGAL4*), but not when reintroduced in glia (*repoGAL4* or *NP0577GAL4*), or in fat body (*dcgGAL4*) (SF 2A-I). Neuroblast reactivation was restored when *bmm* was reintroduced in neuroblasts, glia, and ubiquitously, but only partially, consistent with the notion that genetic rescue can be problematic due to the need for tight regulation of enzyme activity and levels (SF2J-M). Next, to distinguish whether lipids provided maternally or through diet are required for neuroblast reactivation, we knocked down *apolpp* and the single fatty acid binding protein encoded in the *Drosophila* genome, *FABP* using the fat body specific, *r4GAL4*. ApoLpp is transcribed exclusively in the fat body and processed into Lpp, the major hemolymph lipophorin, responsible for lipid transport between tissues. FABP (fatty acid binding protein) is expressed ubiquitously binding fatty acids within cells and in some cases secreted where it functions as an adipokine. We found that neuroblasts still reactivate from quiescence in both conditions suggesting that Lpp mediated transport between tissues and FABP based signaling is not required (Fig. 2G, SF2N-O). However, neuroblasts do stop dividing later in fat body driven-*apolppRNAi* animals indicating that

lipid-based transport between tissues is essential to sustain neuroblast proliferation after reactivation. We conclude that LDs deposited in the brain at freshly hatched stages are consumed locally and are required for neuroblast reactivation. Yet, after neuroblasts reactivate, lipids acquired through diet and transported from gut to brain are required to sustain neuroblast proliferation.

Are fatty acids broken down from LDs within neuroblasts and glia utilized for membrane synthesis, signaling, or ATP production? We first assayed membrane synthesis by assaying neuroblast size and surface area of cortex glial. Neuroblasts increase in size prior to cell cycle re-entry and cortex glia undergo a dramatic expansion in membrane surface area within the first 24 hours. At 24 hours ALH, we found significant reductions in neuroblast size and cortex glial membrane surface area in mutant animals compared to controls (Fig. 2H-L). To further test whether LDs support early neural tissue growth, we next assayed the number of newborn progeny that MB neuroblasts generate. Within the first 24 hours, MB neuroblasts collectively generate on average 75 new progeny in animals fed a BL diet and 40 in animals fed PBS only (Fig. 2M). LDs were consumed under both conditions. In *jabba* and *bmm* mutants, fewer progeny were generated in PBS fed animals compared to control, suggesting that LD availability supports MB neuroblast proliferation during nutrient restriction, whereas Lsd-2 mutants generated fewer under both conditions (Fig. 2M). Next, we examined neuroblast reactivation in *whd* (*withered*) mutants. Whd, is part of the carnitine shuttle needed for transferring long chain fatty acids into the mitochondrial matrix for beta-oxidation. We found reduced neuroblast reactivation in whole animal mutants. We conclude that LDs

are used for synthesizing new membrane and also support stem cell proliferation during dietary nutrient restriction.

Maternal lipid enables Dilp-2 signal reception during feeding

To further understand growth and reactivation defects associated with LD dysfunction, we next assayed upstream and downstream components of the Insulin/PI3-kinase signaling pathway. We found that the InR (insulin receptor) ligand Dilp-2 was synthesized and secreted in response to feeding on a BL diet in both *bmm* mutants and in Oregon R animals (Fig. 3A,B). Dilp-2 is required for neuroblast reactivation and cortex glia growth and is released from the IPCs (insulin producing cells) both systemically and locally into the brain. Next, we assayed InR and found that neuroblasts in both *bmm* mutants and in Oregon R animals express InR but that InR levels were consistently higher in *bmm* mutant neuroblasts (Fig. 3C,D). This suggests that InR signaling is not active in *bmm* mutants, given that InR is a Foxo target gene. Foxo, a negative regulator of Insulin/PI3-kinase signaling is active when PI3-kinase is not, and in S2 and mammalian cells, Foxo positively regulates InR transcript and protein levels. Next, using bi-molecular fluorescence complementation, we assayed PI3-kinase activity. PI3-kinase is a lipid kinase that phosphorylates PIP2 (phosphatidylinositol 4,5-bisphosphate) at the 3' position, converting it to PIP3 (phosphatidylinositol 3,4,5-trisphosphate) (Fig. 3K). When PI3-kinase is active, N- and C-terminal halves of GFP-PH (Pleckstrin homology domain) are reconstituted along the plasma membrane where PIP3 is found. PIP3 serves as a binding site for Pleckstrin homology containing proteins including Akt leading to downstream activation of growth signaling. After 24 hours of feeding on a BL diet, neuroblasts in control animals have active PI3-kinase signaling based on expression of the PIP3 sensor along their cell

membrane (Fig. 3E, mean=57% of neuroblasts, s.e.m.=3.2%, n=5 brain hemispheres from 5 animals). In contrast, no PIP3 sensor signal was found in *bmm* mutants after feeding (Fig. 3F, mean=2%, s.e.m.=0.8%, n=5 brain hemispheres from 5 animals). Next, we expressed a constitutively active version of PI3-kinase (*UAS-dp110*) to rescue the neuroblast reactivation phenotype in *bmm* mutants. *bmm* mutant neuroblasts expressing *dp110* (*worGAL4*) did not reactivate after feeding on a BL diet for 24 hours, although activity of PI3K was not directly measured in these cells (Fig. 3G,H,J). This was surprising given that ectopic *dp110* expression is sufficient to keep non-MB neuroblasts proliferating during non-feeding freshly hatched larval stages. Thus, while the nutrient-dependent cue controlling neuroblast reactivation is intact, neuroblasts with LD defects are not able to respond. Furthermore, because ectopic *dp110* is not sufficient to rescue, this suggests that membrane phospholipid composition is altered in animals with LD defects.

Next, we expressed *dp110* in glia given that PI3-kinase activation in glia positively regulates neuroblast reactivation. In contrast to neuroblast specific *dp110* expression, we found that ectopic *dp110* expression in glia led to increased neuroblast reactivation in *bmm* mutants (Fig. 3I,J). PI3-kinase in glia could promote neuroblast reactivation non-autonomously through increased Dilp although this seemed unlikely given that InR/PI3K signal reception in neuroblasts is compromised. To test this possibility, we expressed *dilp2* in glia in *bmm* mutants, but found that animals died soon after hatching from their egg casings making further analysis untenable. Alternatively, ectopic expression of *dp110* in glia could lead to intrinsic changes in cellular metabolism that promote neuroblast reactivation in a PI3-kinase independent manner. Next, we knocked down *SREBP* (Sterol regulatory element binding protein), a master regulator of lipid biosynthesis, and ACC

(Acetyl Co-A carboxylase), an enzyme that catalyzes a rate limiting step in fatty acid synthesis, in either neuroblasts or glia. When *SREBP* or *ACC* were knocked down in either neuroblasts or glia, we found reductions in neuroblast reactivation (SF3A). This suggests that lipid and fatty acid metabolism promote neuroblast reactivation in both a cell autonomous and non-autonomous manner.

Maternal diet controls neuroblast reactivation in offspring during feeding stages

Because LDs are deposited maternally, we investigated whether neuroblast reactivation during larval feeding stages could be controlled by maternal diet. We fed adults different diets to alter the amount of lipid deposited maternally into the egg (Fig. 4A). After seven days of feeding on either a BL diet or a lipid-depleted diet (LDD), we measured triglyceride (TAG) levels in adult females. LDD is composed of 10 percent yeast autolysate, 10 percent glucose and 1 percent agar [32]. Levels were reduced in females fed the LDD diet compared to the BL diet (Fig. 4G). Next, we assayed numbers of LDs in brains of their progeny at freshly hatched larval stages. We found that numbers were significantly reduced in progeny whose moms were fed a LDD diet compared to BL diet (Fig. 4B-D', H). Next, we assayed neuroblast reactivation. After 24 hours of feeding, larvae born from moms fed lipid-depleted diets had reductions in the number of EdU positive neuroblasts compared to those whose moms were fed a BL diet (Fig. 4E-F, I). We conclude that maternal lipid sources support neuroblast reactivation during feeding stages. Importantly, these results also reveal that stem cell behavior in offspring can be modulated by maternal diet.

Our work so far provides support that LDs deposited maternally and stored in neural tissues are necessary for timely reactivation of neuroblasts in response to animal feeding. Next, we asked whether neuroblasts could reactivate earlier if given access to fatty acids stored in LDs early. We knocked down Lsd-2 in neuroblasts (*worGAL4*) and in glia (*repo*). Lsd-2 protects LDs from premature lipase activity and in the absence of *Lsd-2*, animals are lean and starvation sensitive. We found an increased percentage of reactivated neuroblasts in animals expressing *Lsd-2 RNAi* in glia (Supp. Fig. 4A). We conclude that LD accessibility controls timing of neuroblast reactivation.

Discussion

In response to animal feeding, insulin-like peptides are synthesized and released both locally and systemically, leading to InR/PI3-kinase pathway activation and organism-wide increases in cell number and tissue size [15,20,21]. Beyond acquisition of nutrients through feeding, we show here that stored nutrients also control InR/PI3-kinase pathway activation on the signal receiving end (Fig. 3). During development, it is the mom that supplies lipid in the egg that will be stored in LD-form and used later to reactivate quiescent neuroblasts [22,23]. We speculate that the stored lipid controls phospholipid composition at the neuroblast plasma membrane, especially that of phosphoinositide which is needed to transmit the insulin-like peptide nutrient cue from InR to downstream pathway effectors. We find that neuroblast reactivation can be modulated by maternal diet, underscoring the need for better understanding of diet makeup and its impacts on development, as well as maternal health and wellness. In fact, fatty acids acquired through diet strongly influence the phospholipid composition of membranes in tissues

throughout the animal [24]. In diapause mouse embryos and in quiescent mammalian neural stem cells, stored lipids are used as the primary energy source [25]. Whether free fatty acids or LD numbers somehow trigger quiescence remains unclear, yet it is clear that free fatty acids are required for stem cell maintenance and reactivation from both quiescence and diapause across a range of animal species. When yeast from the stationary phase are transferred to fresh medium and proliferation induced, LDs are consumed rapidly supporting proliferation and increases in cell numbers [26]. What controls LD breakdown in quiescent stem cells including *Drosophila* neuroblasts is unclear, however exercise and caloric restriction can both trigger LD break down and both lead to increased neurogenesis in adult rodents.

Materials and methods

Drosophila strains, genetics, and staging

All animals were raised in uncrowded conditions at 25˚C on BL food in control light dark cycles unless stated otherwise. The following stocks were used: *Oregon R (OR), bmm*^{1}, *Hsl*^{1}, *jabba*^{DL}, *jabba*^{DL}, *Lsd2*^{KG00149}, *klar*^{YG3}, *UAS-Lsd2RNAi*, *UAS-bmmRNAi*, UAS-*SREBPRNAi*, UAS-*apoLppRNAi*, *UASFABPRNAi*, *UAS-ACCRNAi*, *UAS-bmm*, *UAS-N-Venus-PH-GRP*, *UAS-C-Venus-PH-GRP*, UAS-mCD8GFP, *worGAL4*, *NP0577GAL4*, *repoGAL4*, *r4GAL4*

Diets

The BL diet used was commercially purchased from Archon Scientific and is referenced as the W1 recipe. The lipid depleted (LDD) diet consisted of 10% yeast autolysate (Sigma), 10% glucose, and 1% agar.

Triglyceride and protein measurements

After feeding on BL or LDD diets for seven days, single adult females were sonicated three times for 10 seconds each time in 140 mM NaCl, 50 mM Tris-HCl, pH 7.4, 0.1% Triton X-100 with protease inhibitors (Roche). Following clearing by centrifugation at 4°C, supernatants were transferred to new tubes. Triglyceride (Liquicolor Test, Stanbio) and protein (BCA assay, Pierce) were measured in each sample, and triglyceride levels were normalized to protein levels.

Immunofluorescence and confocal imaging

Larval brains were fixed and stained as previously described. In brief, larval brains were dissected and fixed in 4% EM grade formaldehyde in PEM (Pipes, EGTA, Magnesium chloride) buffer with 0.1% Triton-X for 20 mins. Tissues were washed in 1X PBT with 0.1% TritonX-100 and blocked overnight at 4˚C in 1X PBT with 10% normal goat serum. Primary antibodies used in this study include: chicken anti-GFP (1:500, Abcam), rat anti-Deadpan (1:100, Abcam), rabbit anti-Scribble (1:1000), mouse anti-Repo (1:5, DSHB, 8D12), guinea-pig anti-InR (1:300), rabbit anti-Dilp2 (1:1000). Primary antibodies were detected using Alexa Fluor-conjugated secondary antibodies. LDs were detected using Nile Red. Brains were imaged using a Leica SP8 laser scanning confocal microscope equipped with a 63X, 1.4 NA oil-immersion objective. For glia surface measurements, Z

stacks were acquired at 0.5 µm steps using the same confocal settings. All other confocal data were collected at 1.0 µm steps. Images were processed using Fiji.

EdU labeling and LD staining

For EdU labeling, animals were fed 0.1mg/ml EdU mixed in with BL food and animals fed for designated amounts of time. LDs were detected using Nile Red applied for 30 mins. at a concentration of 500 ug/ml after the secondary antibody washes.

Quantification of neuroblast EdU number, LD number, and glia membrane surface area

For neuroblast EdU quantification, the number of EdU-positive, Dpn-positive neuroblasts were counted using the “cell counter” plugin in Fiji and divided by the total number of Dpn-positive neuroblasts. Neuroblast diameter was calculated based on the average length of two perpendicular lines drawn through the center of the neuroblast at its widest point. Custom Fiji plugins were used to quantify both LD number and glial membrane surface area. The top 50 µms from the dorsal surface were analyzed. To count the number of lipid droplets we used MaxEntropy thresholding with a minimum object size to be 11 voxels and maximum object size set at 1000 voxels based on a set image size. For glial membrane, moments thresholding was used.

Statistical analysis

Student’s t-tests and one-way ANOVAs were performed using Prism 10. For box plots, the boundary of the box closest to zero indicates the 25th percentile, a line within the box marks the median, and the boundary of the box farthest from zero indicates the 75th

percentile. Whiskers (error bars) above and below the box indicate the maximum and minimum, respectively. The data in plots and the text are presented as means ± SEM.

Figures:

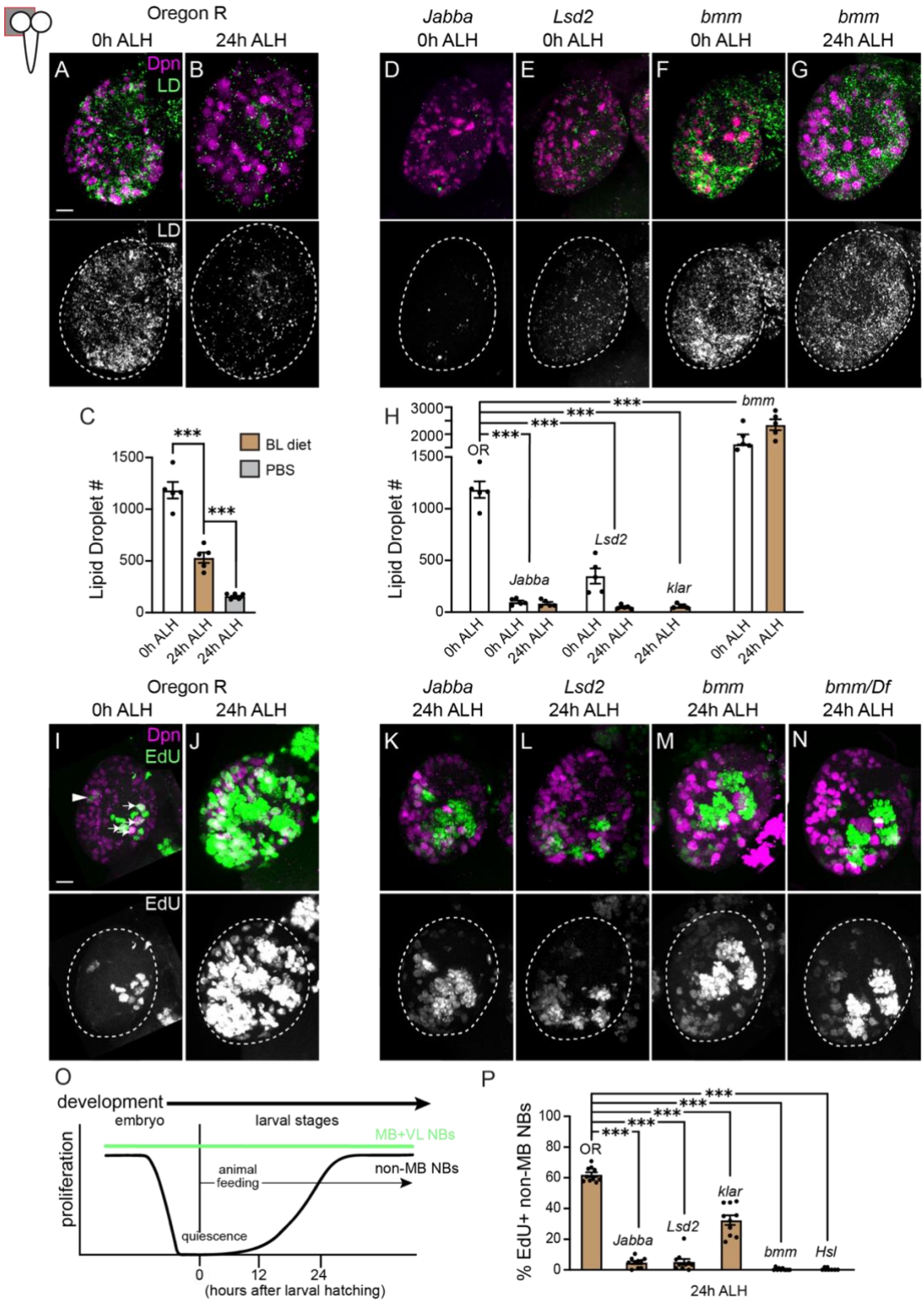
Oregon R
0h ALH
24h ALH
A
Dpn
LD
B
LD
Jabba
0h ALH
Lsd2
0h ALH
bmm
0h ALH
bmm
24h ALH
D
E
F
G
C
***
***
BL diet
PBS
Lipid Droplet #
1500
1000
500
0
0h ALH
24h ALH
24h ALH
H
3000
2000
1500
1000
500
0
***
***
***
***
bmm
OR
Jabba
Lsd2
klar
Lipid Droplet #
0h ALH
0h ALH
24h ALH
0h ALH
24h ALH
24h ALH
0h ALH
24h ALH
Oregon R
0h ALH
24h ALH
I
Dpn
EdU
J
EdU
Jabba
24h ALH
Lsd2
24h ALH
bmm
24h ALH
bmm/Df
24h ALH
K
L
M
N
O
development
embryo
larval stages
MB+VL NBs
non-MB NBs
animal
feeding
proliferation
quiescence
0
12
24
(hours after larval hatching)
P
***
***
***
***
***
100
80
60
40
20
0
% EdU+ non-MB NBs
OR
Jabba
Lsd2
klar
bmm
Hsl
24h ALH

Figure 1: Lipid droplet consumption correlates with neuroblast reactivation.

(A,B, D-G) Maximum intensity projections (MIPs) of single brain hemispheres. Cartoon upper left depicts image location (gray highlight) in panels: anterior is to the top, and midline, right. Time points and genotypes listed above and markers within panels in this and all subsequent figures. Dpn (Deadpan), a transcription factor, labels neuroblasts and Nile Red, Lipid droplets (LD). Top panels, colored overlays with grayscale images below with brain hemispheres outlined. (C,H) Quantification of LD number in OR and mutant animals at different times and different conditions: a white colored column in this and all subsequent histograms denotes no food, brown denotes Bloomington food (BL), and gray, Phosphate buffered saline (PBS) only. (I-N) MIPs of single brain hemispheres after EdU feeding on PBS only for 3 hours (I) or on BL food for 24 hours (J-N) with quantification (P). Top panels, colored overlays with grayscale images below. (O) Timeline of neuroblast entry into quiescence and exit from quiescence in response to BL feeding. MB (mushroom body, four per brain hemisphere, arrows in I) and the single VL (ventro-lateral, arrowhead in I) neuroblasts divide continually during the embryonic to larval transition. Each data point (C,H,P) represents one brain hemisphere from one animal. Mean and SEM. ***$p \leq 0.001$ (Student two-tailed t-test). Scale bar (A,I) equals 10 micrometers.

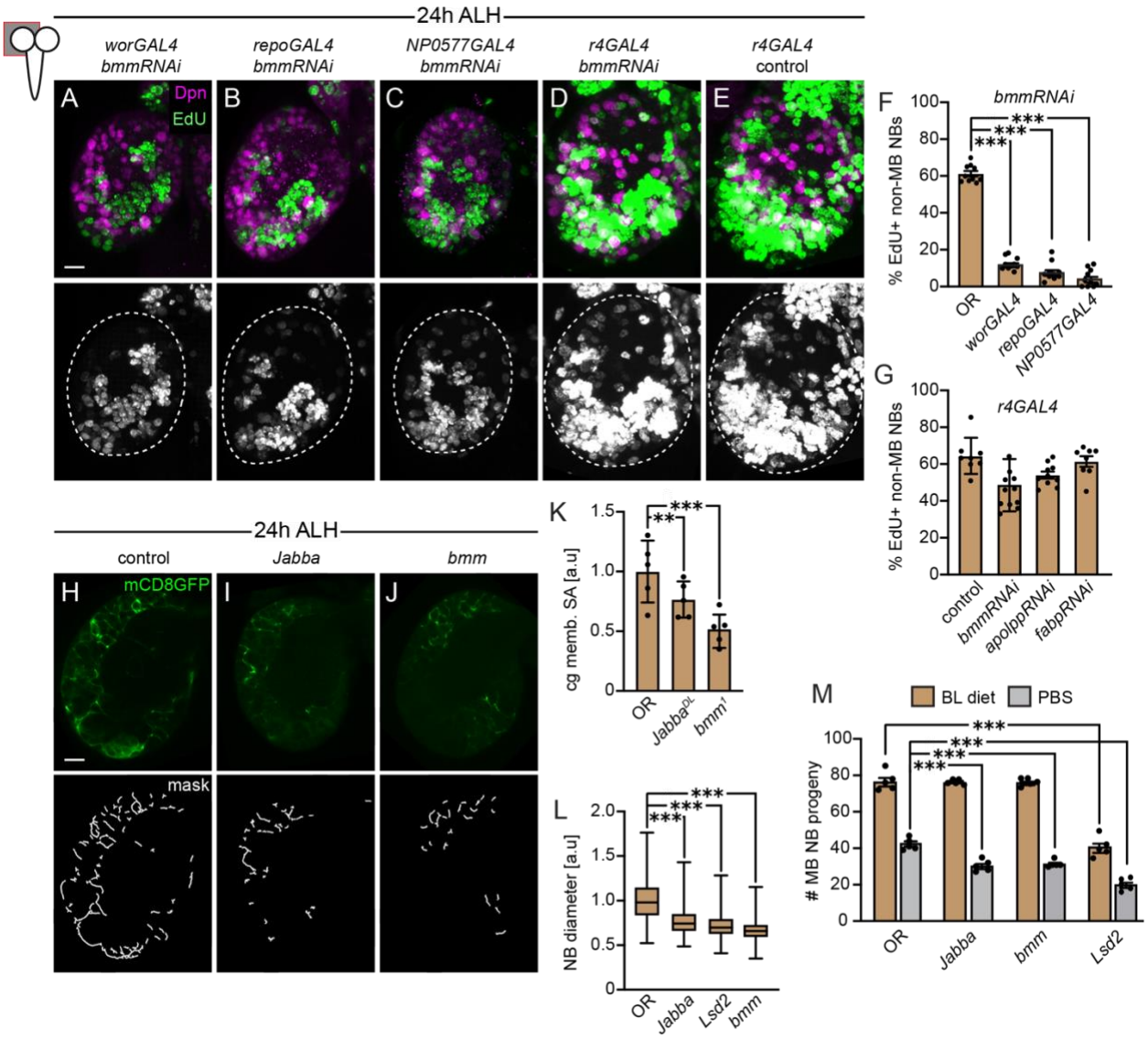

Figure 2: Maternally deposited brain LDs promote early neural tissue growth during feeding stages.

(A-E) MIPs of single brain hemispheres. Cartoon upper left depicts image location (gray highlight) in panels. Time points and genotypes listed above and markers within panels. Top, colored overlay with grayscale image below with brain hemispheres outlined. (F,G) Percentage of non-MB NBs that are EdU positive after 24 hours of BL feeding. (H-J)

Single optical sections of brain hemispheres. Top panels membrane tagged GFP driven by *NP0577GAL4* (cortex glia) and bottom panels are masks used in quantification (K). (L) Neuroblast size based on diameter. Each box and whiskers represent 150 neuroblasts quantified from three brain hemispheres from three animals (50 each). (M) Number of MB neuroblast progeny that are EdU positive after 24 hours of BL or PBS feeding. Each data point (F,G,K,M) represents one brain hemisphere from one animal. Mean and SEM. ***p≤0.001 (Student two-tailed t-test). Scale bar (A,H) equals 10 micrometers. [a.u], arbitrary unit.

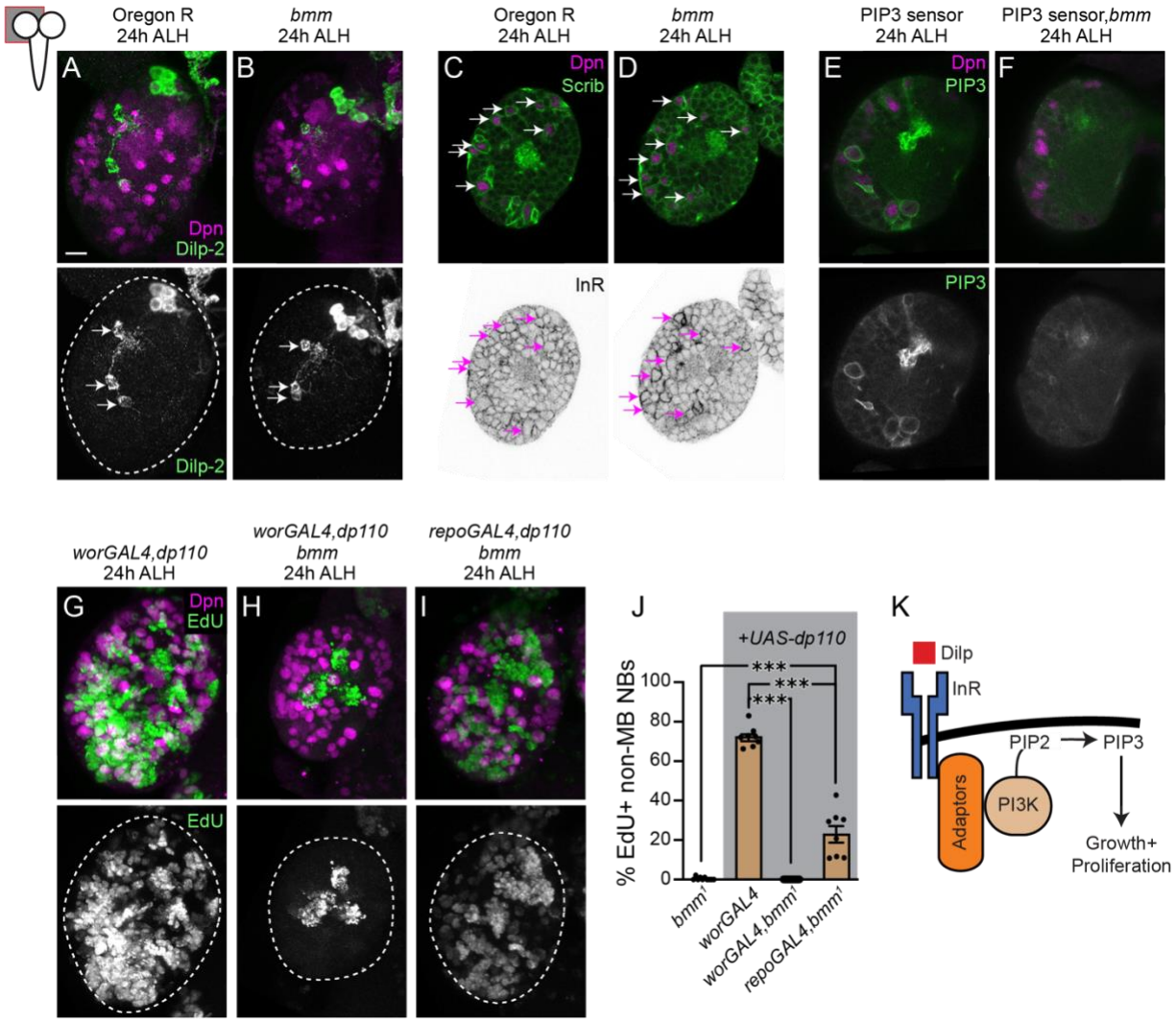

Figure 3: Maternal LDs control reception of Dilp nutrient signals.

(A-B) MIPs of single brain hemispheres. Cartoon upper left depicts image location (gray highlight) in panels. Time points and genotypes listed above and markers within panels. Top, colored overlay with grayscale image below with brain hemispheres outlined. Arrows point to the DRNs (Dilp-2 recruiting neurons) which capture Dilps released from IPCs. (C,D) Single Z images. Top, colored overlay and below same Z with inverted grayscale

image showing InR labeling. Arrows point to neuroblasts and in *bmm* mutants, neuroblasts have higher InR compared to OR animals. (E,F) Single Zs with colored overlay (top) and grayscale image. (G-I) MIPs of single brain hemispheres after EdU feeding on BL food for 24 hours with quantification (J). Top panels, colored overlays with grayscale images below. Each data point (J) represents one brain hemisphere from one animal. (K) Schematic of InR/PI3-kinase signaling pathway. Mean and SEM. ***p≤0.001 (Student two-tailed t-test). Scale bar (A) equals 10 micrometers and all images scaled to panel A.

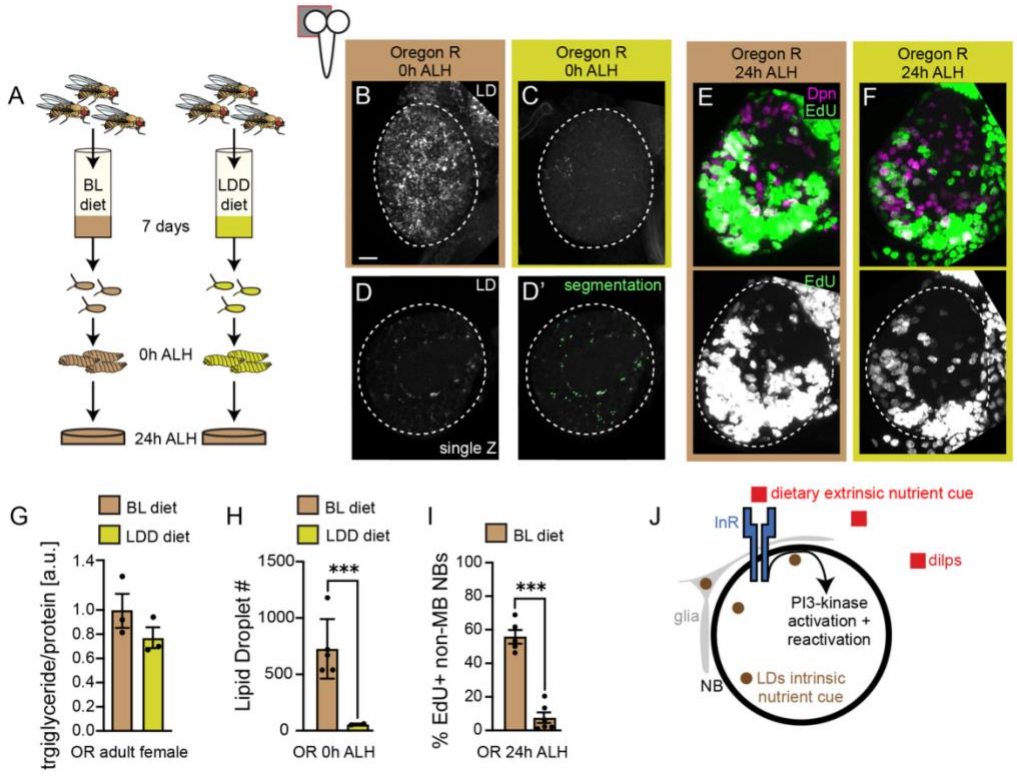

Figure 4: Maternal diets control neuroblast reactivation during larval feeding stages.

(A) Schematic of feeding paradigm. One day old adults were transferred and maintained on designated diets for seven days. Eggs were collected and larvae allowed to hatch. Freshly hatched larvae from animals fed different diets were placed on the same diet as larvae. (B,C) MIPs of single brain hemispheres of freshly hatched larvae (0h ALH) collected from adults fed different diets. Cartoon upper left depicts image location (gray highlight) in panels. LD image alone with brain hemispheres outlined. (D, D') Example of LD segmentation used for quantification with single Z grayscale image on left with LD segmentation (green) overlay on right. (E,F) MIPs of single brain hemispheres after EdU

feeding on BL food for 24 hours. Top panels, colored overlays with grayscale images below with brain hemispheres outlined. (G) Normalized TAG levels in single adult females after seven days on designated diets. Each data point is one female. (H) Quantification of LD numbers in brain hemispheres. Each data point represents one brain hemisphere from one animal. (I) Quantification of EdU positive neuroblasts after feeding on a BL diet. Each data point represents one brain hemisphere from one animal. Mean and SEM. ***p≤0.001 (Student two-tailed t-test). Scale bar (B) equals 10μms and all images scaled to panel B. (J) Model.

Supplementary Figures:

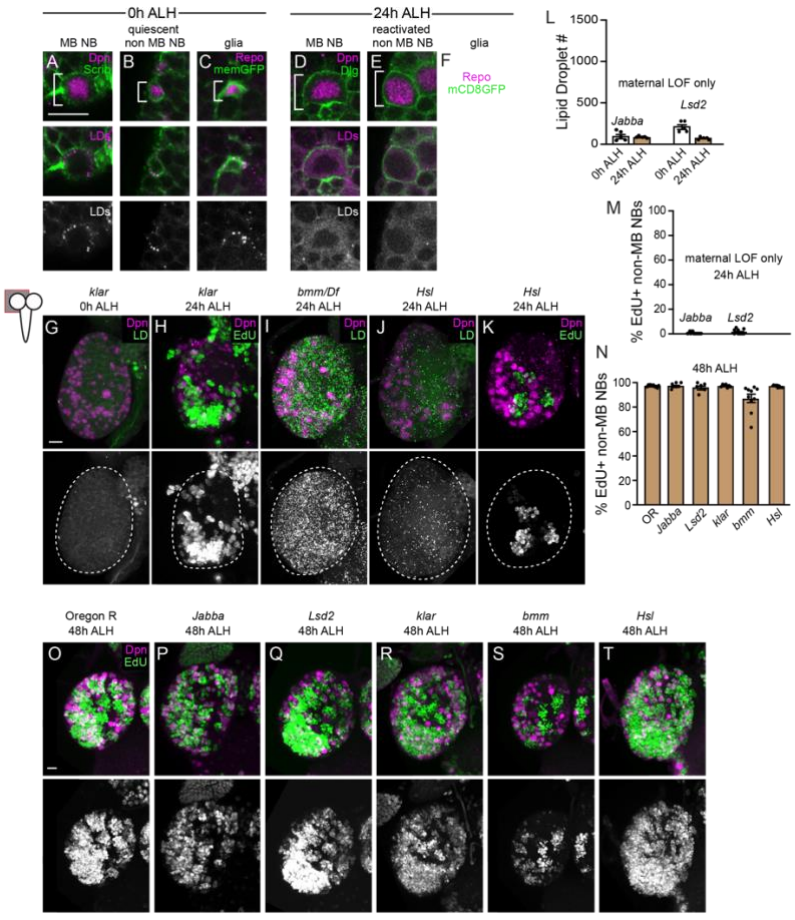

Supplemental Figure 1: Related to Figure 1, Lipid droplet consumption correlates with neuroblast reactivation.

(A-F) Single Z images of the distribution of LDs in neuroblasts (non-MB neuroblasts and MB neuroblasts) and in glia at 0h ALH and 24 hours later. (G-K) MIPs of single brain hemispheres. Cartoon upper left depicts image location (gray highlight) in panels. Time points and genotypes listed above and markers within panels. Top panels, colored overlays with grayscale images below with brain hemispheres outlined. (L) Quantification of LD number and (M) EdU percentage in maternal mutants with wildtype zygotic

(paternal) gene copy. Each data point represents one brain hemisphere from one animal. Mean and SEM. ***p≤0.001 (Student two-tailed t-test). (N) Quantification of EdU percentage at 48 hours ALH in BL fed animals. Genotypes listed below and each data point represents one brain hemisphere from one animal. Mean and SEM. ***p≤0.001 (Student two-tailed t-test). (O-T) MIPs of single brain hemispheres. Time points and genotypes listed above and markers within panels. Top panels, colored overlays with grayscale images below with brain hemispheres outlined. Scale bars in panels A, G, O equal 10 micrometers. Panels B-E scaled to A, panels H-K scaled to G, and panels P-T scaled to O.

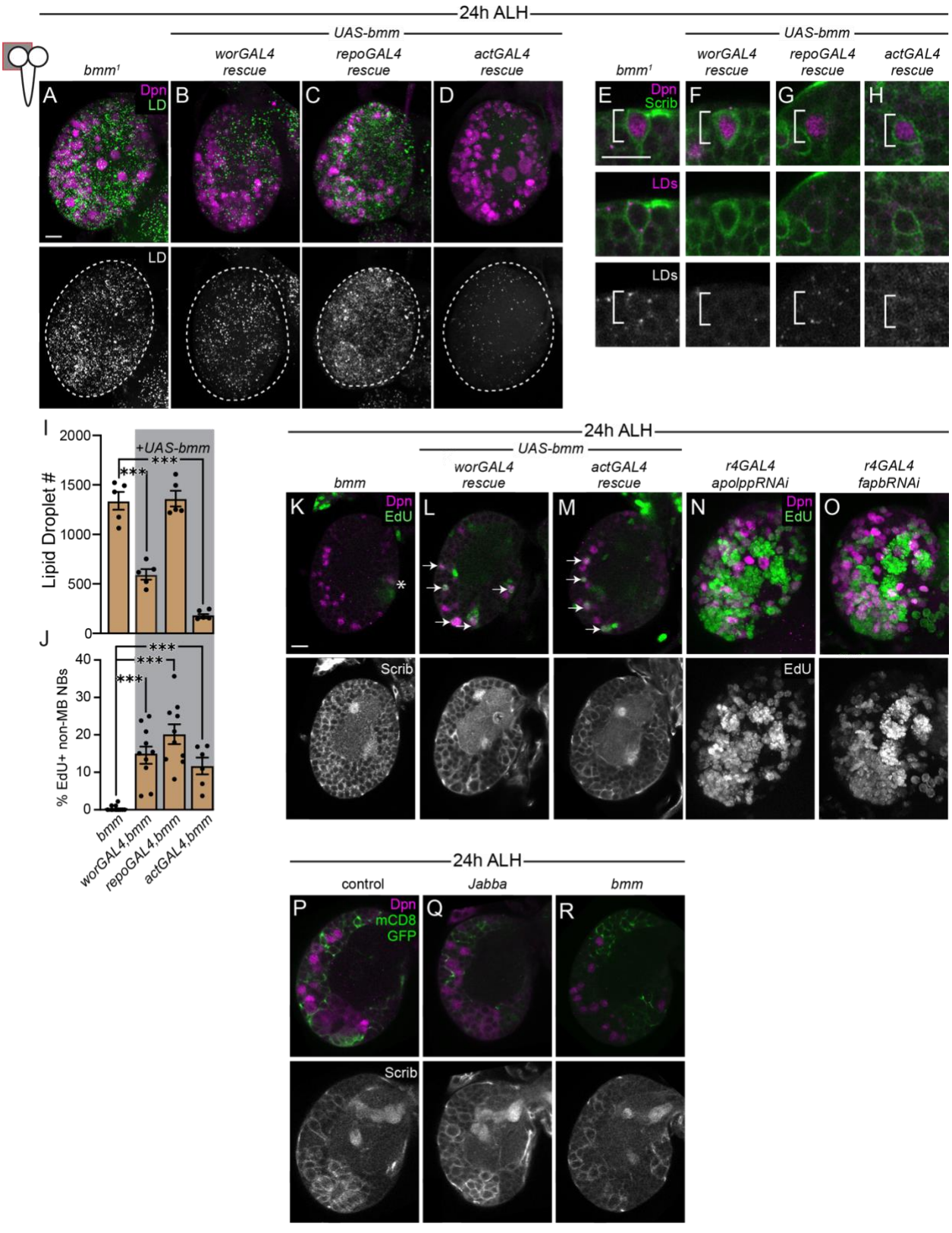
24h ALH
UAS-bmm
bmm¹
worGAL4 rescue
repoGAL4 rescue
actGAL4 rescue
A
Dpn
LD
B
C
D
LD
E
Dpn
Scrib
F
G
H
LDs
LDs
I
Lipid Droplet #
2000
1500
1000
500
0
+UAS-bmm
***
***
J
% EdU+ non-MB NBs
40
30
20
10
0
***
***
***
bmm
worGAL4,bmm
repoGAL4,bmm
actGAL4,bmm
24h ALH
UAS-bmm
bmm
worGAL4 rescue
actGAL4 rescue
r4GAL4 apolppRNAi
r4GAL4 fapbRNAi
K
Dpn
EdU
L
M
N
Dpn
EdU
O
Scrib
EdU
24h ALH
control
Jabba
bmm
P
Dpn
mCD8
GFP
Q
R
Scrib

Supplemental Figure 2: Related to figure 2, Maternally deposited brain LDs promote early neural tissue growth during feeding stages.

(A-D) MIPs of single brain hemispheres. Cartoon upper left depicts image location in panels. Time points and genotypes listed above and markers within panels in this and all subsequent figures. All are homozygous *bmm* mutants. Top panels, colored overlays with grayscale images below with brain hemispheres outlined. (E-H) High mag single Z images of neuroblasts in *bmm* rescue animals. All are cell type specific rescue in the *bmm* homozygous mutant background. White brackets indicate neuroblasts. Top panel colored overlay with grayscale images below. (I) Quantification of LD number and quantification of EdU percentages (J) in different rescue backgrounds. Each data point represents one brain hemisphere from one animal. Mean and SEM. ***p≤0.001 (Student two-tailed t-test). (K-O) MIPs of single brain hemispheres. Time points and genotypes listed above and markers within panels. Top panels, colored overlays with grayscale images below with brain hemispheres outlined. Scale bars are 10 μms and B-D scaled relative to A, panel F-H scaled to E, and panel L-R scaled to K.

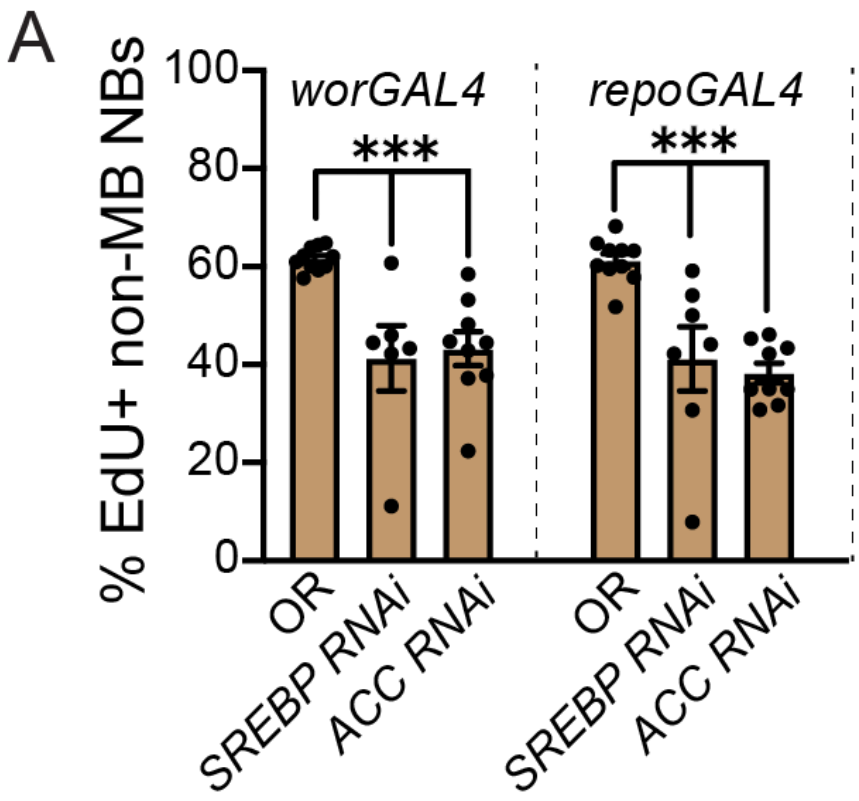

Supplemental Figure 3: Related to figure 3, Maternal LDs control reception of Dilp nutrient signals.

(A) Quantification of the percentage of EdU positive neuroblasts after 24 hours of BL feeding. Genotypes listed below and GAL4 drivers above. Each data point represents one brain hemisphere from one animal. Mean and SEM. ***p≤0.001 (Student two-tailed t-test).

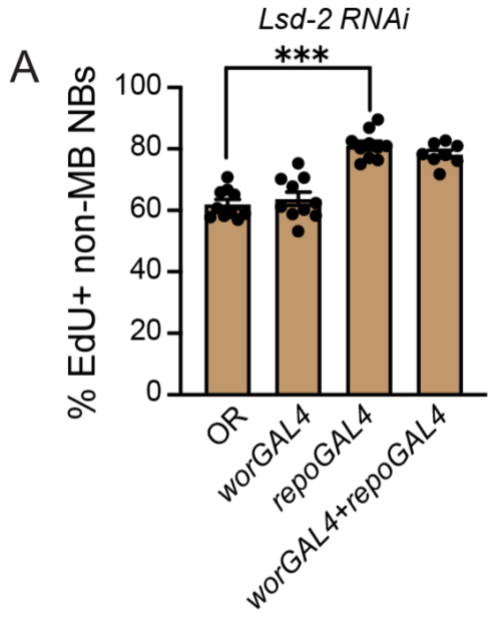

Supplemental Figure 4: Related to figure 4, Maternal diets control neuroblast reactivation during larval feeding stages.

(A) Quantification of the percentage of EdU positive neuroblasts after 24 hours of BL feeding. Genotypes listed below and GAL4 drivers above. Each data point represents one brain hemisphere from one animal. Mean and SEM. ***p≤0.001 (Student two-tailed t-test).

References:

1. Parra-Peralbo E, Culi J. Drosophila Lipophorin Receptors Mediate the Uptake of Neutral Lipids in Oocytes and Imaginal Disc Cells by an Endocytosis-Independent Mechanism. *PLOS Genet*. 2011;7(2):e1001297. doi:10.1371/journal.pgen.1001297
2. Truman JW, Bate M. Spatial and temporal patterns of neurogenesis in the central nervous system of Drosophila melanogaster. *Dev Biol*. 1988;125(1):145-157. doi:10.1016/0012-1606(88)90067-x
3. Kimmel CB, Ballard WW, Kimmel SR, Ullmann B, Schilling TF. Stages of embryonic development of the zebrafish. *Dev Dyn Off Publ Am Assoc Anat*. 1995;203(3):253-310. doi:10.1002/aja.1002030302
4. Roberts A, Blight AR. Anatomy, physiology and behavioural rôle of sensory nerve endings in the cement gland of embryonic xenopus. *Proc R Soc Lond B Biol Sci*. 1975;192(1106):111-127. doi:10.1098/rspb.1975.0153
5. Hartenstein V. The neuroendocrine system of invertebrates: a developmental and evolutionary perspective. *J Endocrinol*. 2006;190(3):555-570. doi:10.1677/joe.1.06964
6. Padilla PA, Ladage ML. Suspended animation, diapause and quiescence. *Cell Cycle*. 2012;11(9):1672-1679. doi:10.4161/cc.19444
7. Brown DD, Cai L. Amphibian metamorphosis. *Dev Biol*. 2007;306(1):20-33. doi:10.1016/j.ydbio.2007.03.021
8. Tennessen JM, Thummel CS. Coordinating growth and maturation - insights from Drosophila. *Curr Biol CB*. 2011;21(18):R750-757. doi:10.1016/j.cub.2011.06.033
9. Urbán N, Guillemot F. Neurogenesis in the embryonic and adult brain: same regulators, different roles. *Front Cell Neurosci*. 2014;8:396. doi:10.3389/fncel.2014.00396
10. Bestman JE, Cline HT. The RNA binding protein CPEB regulates dendrite morphogenesis and neuronal circuit assembly in vivo. *Proc Natl Acad Sci U S A*. 2008;105(51):20494-20499. doi:10.1073/pnas.0806296105
11. Spéder P, Liu J, Brand AH. Nutrient control of neural stem cells. *Curr Opin Cell Biol*. 2011;23(6):724-729. doi:10.1016/j.ceb.2011.08.004
12. Cavallucci V, Fidaleo M, Pani G. Neural Stem Cells and Nutrients: Poised Between Quiescence and Exhaustion. *Trends Endocrinol Metab*. 2016;27(11):756-769. doi:10.1016/j.tem.2016.06.007
13. Britton JS, Edgar BA. Environmental control of the cell cycle in Drosophila: nutrition activates mitotic and endoreplicative cells by distinct mechanisms. *Dev Camb Engl*. 1998;125(11):2149-2158. doi:10.1242/dev.125.11.2149
14. Chell JM, Brand AH. Nutrition-responsive glia control exit of neural stem cells from quiescence. *Cell*. 2010;143(7):1161-1173. doi:10.1016/j.cell.2010.12.007
15. Yuan X, Sipe CW, Suzawa M, Bland ML, Siegrist SE. Dilp-2–mediated PI3-kinase activation coordinates reactivation of quiescent neuroblasts with growth of their glial stem cell niche. *PLoS Biol*. 2020;18(5):e3000721. doi:10.1371/journal.pbio.3000721
16. Nässel DR, Vanden Broeck J. Insulin/IGF signaling in Drosophila and other insects: factors that regulate production, release and post-release action of the insulin-like peptides. *Cell Mol Life Sci CMLS*. 2016;73(2):271-290. doi:10.1007/s00018-015-2063-3
17. Bai H, Kang P, Tatar M. Drosophila insulin-like peptide-6 (dilp6) expression from fat body extends lifespan and represses secretion of Drosophila insulin-like peptide-2 from the brain. *Aging Cell*. 2012;11(6):978-985. doi:10.1111/acel.12000
18. Manning BD, Toker A. AKT/PKB Signaling: Navigating the Network. *Cell*. 2017;169(3):381-405. doi:10.1016/j.cell.2017.04.001
19. Leevers SJ, Weinkove D, MacDougall LK, Hafen E, Waterfield MD. The Drosophila phosphoinositide 3-kinase Dp110 promotes cell growth. *EMBO J*. 1996;15(23):6584-6594.
20. Murphy DJ. The dynamic roles of intracellular lipid droplets: from archaea to mammals. *Protoplasma*. 2012;249(3):541-585. doi:10.1007/s00709-011-0329-7

21. Olzmann JA, Carvalho P. Dynamics and functions of lipid droplets. *Nat Rev Mol Cell Biol*. 2019;20(3):137-155. doi:10.1038/s41580-018-0085-z
22. Liu L, Zhang K, Sandoval H, et al. Glial lipid droplets and ROS induced by mitochondrial defects promote neurodegeneration. *Cell*. 2015;160(1-2):177-190. doi:10.1016/j.cell.2014.12.019
23. Xie M, Roy R. AMP-Activated Kinase Regulates Lipid Droplet Localization and Stability of Adipose Triglyceride Lipase in C. elegans Dauer Larvae. *PLOS ONE*. 2015;10(6):e0130480. doi:10.1371/journal.pone.0130480
24. Zhang W, Xu L, Zhu L, Liu Y, Yang S, Zhao M. Lipid Droplets, the Central Hub Integrating Cell Metabolism and the Immune System. *Front Physiol*. 2021;12. doi:10.3389/fphys.2021.746749
25. Sipe CW, Siegrist SE. Eyeless uncouples mushroom body neuroblast proliferation from dietary amino acids in Drosophila. *eLife*. 6:e26343. doi:10.7554/eLife.26343
26. Brogiolo W, Stocker H, Ikeya T, Rintelen F, Fernandez R, Hafen E. An evolutionarily conserved function of the Drosophila insulin receptor and insulin-like peptides in growth control. *Curr Biol CB*. 2001;11(4):213-221. doi:10.1016/s0960-9822(01)00068-9
27. Welte MA. As the fat flies: The dynamic lipid droplets of Drosophila embryos. *Biochim Biophys Acta BBA - Mol Cell Biol Lipids*. 2015;1851(9):1156-1185. doi:10.1016/j.bbalip.2015.04.002
28. Kilwein MD, Dao TK, Welte MA. Drosophila embryos allocate lipid droplets to specific lineages to ensure punctual development and redox homeostasis. *PLoS Genet*. 2023;19(8):e1010875. doi:10.1371/journal.pgen.1010875
29. Carvalho M, Sampaio JL, Palm W, Brankatschk M, Eaton S, Shevchenko A. Effects of diet and development on the Drosophila lipidome. *Mol Syst Biol*. 2012;8(1):600. doi:10.1038/msb.2012.29
30. Knobloch M, Jessberger S. Metabolism and neurogenesis. *Curr Opin Neurobiol*. 2017;42:45-52. doi:10.1016/j.conb.2016.11.006
31. Kurat CF, Wolinski H, Petschnigg J, et al. Cdk1/Cdc28-Dependent Activation of the Major Triacylglycerol Lipase Tgl4 in Yeast Links Lipolysis to Cell-Cycle Progression. *Mol Cell*. 2009;33(1):53-63. doi:10.1016/j.molcel.2008.12.019
32. Carvalho M, Schwudke D, Sampaio JL, et al. Survival strategies of a sterol auxotroph. Development. 2010;137(21):3675-3685. doi:10.1242/dev.044560

Chapter 3

The microtubule-associated protein Toucan (Toc) controls neural stem cell asymmetric cell division (ACD) in *Drosophila*

Abstract:

Microtubule-associated proteins (MAPs) are evolutionarily conserved from yeast to humans and play critical roles during cell division, including metaphase plate formation, chromosome segregation, and cytokinesis. Our research demonstrates that the microtubule-binding protein Toucan (Toc) is essential for the proliferation of neuroblasts (NBs) in the *Drosophila* brain. In Toc mutant larval brains, quiescent NBs fail to re-enter the cell cycle, while mushroom body (MB) NBs exit the cell cycle and exhibit defects in their asymmetric cell division. Loss of Toc causes nuclear accumulation of Prospero in the MB NBs and leads to their terminal differentiation.

Introduction:

Asymmetric cell division (ACD) is an evolutionarily conserved proliferation mechanism used by stem and progenitor cells across various tissue types. This process enables these cells to self-renew the progenitor pool while producing differentiated progenies. To create two different cell types after cell division, a cell-determining factor, such as a protein or RNA, must be asymmetrically partitioned into only one of the two daughter cells post-cytokinesis. This typically occurs through the alignment of the mitotic spindle orthogonal to the cell-determining factor [1–3]. Although many proteins are known

to control the mechanics of ACD, several questions remain unanswered. Notably, it is still unclear how the mitotic spindle communicates with the cell cortex to achieve both spindle positioning and the asymmetric segregation of cell fate determinants.

Neural stem and progenitor cells (NSPCs) predominantly use ACD to sustain their population while producing diverse types of neurons and glial cells throughout development. *Drosophila* neural stem cells, known as neuroblasts (NBs), are an excellent model system for studying the mechanism of ACD. NBs divide asymmetrically, self-renewing the stem cell pool while simultaneously producing a smaller daughter cell that differentiates into a neuron or glial cell. This process involves several steps: establishing an apical-basal polarity axis, aligning the microtubule spindle along this polarity axis, and segregating the basal cell fate determinant proteins into the smaller daughter cell before cytokinesis [1]. The evolutionarily conserved apical Par complex proteins are crucial for proper mitotic spindle orientation and the segregation of the cell fate determinants Numb, Miranda, and Prospero to the basal cortex. The Par complex protein aPKC phosphorylates Miranda and Numb, which is critical for their basal cortical localization [4–9]. Proper mitotic spindle alignment along the NBs' apical-basal axis is essential for the correct segregation of cell fate-determining factors. NBs with misoriented mitotic spindles fail to segregate polarity proteins and divide symmetrically [10]. Although this is the current model mediating unequal segregation, it still remains unclear exactly how the NB intrinsic polarity cues interact with the microtubule network to segregate basal cell fate determinants.

The neuroblast daughter cell that inherits the basal polarity proteins is known as a ganglion mother cell (GMC) and is smaller in size compared to the neuroblast mother cell

[1,9]. This physical size asymmetry is presumably achieved by positioning the cleavage furrow asymmetrically during mitosis. Experiments in *Drosophila* spermatocytes and S2 cells have demonstrated that a stable population of spindle microtubules determines the site of cleavage furrow positioning. According to this model, microtubule-associated proteins (MAPs), such as Pavarotti (Pav) and Tumbleweed (Tum), travel along central spindle microtubules and activate RhoA kinase signaling at their point of contact at the NB cortex, thereby determining the point of cleavage furrow positioning [11–13]. MAPs play key roles throughout mitosis, and their loss causes defects in spindle formation and cytokinesis [11,13–17]. While the microtubule network is crucial during ACD in NBs, cleavage furrows can still form even in their absence or dysfunction. A recent experiment showed that misorientation of the mitotic spindle in NBs leads to the appearance of two cleavage furrows instead of one. The first cleavage furrow appears at the original basal cortex, and the second one emerges centered on the newly positioned central spindle [10,18,19]. This observation suggests that NB intrinsic polarity cues and spindle microtubules complement each other in cleavage furrow positioning and achieving physical cell size asymmetry in NB daughter cells.

Here, we report the identification of a microtubule-associated protein, Toucan (Toc), in controlling the asymmetric cell division of a subset of neuroblasts, specifically mushroom body neuroblasts (MB NBs). Toc was first reported to be expressed in the germline, where it plays a key role in somatic cell patterning during oogenesis [20]. An antibody raised against the N terminus of the Toc protein revealed that Toc localized to microtubules [21]. Toc is a microtubule-associated protein (MAP) and, during embryonic

syncytial nuclear division, colocalizes with the microtubule network throughout all phases of mitosis. It was also reported that Toc is maternally deposited and becomes depleted by maternal embryonic stage 14 [22,23]. We have found that Toc is also expressed in the larval brain. In the absence of Toc, non-MB NBs fail to reactivate from developmental quiescence, and MB NBs stop proliferating within the first 24 hours after larval hatching (ALH). Additionally, Toc mutant MB NBs exhibit cytokinesis defects and fail to segregate basal cell fate determinant proteins Miranda, Prospero, and Numb. As a result, most MB NBs terminally differentiate with elevated levels of nuclear Prospero.

Results

Identification of *toucan (toc)* as a gene involved in NB proliferation

We were initially focused on exploring the impact of lipid metabolism on neuroblast (NB) proliferation in the *Drosophila* brain during the early stages of larval development using an allele of the *midway* gene called mdy^{QX25}. Midway (Mdy) converts DAG to TAG in *Drosophila.* We found that mutant larvae homozygous for the mdy^{QX25} allele died by 48 hours ALH. Upon examination of the brains of mdy^{QX25} mutant larvae, we found that the non-MB NBs in freshly hatched mdy^{QX25} mutant larval brains failed to reactivate from developmental quiescence. Additionally, MB NBs stopped proliferation by 24 hours ALH and most of them were binucleate. By 40 hours ALH, most of the MB NBs had terminally differentiated and showed nuclear accumulation of Prospero. Interestingly, we failed to replicate the mutant phenotypes when we crossed the mdy^{QX25} line with a deficiency line of *midway* (*Df(2L)Exel6039*, BDSC #7522). Because the mdy^{QX25} allele was generated using ethyl methane sulfonate (EMS) mutagenesis, we reasoned that the chromosome likely carried additional background mutations which were responsible for the observed

phenotypes. We isolated the unknown gene causing larval lethality and NBs cytokinesis defects from the original *mdy*^{QX25} allele and named it *toc*^{9}. We decided to identify the unknown gene of interest by using the meiotic mapping technique (chapter 3, Fly pushing book). We used fly lines *al[1] dpy[ov1] b[1] pr[1] c[1] px[1] speck[1]* and *al[1] dpy[ov1] b[1] pr[1] Bl[1] c[1] px[1] speck[1]/SM1* from the Bloomington *Drosophila* Stock Center (BDSC) for this purpose. By following the meiotic mapping technique, we were able to narrow down the location of the unknown gene of interest to somewhere between the alleles *al*^{1} and *dpy*^{ov1} **(Fig. 3.1 G, a)**, which encompass about 4 million base pairs of genomic DNA in chromosome 2L. Next, we acquired 18 individual deficiency lines from BDSC that together cover the entire 4 million base pairs **(Fig. 3.1 G, b)**. We crossed the deficiency lines with original *mdy*^{QX25} line and screened for the homozygous lethality phenotype at 48 hours ALH. Only deficiency line *Df(2L)ED4651/SM6a* when crossed with *mdy*^{QX25} showed larval lethality at 48 hours ALH and NBs at 40h ALH displayed the distinctive cytokinesis and differentiation phenotype **(Fig 3.1 A)**. *Df(2L)ED4651/SM6a* covers almost 0.6 million base pairs and 100 genes. We narrowed down the location of our unknown gene of interest by using smaller deficiency lines covering the entire 0.6 million base pairs deleted in *Df(2L)ED4651/SM6a* **(Fig. 3.1 G, c)**. One of these smaller deficiency lines *Df(2L)BSC238/CyO* , when crossed with mdy^{QX25} allele, replicated all the aforementioned phenotypes and thus possibly had our unknown gene of interest deleted in it **(Fig 3.1 B)**. *Df(2L)BSC238/CyO* covered 15 genes and by literature search we narrowed our list of target genes to three genes; *glaikit* (*gkt*), *Mothers against dpp* (*Mad*) and *toucan* (*toc*). We acquired individual mutant alleles for *gkt*, *Mad* and *toc* from BDSC. When the *toc* allele *toc*$^{A1-1}$ was crossed with *Df(2L)BSC238/CyO* and *toc*^{9}, the larvae died by 48 hours

ALH and the MB NBs were binucleate and terminally differentiated with nuclear Pros. We conclude that *toc* is most likely our unknown gene of interest **(Fig 3.1 C-E)**.

Toucan, a microtubule-associated protein, regulates ACD in MB NBs

We used the previously generated N-terminal Toc antibody that was reported to detect the maternal Toc in egg chambers and early staged embryos. We asked whether we could detect Toc in the freshly hatched larval brain using this antibody. Unfortunately, we failed to detect Toc in larval brains using this antibody (data not shown). Therefore, we developed a new antibody to detect the C-terminal end of the Toc protein. Using this new antibody, we detected Toc colocalized with microtubules in the mitotic spindle during metaphase in the brains of freshly hatched control animals (Oregon R) **(Fig 3.2 A-B).**

Next, we asked whether the mutant allele of *Toc, toc*^{9} identified from the *mdy*^{QX25} chromosome, exhibited a neuroblast microtubule defect, since it is known that Toc depleted embryos have spindle defects. We used an alpha-tubulin antibody to visualize microtubules in Toc mutant MB NBs at 24 hours ALH. In preliminary work, we observed abnormal numbers of centrosomes (four instead of two) and some short, abnormally formed spindles **(Fig 3.2 C).** We have also observed other MB NBs with seemingly normal telophase profiles. More work will need to be done to determine whether Toc affects spindle assembly and dynamics throughout mitosis or if Toc functions in a stage specific manner. We conclude that Toc is a microtubule associated protein required for proper microtubule network function during mitosis.

Toucan controls NB reactivation from quiescence and is required to sustain MB NB continuous proliferation

Next, we assayed whether Toc is required for the NBs proliferation during early stages of larval brain development. Most of the NBs in the *Drosophila* freshly hatched larval brain are in quiescence. Only the Mushroom body neuroblasts (MB NBs) do not enter quiescence at the end of the embryonic stage and continue to proliferate in the freshly hatched larval brain. We fed freshly hatched Toc mutant larvae with EdU for 3 hours and then dissected and stained their brains with antibodies against the neuroblast marker, Deadpan, and the membrane marker, Scribble, in order to study NB proliferation in the freshly hatched larva brain. As in wild type Oregon R freshly hatched larval brains, only the MB NBs incorporated EdU in the Toc mutant larvae brain **(Fig 3.3 A-B)**. Next, we fed the freshly hatched larvae EdU for 24 hours to investigate whether the Toc mutation affects non-MB NB reactivation from quiescence and MB NB continuation of proliferation. During 24 hours ALH, non-MB NBs failed to incorporate EdU into their DNA indicating that they did not reactivate from developmental quiescence. Additionally, MB NBs also stopped EdU incorporation by 24 hours ALH **(Fig 3.3 C-D)**. We conclude that the Toc mutation causes MB NBs to stop proliferating and prevents the non-MB NBs to reactivate from quiescence.

Some MB NBs in Toucan mutants are binucleate, indicating a defect in cytokinesis

Next, we used Deadpan (Dpn), Scribble (Scrib), alpha-tubulin (aTub) and PHH3 staining to study the mitosis defects in the MB NBs. At 24 hours ALH, MB NBs in Toc mutant brains were found to be binucleated Dpn+ **(Fig 3.4 B)**. No such binucleated MB

NBs were observed in the wild type *Oregon R* larval brain at 24 hours ALH **(Fig 3.4 A)**. We conclude that the Toc mutation causes cytokinesis defects in the proliferating MB NBs.

Asymmetric segregation of the basal cell fate determinants is disrupted in Toc mutants in the absence of Toc

Next, we investigated the asymmetric localization of cell fate determinants in MB NBs. Just prior to the onset of mitosis, apical polarity protein aPKC phosphorylates Mira and Numb which is important for their basal cortical localization. During metaphase, aPKC forms a tight crescent at the apical cortical surface whereas Mira and Numb form a similar crescent at the opposite basal cortical surface. In the freshly hatched and 24-hour ALH brain, aPKC localization was normal in the Toc mutant MB NBs. Next, we looked at Miranda localization. At 24 hours ALH, we found that Miranda was mislocalized in toc9/Df9713 mutant MB NBs compared to the control **(Fig 3.5 A-B)**. We also observed defects in Prospero localization and found increasing levels of nuclear Prospero in Toc mutant neuroblasts during 24 hours ALH **(Fig 3.5 C)**. Next, we examined Numb localization and found that Numb was uniformly cortical in the Toc mutant MB NBs **(Fig 3.5 D)**. We conclude that Toc mutants have defects in the asymmetric localization of key polarity proteins that govern cell fates.

Notch signaling is attenuated in the MB NBs

Because Numb was no longer partitioned asymmetrically to the GMC after cytokinesis in toc mutant neuroblasts, we next examined whether Notch signaling remains active in neuroblasts. Numb is an inhibitor of Notch signaling and normally during asymmetric cell division, Numb is partitioned exclusively to the GMC where it turns off Notch. We used the Notch activity reporter Espl-mγGFP to determine whether Notch signaling is active in Toc mutant MB NBs. We found that Notch signaling is not active consistent with the observed mislocalization of Numb **(Fig 3.6 A-B)**. We conclude that Toc sustains MB NB proliferation by controlling Numb localization.

Progressive accumulation of Prospero leads to the terminal differentiation of the MB NBs

Pros is inherited by the GMCs during NB asymmetric cell division where it induces GMCs to differentiate into neurons [4]. We investigated whether mislocalized Pros might cause MB NB terminal differentiation. We used Dpn and Pros antibody staining to detect their relative levels in the brains of freshly hatched, 24h, and 48h ALH animals. In the MBNBs of freshly hatched Toc mutant larval brains, Pros levels were low and similar to the wild-type Oregon R freshly hatched larval brain **(Fig 3.7 A)**. However, Prospero became nuclear by 24 hours ALH in the Toc mutant MB NBs, and the ratio of nuclear Dpn/Pros was significantly lower in the mutant brain than in controls **(Fig 3.7 B)**. By 48 hours ALH, a significant number of the MB NBs were completely differentiated into Dpn^{-} $Pros^{+}$ cells and the Dpn/Pros levels were even lower **(Fig 3.7 C)**. We conclude that loss

of Toc causes MB NB terminal differentiation due to gradual nuclear accumulation of Pros.

Discussion:

Here we report that the microtubule binding protein Toc is expressed in the freshly hatched *Drosophila* larval brain. Earlier studies showed that Toc is maternally deposited in the embryo and plays a critical role in nuclear division during the formation of the syncytial blastoderm in early-stage embryos. The same group also reported that the maternal pool of Toc is exhausted by embryonic stage 14 and no longer detected in the larvae [20–22]. According to the Flybase, there are 10 different annotated transcripts and 10 unique polypeptides of Toc in *Drosophila*. It is possible that various isoforms of Toc are expressed across different tissue types during distinct developmental stages.

Loss of Toc severely affects NB proliferation during early stages of larval brain development. The fact that non-MB NBs do not reactivate from developmental quiescence in Toc mutant brains indicates that a stable microtubule population might be necessary for NB to re-enter in the cell cycle. *Drosophila* Toc expressed in mammalian cell lines has demonstrated that Toc is necessary for the stability of the microtubule structures [23]. Loss of Toc also affects proliferating MB NBs in the early-stage larval brain. Although Toc mutant MB NBs incorporate EdU and go through a few rounds of cell division in the freshly hatched larvae brain, they exit the cell cycle by 24 hours ALH. Studies in which maternal Toc transcripts were depleted in a dose dependent manner

using RNAi showed that loss of Toc could affect cell division during any stage of mitosis depending on the level of Toc depletion. Based on EdU incorporation and Phh3 labeling, we have observed that MB NBs exit the cell cycle and remain stuck at various stages of the cell cycle. The most common mitosis defects we've observed in Toc mutant MB NBs are instances where they become stuck as double Dpn+ bi-nucleate cells. We have also observed an abnormal number of centrosomes in the Toc mutant MB NBs which suggests that Toc also plays a role in centrosome homeostasis in the NBs.

Another striking phenotype observed in the Toc mutant MB NBs is the mislocalization of the basal cell fate determinant proteins Numb, Miranda and Prospero. aPKC mediated phosphorylation of Miranda and Numb at the onset of mitosis is critical for their dissociation from the NB cortex [5,6,24,25]. However, how Miranda and Numb are localized to the basal cell cortex during metaphase remains unknown. A recent study has suggested that spindle microtubules might be involved in basal cell fate determinant localization since NBs with misoriented spindle microtubules are divided symmetrically due to improper segregation of the cell fate determinants [10]. However, the mechanism controlling spindle microtubule mediated segregation of the basal cell fate determinants remains unknown. Our findings suggest that microtubules might play a role in proper localization of the basal cell fate determinants.

We have also observed that Toc mutant MB NBs progressively accumulate Prospero in their nucleus which leads to their terminal differentiation. This could be explained in two different ways **(Fig 3.8)**. In the first scenario, mislocalization of Numb

turns off Notch signaling which causes inhibition of Deadpan (Dpn) expression. Loss of Dpn leads to the expression of Prospero which eventually leads to the MB NBs terminal differentiation. In the second scenario, mislocalization of Miranda leads to mislocalization of Prospero in the Toc mutant non-proliferative MB NBs. Nuclear localization of Prospero due to microtubule network failure leads to MB NBs terminal differentiation. Our future work will focus on determining the mechanism behind MB NBs terminal differentiation in the Toc mutant larval brain.

Material and methods:

Fly stocks

All animals were raised in uncrowded conditions at 25˚C on BL food in a controlled light dark cycles unless stated otherwise. The following fly lines were used: *mdy*^{QX25} (Michelle Bland lab), *toc*^{9} (isolated from *mdy*^{QX25}), *toc*$^{A1\text{-}1}$ (BDSC #). Bigger deficiency lines used: *Df(2L)ED50001 (BDSC #24626), Df(2L)ED5878 (BDSC #9353), Df(2L)ED19 (BDSC #8901), Df(2L)BSC106 (BDSC #8672), Df(2L)BSC107 (BDSC #8673), Df(2L)ED94 (BDSC #8908), Df(2L)ED105 (BDSC #24118), Df(2L)Exel6005 (BDSC #7492), Df(2L)BSC688 (BDSC #26540), Df(2L)BSC455 (BDSC #24959), Df(2L)Exel7011 (BDSC #7783), Df(2L)C144 (BDSC #90), Df(2L)ED4651 (BDSC #94697), Df(2L)BSC292 (BDSC #23677), Df(2L)ED247 (BDSC #24123), Df(2L)Exel6009 (BDSC #7495), Df(2L)BSC295 (BDSC #23680), Df(2L)ED250 (BDSC #9270)*. Smaller deficiency lines used: *Df(2L)ED206 (BDSC #8038), Df(2L)ED4559 (BDSC #24121), Df(2L)BSC164 (BDSC #9599), Df(2L)BSC238 (BDSC #9713).* Lines used for meiotic mapping: *al[1] dpy[ov1]*

b[1] pr[1] c[1] px[1] speck[1] (BDSC #156) and *al[1] dpy[ov1] b[1] pr[1] Bl[1] c[1] px[1] speck[1]/SM1* (BDSC #213)

Immunofluorescence and confocal imaging

Larval brains were fixed and stained as previously described. (Reference) In brief, larval brains were dissected and fixed in 4% EM grade formaldehyde in PEM (Pipes, EGTA, Magnesium chloride) buffer with 0.1% Triton-X for 20 mins. Tissues were washed in 1X PBT with 0.1% TritonX-100 and blocked overnight at 4˚C in 1X PBT with 10% normal goat serum. Primary antibodies used in this study include: rat anti-Deadpan (1:100, Abcam), rabbit anti-Scribble (1:1000, Doe lab), rat anti-Miranda (1:300), guinea-pig anti-Numb (1:3000), mouse anti-Prospero (1:1000, DSHB), rabbit anti-aPKC (1:200), rabbit anti-phh3 (1:1000, Abcam). Primary antibodies were detected using Alexa Fluor-conjugated secondary antibodies. Brains were imaged using a Leica SP8 laser scanning confocal microscope equipped with a 63X, 1.4 NA oil-immersion objective. Images were processed using Fiji.

EdU labeling

For EdU labeling, animals were fed 0.1mg/ml EdU mixed in with BL food for indicated time periods in the figure. Larval brains were dissected in PBT and fixed in 4% paraformaldehyde/PEM for 20 min, followed by detection of EdU using the Click-iT EdU imaging kit (Molecular Probes, Eugene, OR).

Data quantification

Leica confocal image files were analyzed with Fiji. NBs were identified based on their Deadpan expression, and they were quantified manually. In non-mitotic MB NBs, Deadpan was used as a marker for the nucleus. Nuclear Prospero and Deadpan levels were quantified manually by measuring the nuclear fluorescence signals of Deadpan and Prospero.

Figures:

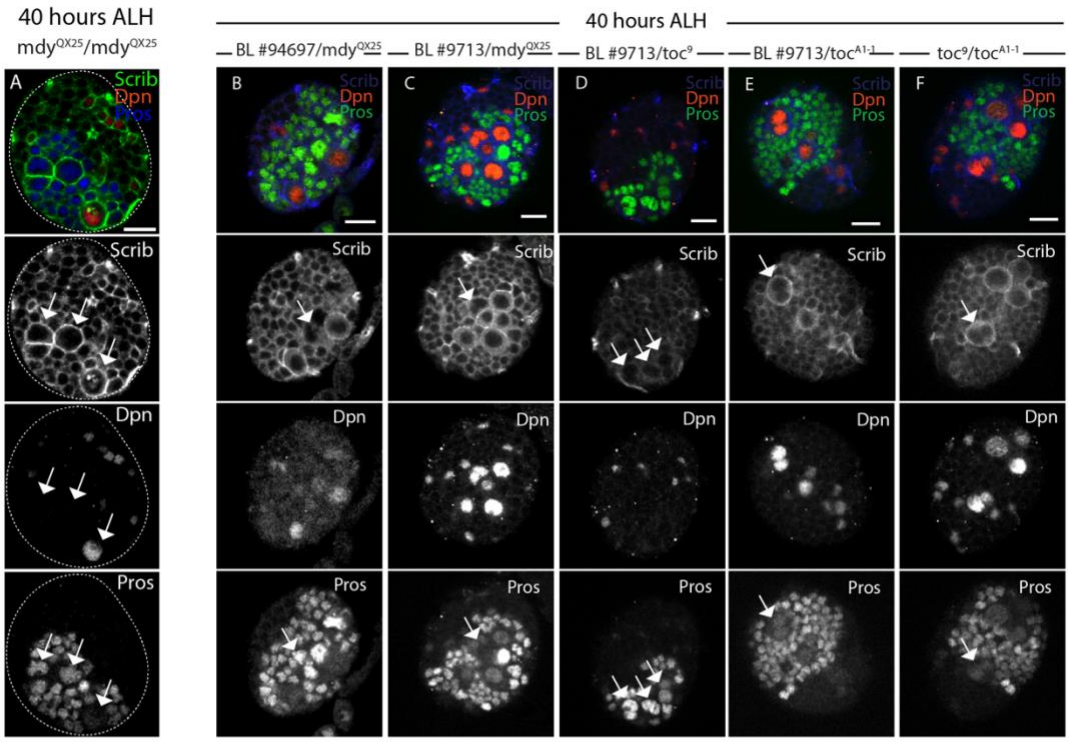
40 hours ALH
mdy^QX25/mdy^QX25
40 hours ALH
BL #94697/mdy^QX25
BL #9713/mdy^QX25
BL #9713/toc^9
BL #9713/toc^A1-1
toc^9/toc^A1-1
A
B
C
D
E
F
Scrib
Dpn
Pros

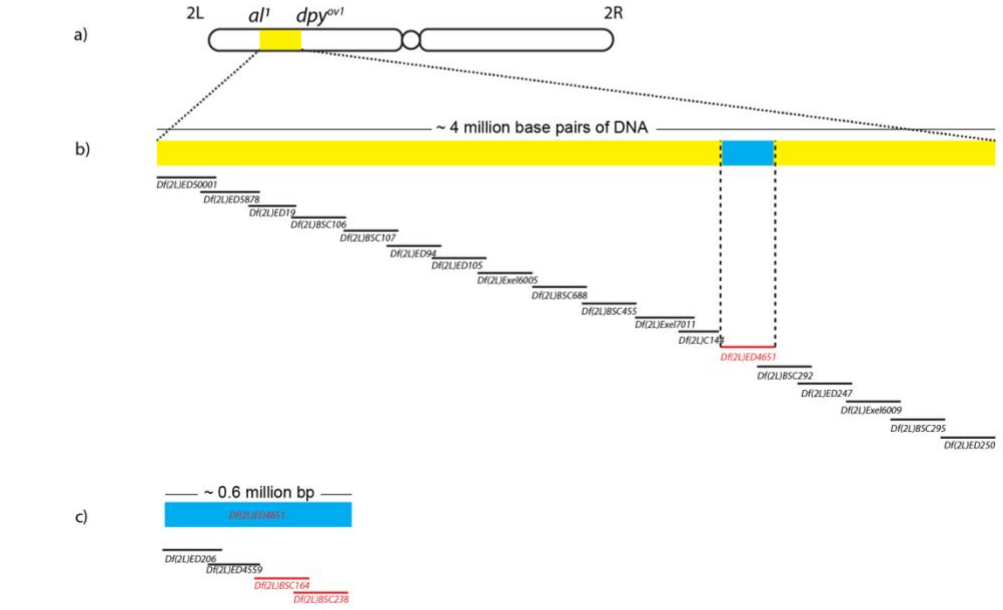
G
a)
2L
al^1
dpy^ov1
2R
b)
~ 4 million base pairs of DNA
Df(2L)ED5001
Df(2L)ED5878
Df(2L)ED19
Df(2L)BSC106
Df(2L)BSC107
Df(2L)ED94
Df(2L)ED105
Df(2L)Exel6005
Df(2L)BSC688
Df(2L)BSC455
Df(2L)Exel7011
Df(2L)JC142
Df(2L)ED4651
Df(2L)BSC292
Df(2L)ED247
Df(2L)Exel6009
Df(2L)BSC295
Df(2L)ED250
c)
~ 0.6 million bp
Df(2L)ED4651
Df(2L)ED206
Df(2L)ED4559
Df(2L)BSC164
Df(2L)BSC238

Figure 3.1: Identification of *toucan* as our unknown gene of interest using meiotic and deficiency mapping. Single optical sections showing MB NBs in a single brain lobe. Arrows indicate bi-nucleate MB NBs with high levels of Prospero **(A)** In mdy^{QX25} mutant brain, MB NBs show cytokinesis defects and undergoes terminal differentiation by 40 hours ALH **(B)** Deficiency line *Df(2L)ED4651* when crossed with mdy^{QX25} produces the phenotypes observed in the original mdy^{QX25} allele. MB NBs are binucleate and contain Pros in their nucleus at 40 hours ALH **(C)** A smaller deficiency line *Df(2L)BSC238* when crossed with mdy^{QX25} replicates the phenotype. **(D)** The smaller deficiency line *Df(2L)BSC238* when crossed with another *toc* allele toc^{A1-1} reproduced the phenotypes. **(E-F)** toc^{9} allele when crossed with the deficiency line *Df(2L)BSC238* and allele toc^{A1-1} showed cytokinesis defects and differentiation of the MB NBs at 40 hours ALH. Scale bar is 10 micrometers. **(G)** Illustration of the deficiency mapping technique used to identify a single small deficiency line *Df(2L)BSC238* that produced all the original MB NBs phenotypes when crossed to *toc* mutant alleles.

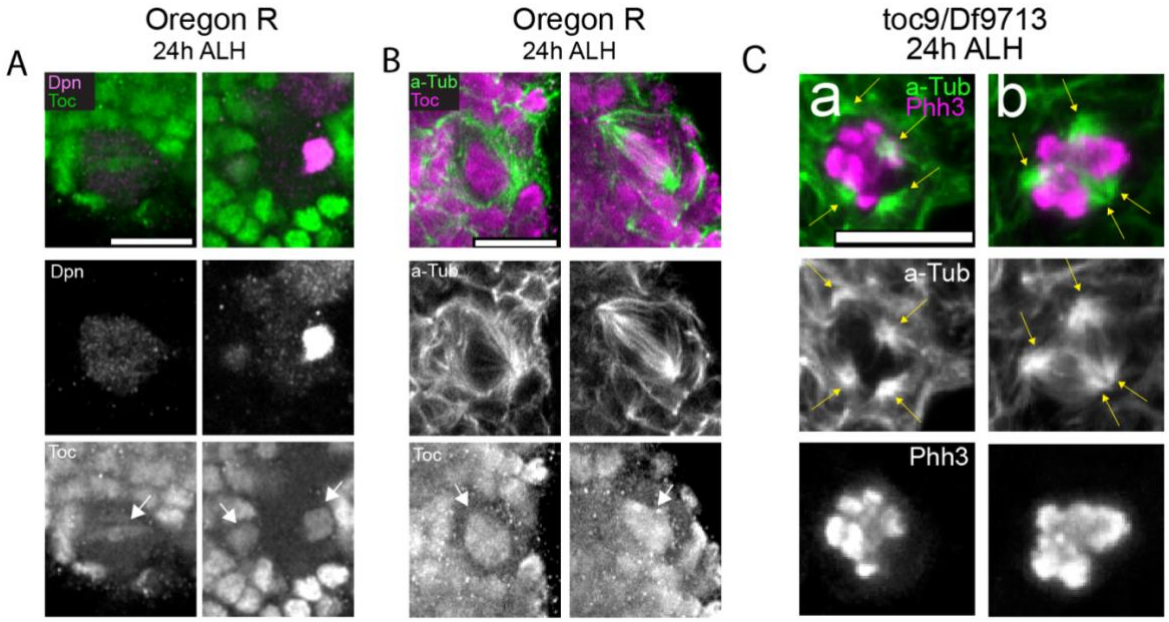

Fig 3.2: Toc is a microtubule binding protein. (A) Single optical section of *Drosophila* 24h ALH larvae brain showing Toc antibody staining in a single MB NB. Deadpan (magenta) marks the MB NB nucleus and Toc is in green. (B) Single optical section of *Drosophila* 24h ALH larvae brain showing Toc antibody staining in a single MB NB. Alpha-tubulin staining is in green and Toc is in magenta **(C, a-b)** At 24 hours ALH, alpha-tubulin staining in toc9/Df9713 mutant brain shows the presence of an extra pair of centrosomes (arrows) in one of the MB NBs. Scale bar is 10 micrometers.

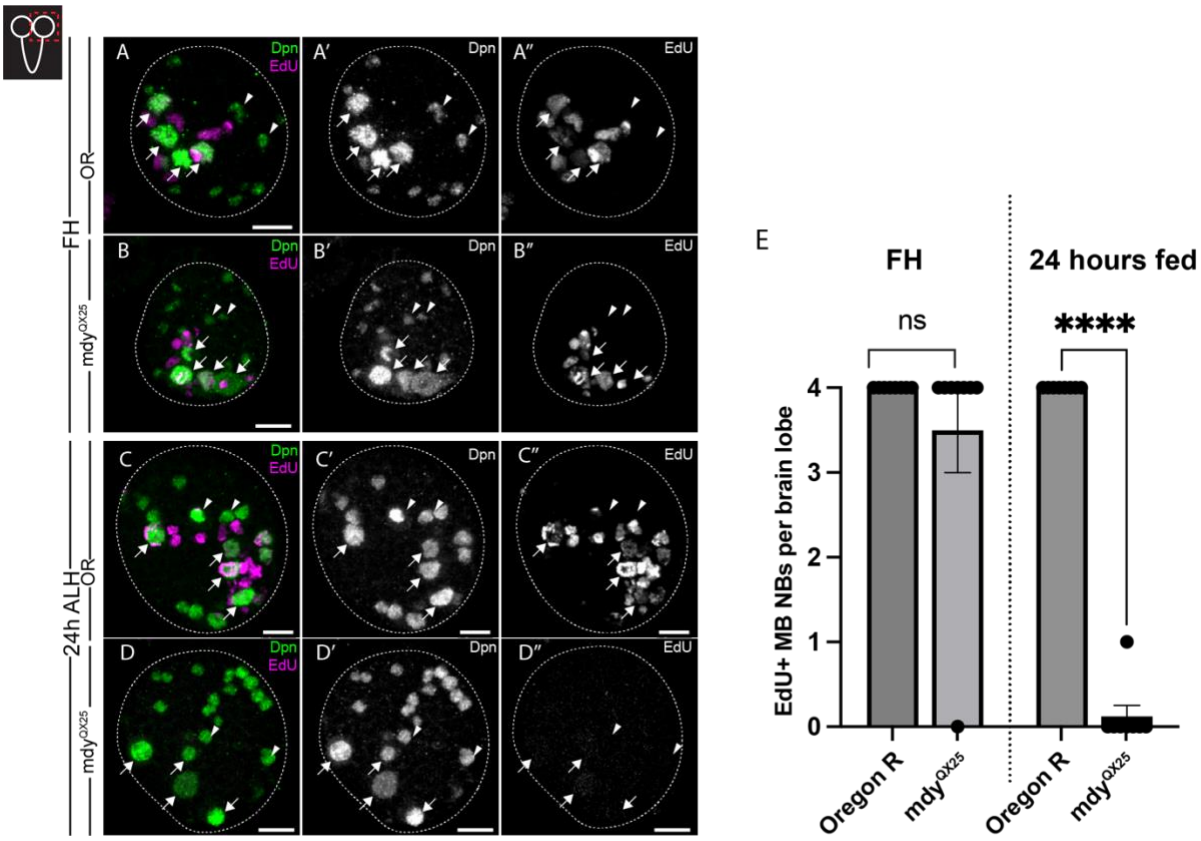

Fig 3.3: Non-MB NBs failed to reactivate from developmental quiescence while MB NBs exit the cell cycle in the Toc mutant 24 hours fed larvae brain. (A-B) maximum intensity projections of ten dorsal-most Z sections from freshly hatched (FH) larval brains show that MB NBs continue to incorporate EdU both in the wild type Oregon R and Toc mutant brain. **(C)** In the Oregon R control brain, MB NBs continue to incorporate EdU while non-MB NBs resume proliferation as indicated by their incorporation of EdU at 24 hours ALH **(D)** In contrast, non-MB NBs never incorporate EdU in their DNA and MB NBs exit cell cycle by 24 hours ALH in Toc mutant brain. Arrows indicate MB NBs and arrowheads indicate non-MB NBs **(E)** Quantification of the data shown in panel A-D. Scale bar is 10 micrometers. Student's t-test was used to test statistical significance. **** $p<0.0001$.

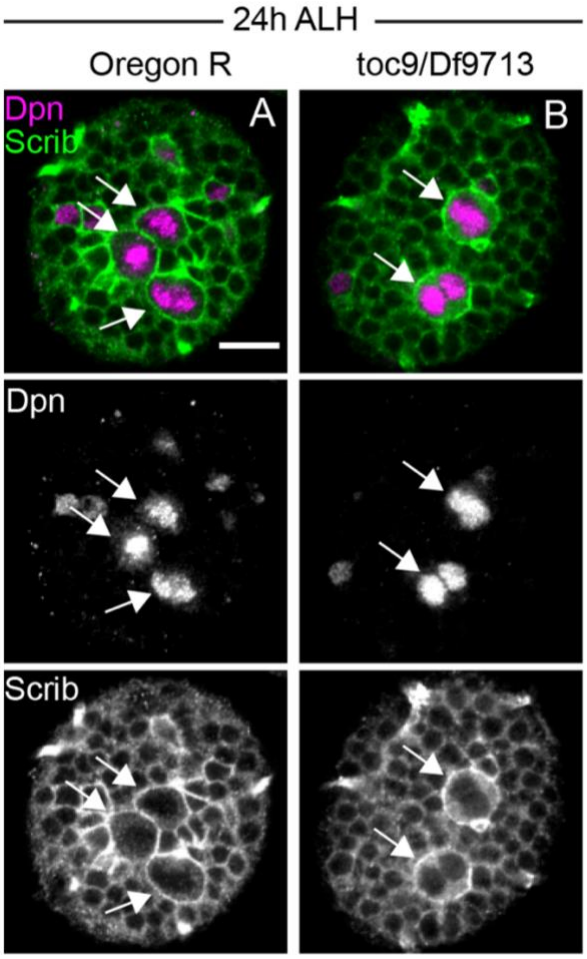

Fig 3.4: toc^{9}/Df9713 mutant MB NBs show cytokinesis defects. Single optical section showing a single brain hemisphere of a 24-hour ALH larval brain **(A)** In wild type Oregon R animals, all MB NBs have a single Dpn+ nucleus at 24 hours ALH. **(B)** In comparison, in toc^{9}/Df9713 animals MB NBs are Dpn+ and binucleated which is indicative of cytokinesis defects. Scale bar is 10 micrometers.

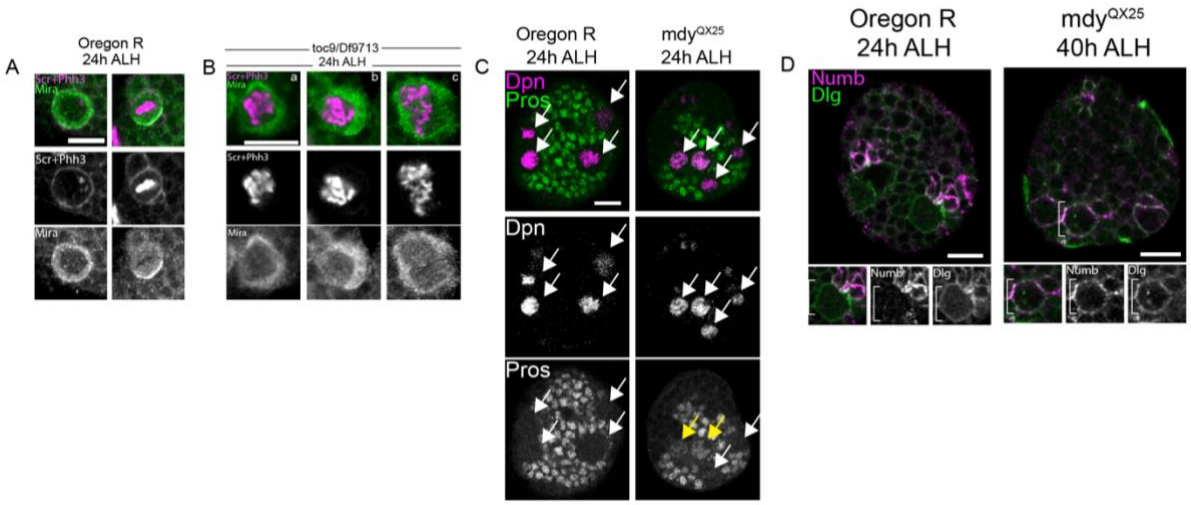

Fig 3.5: Asymmetric segregation of the basal cell fate determinants Miranda, Prospero and Numb is disrupted in Toc mutant MB NBs. Single optical section showing a single brain hemisphere in indicated genotypes **(A-B)** Antibody staining against Miranda shows Miranda localization in Oregon R and toc9/Df9713 mutant MB NB during 24h ALH. **(C)** MB NBs show nuclear Prospero localization by 24 hours ALH in Toc mutant MB NBs compared to the control Oregon R brain **(D)** Numb is mislocalized in the Toc mutant MB NBs at 40 hours ALH. Scale bar is 10 micrometers.

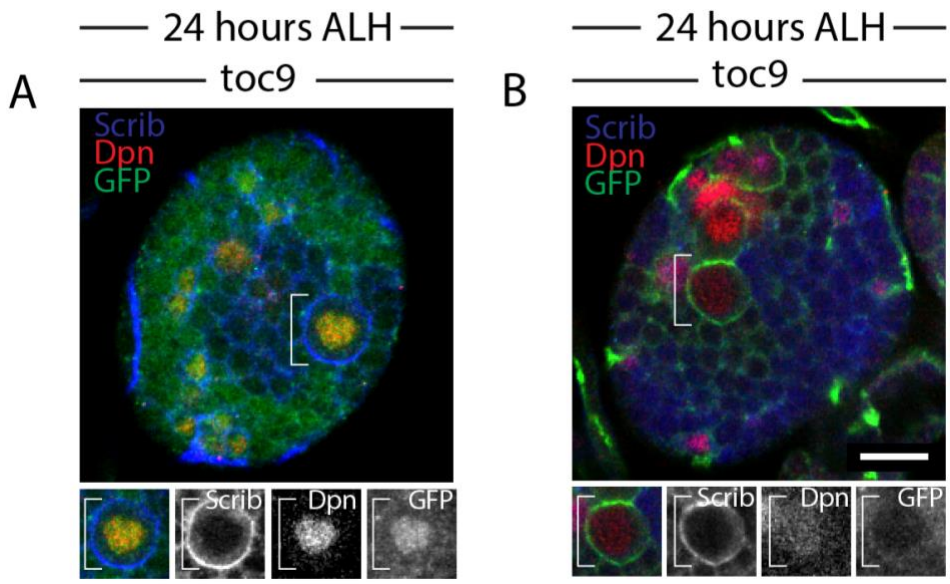

Fig 3.6: Notch signaling is attenuated in the MB NBs at 24 hours ALH in the Toc mutant brain. Single optical section of a brain hemisphere showing expression of a Notch reporter activity (GFP). **(A-B)** Notch signaling is attenuated in some of the MB NBs at 24 hours ALH. Scale bar is 10 micrometers.

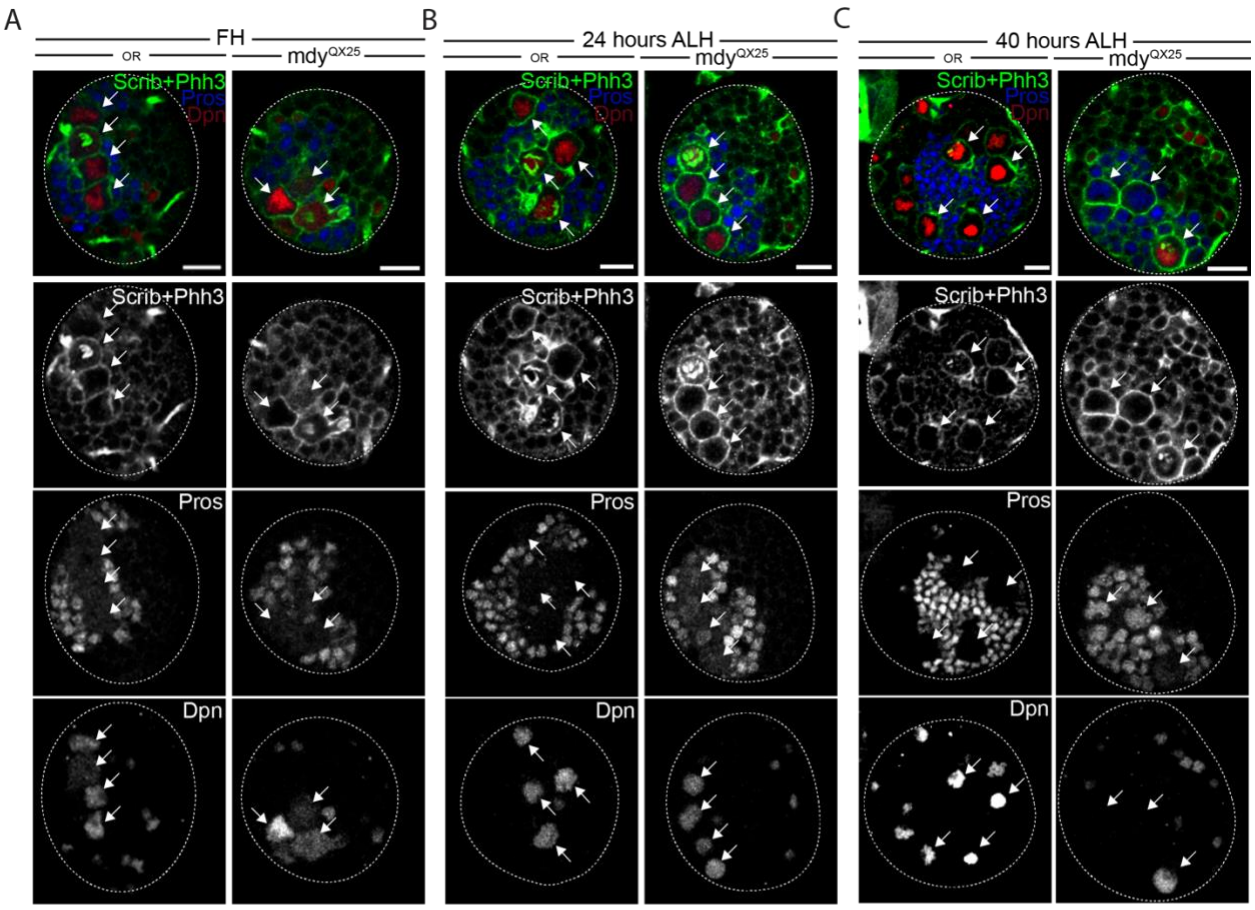
A
FH
OR
mdy^QX25
B
24 hours ALH
OR
mdy^QX25
C
40 hours ALH
OR
mdy^QX25
Scrib+Phh3
Pros
Dpn

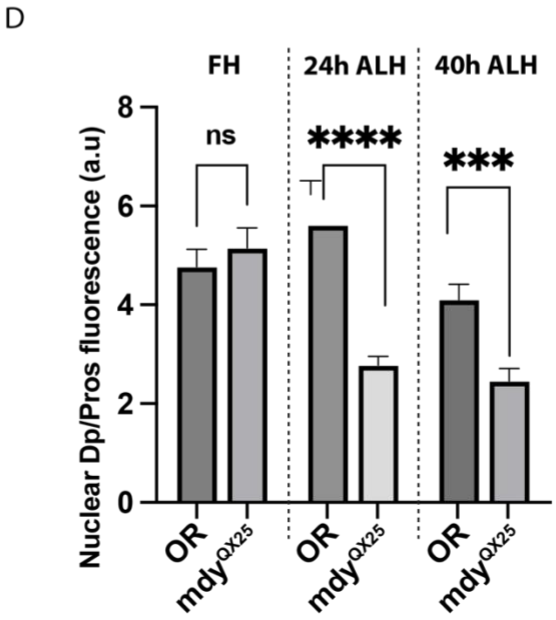
D
FH
24h ALH
40h ALH
ns
****
***
Nuclear Dp/Pros fluorescence (a.u)
0
2
4
6
8
OR
mdy^QX25

Fig 3.7: MB NBs are terminally differentiated by 40 hours ALH in the Toc mutant brain. (A-C) Single optical sections of brain hemispheres show dynamic changes in Dpn and Pros protein levels over time in wild type Oregon R and Toc mutant brains. Arrows indicate MB NBs. **(A)** In freshly hatched larval brains, Pros level is very similar in wild type Oregon R and Toc mutant MB NBs. **(B)** By 24 hours ALH, there is a significant increase in nuclear Pros level in the Toc mutant MB NBs compared to the wild type MB NBs. **(C)** By 40 hours ALH, nuclear Pros level is even higher in the Toc mutant MB NBs while Pros is absent in the wild type MB NBs. Some of the MB NBs terminally differentiate due to their increased level of nuclear Pros. **(D)** Quantification of the data. Student's t-test was used for statistical significance. ***$p < 0.001$, ****$p < 0.0001$. Scale bar is 10 micrometers.

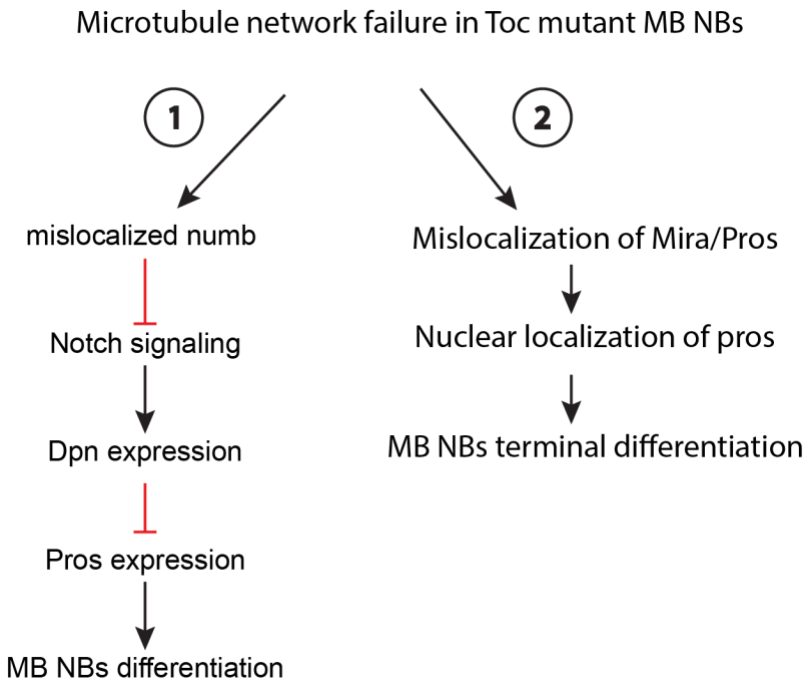

Fig 3.8: Proposed mechanisms behind MB NB terminal differentiation in the Toc mutant brain. (1) Failure in the microtubule network leads to the mislocalization of Numb, which in turn deactivates Notch signaling in the MB NBs. The disruption in Notch signaling results in reduced Deadpan expression and increased Prospero expression, ultimately causing the terminal differentiation of MB NBs. (2) Failure in the microtubule network in Toc mutants causes Miranda to mislocalize and leads to the nuclear accumulation of Prospero in the MB NBs. This results in their terminal differentiation by 40 hours after larval hatching (ALH).

References:

1. Gallaud E, Pham T, Cabernard C. Drosophila melanogaster Neuroblasts: A Model for Asymmetric Stem Cell Divisions. In: Tassan JP, Kubiak JZ, eds. *Asymmetric Cell Division in Development, Differentiation and Cancer*. Results and Problems in Cell Differentiation. Springer International Publishing; 2017:183-210. doi:10.1007/978-3-319-53150-2_8

2. Sunchu B, Cabernard C. Principles and mechanisms of asymmetric cell division. *Dev Camb Engl*. 2020;147(13):dev167650. doi:10.1242/dev.167650

3. Gönczy P. Mechanisms of asymmetric cell division: flies and worms pave the way. *Nat Rev Mol Cell Biol*. 2008;9(5):355-366. doi:10.1038/nrm2388

4. Doe CQ, Chu-LaGraff Q, Wright DM, Scott MP. The prospero gene specifies cell fates in the Drosophila central nervous system. *Cell*. 1991;65(3):451-464. doi:10.1016/0092-8674(91)90463-9

5. Knoblich JA, Jan, Nung Jan Y. Asymmetric segregation of Numb and Prospero during cell division. *Nature*. 1995;377(6550):624-627. doi:10.1038/377624a0

6. Shen CP, Jan LY, Jan YN. Miranda Is Required for the Asymmetric Localization of Prospero during Mitosis in Drosophila. *Cell*. 1997;90(3):449-458. doi:10.1016/S0092-8674(00)80505-X

7. Hirata J, Nakagoshi H, Nabeshima Y ichi, Matsuzaki F. Asymmetric segregation of the homeodomain protein Prospero duringDrosophila development. *Nature*. 1995;377(6550):627-630. doi:10.1038/377627a0

8. Rhyu MS, Jan LY, Jan YN. Asymmetric distribution of numb protein during division of the sensory organ precursor cell confers distinct fates to daughter cells. *Cell*. 1994;76(3):477-491. doi:10.1016/0092-8674(94)90112-0

9. Homem CCF, Knoblich JA. Drosophila neuroblasts: a model for stem cell biology. *Dev Camb Engl*. 2012;139(23):4297-4310. doi:10.1242/dev.080515

10. Cabernard C, Doe CQ. Apical/basal spindle orientation is required for neuroblast homeostasis and neuronal differentiation in Drosophila. *Dev Cell*. 2009;17(1):134-141. doi:10.1016/j.devcel.2009.06.009

11. Adams RR, Tavares AAM, Salzberg A, Bellen HJ, Glover DM. pavarotti encodes a kinesin-like protein required to organize the central spindle and contractile ring for cytokinesis. *Genes Dev*. 1998;12(10):1483-1494.

12. Goldstein AYN, Jan YN, Luo L. Function and regulation of Tumbleweed (RacGAP50C) in neuroblast proliferation and neuronal morphogenesis. *Proc Natl Acad Sci U S A*. 2005;102(10):3834-3839. doi:10.1073/pnas.0500748102

13. Somers WG, Saint R. A RhoGEF and Rho family GTPase-activating protein complex links the contractile ring to cortical microtubules at the onset of cytokinesis. *Dev Cell*. 2003;4(1):29-39. doi:10.1016/s1534-5807(02)00402-1

14. Lehner CF. The pebble gene is required for cytokinesis in Drosophila. *J Cell Sci*. 1992;103 (Pt 4):1021-1030. doi:10.1242/jcs.103.4.1021

15. Prokopenko SN, Brumby A, O'Keefe L, et al. A putative exchange factor for Rho1 GTPase is required for initiation of cytokinesis in Drosophila. *Genes Dev*. 1999;13(17):2301-2314.

16. Giet R, Glover DM. Drosophila aurora B kinase is required for histone H3 phosphorylation and condensin recruitment during chromosome condensation and to organize the central spindle during cytokinesis. *J Cell Biol*. 2001;152(4):669-682. doi:10.1083/jcb.152.4.669

17. Gao S, Giansanti MG, Buttrick GJ, et al. Australin: a chromosomal passenger protein required specifically for Drosophila melanogaster male meiosis. *J Cell Biol*. 2008;180(3):521-535. doi:10.1083/jcb.200708072

18. Siller KH, Cabernard C, Doe CQ. The NuMA-related Mud protein binds Pins and regulates spindle orientation in Drosophila neuroblasts. *Nat Cell Biol*. 2006;8(6):594-600. doi:10.1038/ncb1412

19. Bowman SK, Neumüller RA, Novatchkova M, Du Q, Knoblich JA. The Drosophila NuMA Homolog Mud regulates spindle orientation in asymmetric cell division. *Dev Cell*. 2006;10(6):731-742. doi:10.1016/j.devcel.2006.05.005

20. Grammont Muriel, Dastugue B, Couderc JL. The Drosophila toucan (toc) gene is required in germline cells for the somatic cell patterning during oogenesis. *Development*. 1997;124(24):4917-4926. doi:10.1242/dev.124.24.4917

21. Grammont M, Berson G, Dastugue B, Couderc JL. Expression and cellular localization of the Toucan protein during *Drosophila* oogenesis. *Mech Dev*. 2000;90(2):289-292. doi:10.1016/S0925-4773(99)00240-3

22. Debec A, Grammont M, Berson G, Dastugue B, Sullivan W, Couderc JL. Toucan protein is essential for the assembly of syncytial mitotic spindles in Drosophila melanogaster. *genesis*. 2001;31(4):167-175. doi:10.1002/gene.10019

23. Mirouse V, Dastugue B, Couderc JL. The Drosophila Toucan protein is a new mitotic microtubule-associated protein required for spindle microtubule stability. *Genes Cells*. 2005;10(1):37-46. doi:10.1111/j.1365-2443.2004.00813.x

24. Hannaford MR, Ramat A, Loyer N, Januschke J. aPKC-mediated displacement and actomyosin-mediated retention polarize Miranda in Drosophila neuroblasts. Yamashita YM, ed. *eLife*. 2018;7:e29939. doi:10.7554/eLife.29939

25. Smith CA, Lau KM, Rahmani Z, et al. aPKC-mediated phosphorylation regulates asymmetric membrane localization of the cell fate determinant Numb. *EMBO J*. 2007;26(2):468-480. doi:10.1038/sj.emboj.7601495

Chapter 4

Discussion and future directions

Proper brain development is dependent on controlled proliferation of the neural stem and progenitor cell (NSPC) population. NSPCs can use both symmetric and asymmetric cell division for their proliferation. Symmetric cell division is often used to amplify the progenitor pool and upon terminal differentiation. However, NSPCs predominantly use asymmetric cell division for proliferation which allows them to maintain a stem cell pool while generating a huge variety of neuronal and glial progenies [1–4]. This asymmetry in the progeny cell fate is normally achieved by segregating cell fate determinant factors, such as polarity proteins, in an asymmetric way. There are numerous factors involved in the asymmetric distribution of the cell fate determinants. NSPC intrinsic polarity cues and the microtubule spindle network are two of the most important factors involved in this process [1,5,6]. Here I will discuss a microtubule associated protein, named Toucan, which we have found to be involved in the regulation of asymmetric cell division in *Drosophila* early-stage larvae brain.

NSPCs also go through periods of quiescence and proliferation throughout development in order to coordinate brain development with body development, and also to maintain tissue homeostasis later in life. The decision between quiescence versus proliferation is dependent on an interplay between NSPC intrinsic and extrinsic factors. Availability of extrinsic nutrients is one of the key factors that affect NSPCs proliferation. Recent studies have highlighted the metabolic state of the NSPCs in dictating their

quiescence versus proliferation decisions [7–9]. Here I will discuss how lipid droplet availability in the freshly hatched *Drosophila* brain affects NBs reactivation from quiescence.

Lipid droplet availability affects NB reactivation from quiescence

Nurse cells deposit a large amount of lipid droplets into the egg during oogenesis in *Drosophila.* These lipid droplets become exhausted by the end of the embryonic stage, suggesting an important role for the lipid droplets during early development [10–12]. *Drosophila* embryos mutant for the Brummer lipase, which is the major TAG lipase in *Drosophila*, show embryonic lethality which highlights the importance of lipid resources during development [13]. A recent study has shown that *Drosophila* development is significantly delayed in mutants that either lack lipid droplets from the maternal source (Lsd2 mutants) or have difficulty with the distribution of lipid droplets in the embryo (Jabba and Klar mutants) [14]. This study again highlights the importance of maternal lipid droplets during early development. However, it is not clear whether the maternal lipid droplets are distributed in a preferential manner to the newly formed tissues of the embryo or if they are distributed evenly. Moreover, it is not clear whether the availability of lipid droplets affects the development of certain tissues more than others. We have found that *Drosophila* freshly hatched larval brains contain lipid droplets and that they are required for the reactivation of the quiescent NBs. We verified our observations with four different mutant lines all of which are involved in lipid droplet homeostasis in the *Drosophila* embryo. Bmm^{1} mutant larvae had defects in lipid droplet breakdown and there was a huge accumulation of lipid droplets in the freshly hatched larval brain. $Lsd2^{KG}$ mutant

larvae had very few lipid droplets in the freshly hatched brain due to their defect in lipid droplet deposition during oogenesis. *Klar*^{YG3} and *Jabba*^{DL} mutant larval brains also contained very few lipid droplets because of their issues with sorting embryonic lipid droplets from the embryo core to the newly formed peripheral tissues. We also observed a significant delay in quiescent NBs reactivation when we knocked down *Bmm* in a NB or glia specific manner. Overall, our data strongly support the idea that maternally deposited lipid droplets play an important role in NB reactivation from quiescence. It will be interesting to know whether lipid droplet availability also affects the development of other tissues such as gut, muscle, etc.

Lipid droplet availability affects PI3K activation in quiescent neuroblasts

PI3K signaling is an evolutionarily conserved signaling pathway that controls cell growth and proliferation. Several factors affect the functioning of the PI3K signaling pathway including the availability of PIP2 in the cell membrane and the relative abundance of saturated and unsaturated fatty acids in the membrane lipids [15,16]. We investigated whether lipid droplet availability affects PI3K activation in the quiescent NBs. Extrinsic nutrient cues are known to activate PI3K signaling in the quiescent NBs in *Drosophila* by inducing the expression of dILP2 from the insulin producing cells [17,18]. We looked at expression of dILP2 and its downstream target InR in the quiescent NBs in Bmm^{1} mutant brains and found that dILP2 and InR expression was normal. This led us to investigate whether PI3K activation was abnormal despite the normal InR expression in the Bmm^{1} mutant quiescent NBs. We found that a PI3K activity reporter failed to turn on in the Bmm^{1} mutant NBs at 24 hours ALH. However, PI3K reporter activity was

completely present by 48 hours ALH in the Bmm^{1} mutant NBs and they achieved complete reactivation. This suggests that lipid droplet availability in the freshly hatched larval brain affects PI3K activity. Our future studies will investigate whether there is a difference between wild type and *bmm^{1}* NBs cell membrane lipid composition if that is sufficient to affect PI3K signaling pathway. Also, are there any key differences in fatty acid chain length and level of saturation in fatty acids found in the lipid droplets and produced by *de novo* lipogenesis which can potentially contribute to the level of PI3K signaling activation?

Role of dietary and *de-novo* lipogenesis in quiescent neuroblast reactivation

Lipids acquired through diet and *de novo* lipogenesis represent two major sources of lipids during the *Drosophila* life cycle. We investigated whether lipids from diet or *de novo* lipogenesis play a role in quiescent NBs reactivation. We knocked down lipoprotein expression, which is required for dietary lipid transport via the hemolymph, in the fat body and found that it did not affect NBs reactivation from quiescence. One earlier study also reported a similar observation [19]. Next, we knocked down key enzymes, acetyl-CoA carboxylase (ACC) and SREBP, involved in lipogenesis in a NB and glia specific manner and found that quiescent NB reactivation was delayed at 24 hours ALH. Multiple studies in mice have reported that FASN mediated *de novo* lipogenesis is crucial for maintaining NSPCs proliferation in the adult brain. Proliferating NSPCs are known to upregulate their lipogenic pathways whereas quiescent NSPCs prefer FAO. Studies have also reported that the lipids produced via *de novo* lipogenesis are mostly used in cell membrane synthesis [7,9,20]. Our data clearly indicates that *de novo* lipogenesis plays a role during

quiescent NB reactivation. It will be interesting to explore the role played by FAO during quiescent NB reactivation in the freshly hatched *Drosophila* brain.

Toucan is a microtubule associated protein and affects NB proliferation

We have identified expression of a microtubule associated protein (MAP), called Toucan (Toc) in the *Drosophila* larval brain. Toc was initially reported to be expressed in the *Drosophila* female germline cells and in the embryo. The maternal pool of Toc in the embryo is depleted by embryonic stage 14 [21,22]. According to Flybase, there are 10 distinct polypeptides of Toc present in *Drosophila*. Therefore, it is likely that different isoforms of Toc are expressed during different developmental stages, presumably in a tissue specific manner. We developed an antibody against the C terminus of the Toc protein and immunostaining has clearly shown that Toc colocalizes to the spindle microtubules during metaphase. Loss of Toc severely affected NB proliferation in the freshly hatched larval brain. Quiescent non-MB NBs failed to reactivate while MB NBs exited the cell cycle by 24 hours ALH. MAPs are known to be involved in every aspect of cell division including centrosome homeostasis, proper chromosome alignment at the metaphase plate, chromosome segregation and cytokinesis [23–26]. Alpha tubulin staining for the microtubules in the Toc mutant MB NBs showed defects in their mitotic spindles. We also saw abnormal numbers of centrosomes in the MB NBs. Previous studies in *Drosophila* embryos showed that loss of Toc affects all stages of mitosis. Another study demonstrated that Toc plays an important role in microtubule network stability [27,28]. Overall, it is clear that Toc is required in the *Drosophila* larval brain for the microtubule network function which affects NB proliferation.

Toucan affects asymmetric cell fate determinant protein segregation

We have also observed defects in segregation of the basal cell fate determinants during asymmetric cell division of the MB NBs in Toc mutant larval brains. Basal cell fate determinant polarity proteins Miranda, Prospero and Numb were all mislocalized in the Toc mutant MB NBs at 24 hours ALH. MB NBs are terminally differentiated due to nuclear Prospero by 40 hours ALH. Previous studies in *Drosophila* NBs have shown that the evolutionarily conserved apical Par protein complex and the mitotic spindle network play very important roles in segregating basal cell fate determinant polarity proteins. Mutations in genes encoding components of the spindle orientation machinery (e.g., Insc, Pins, Mud) disrupt spindle alignment, leading to symmetric divisions and mis-segregation of basal cell fate determinants [23,29–32]. It remains unclear how exactly the interaction between the apical Par complex proteins and the spindle microtubule network ensures basal polarity protein segregation and overall cytokinesis. In Toc mutant MB NBs, it will be interesting to know whether terminal differentiation is due to Notch signaling turning off and causing the downregulation of Deadpan and upregulation of Prospero, or whether it is because of Prospero entering MB NBs nucleus due to failure of the microtubule network to segregate Miranda and Prospero to the basal cortex.

References:

1. Gönczy P. Mechanisms of asymmetric cell division: flies and worms pave the way. *Nat Rev Mol Cell Biol*. 2008;9(5):355-366. doi:10.1038/nrm2388

2. Homem CCF, Knoblich JA. Drosophila neuroblasts: a model for stem cell biology. *Dev Camb Engl*. 2012;139(23):4297-4310. doi:10.1242/dev.080515

3. Homem CCF, Repic M, Knoblich JA. Proliferation control in neural stem and progenitor cells. *Nat Rev Neurosci*. 2015;16(11):647-659. doi:10.1038/nrn4021

4. Sousa-Nunes R, Cheng LY, Gould AP. Regulating neural proliferation in the Drosophila CNS. *Curr Opin Neurobiol*. 2010;20(1):50-57. doi:10.1016/j.conb.2009.12.005

5. Gallaud E, Pham T, Cabernard C. Drosophila melanogaster Neuroblasts: A Model for Asymmetric Stem Cell Divisions. In: Tassan JP, Kubiak JZ, eds. *Asymmetric Cell Division in Development, Differentiation and Cancer*. Results and Problems in Cell Differentiation. Springer International Publishing; 2017:183-210. doi:10.1007/978-3-319-53150-2_8

6. Knoblich JA. Asymmetric cell division: recent developments and their implications for tumour biology. *Nat Rev Mol Cell Biol*. 2010;11(12):849-860. doi:10.1038/nrm3010

7. Knobloch M, Braun SMG, Zurkirchen L, et al. Metabolic control of adult neural stem cell activity by Fasn-dependent lipogenesis. *Nature*. 2013;493(7431):226-230. doi:10.1038/nature11689

8. Knobloch M. The Role of Lipid Metabolism for Neural Stem Cell Regulation. *Brain Plast Amst Neth*. 2017;3(1):61-71. doi:10.3233/BPL-160035

9. Knobloch M, Pilz GA, Ghesquière B, et al. A Fatty Acid Oxidation-Dependent Metabolic Shift Regulates Adult Neural Stem Cell Activity. *Cell Rep*. 2017;20(9):2144-2155. doi:10.1016/j.celrep.2017.08.029

10. Welte MA. As the fat flies: The dynamic lipid droplets of Drosophila embryos. *Biochim Biophys Acta BBA - Mol Cell Biol Lipids*. 2015;1851(9):1156-1185. doi:10.1016/j.bbalip.2015.04.002

11. Li Z, Johnson MR, Ke Z, Chen L, Welte MA. Drosophila lipid droplets buffer the H2Av supply to protect early embryonic development. *Curr Biol CB*. 2014;24(13):1485-1491. doi:10.1016/j.cub.2014.05.022

12. White RP, Welte MA. Visualizing Lipid Droplets in Drosophila Oogenesis. In: Giedt MS, Tootle TL, eds. *Drosophila Oogenesis: Methods and Protocols*. Springer US; 2023:233-251. doi:10.1007/978-1-0716-2970-3_12

13. Grönke S, Mildner A, Fellert S, et al. Brummer lipase is an evolutionary conserved fat storage regulator in Drosophila. *Cell Metab*. 2005;1(5):323-330. doi:10.1016/j.cmet.2005.04.003

14. Kilwein MD, Dao TK, Welte MA. Drosophila embryos allocate lipid droplets to specific lineages to ensure punctual development and redox homeostasis. *PLoS Genet*. 2023;19(8):e1010875. doi:10.1371/journal.pgen.1010875

15. Vanhaesebroeck B, Stephens L, Hawkins P. PI3K signalling: the path to discovery and understanding. *Nat Rev Mol Cell Biol*. 2012;13(3):195-203. doi:10.1038/nrm3290

16. Engelman JA, Luo J, Cantley LC. The evolution of phosphatidylinositol 3-kinases as regulators of growth and metabolism. *Nat Rev Genet*. 2006;7(8):606-619. doi:10.1038/nrg1879

17. Sipe CW, Siegrist SE. Eyeless uncouples mushroom body neuroblast proliferation from dietary amino acids in Drosophila. *eLife*. 6:e26343. doi:10.7554/eLife.26343

18. Yuan X, Sipe CW, Suzawa M, Bland ML, Siegrist SE. Dilp-2–mediated PI3-kinase activation coordinates reactivation of quiescent neuroblasts with growth of their glial stem cell niche. *PLoS Biol*. 2020;18(5):e3000721. doi:10.1371/journal.pbio.3000721

19. Palm W, Sampaio JL, Brankatschk M, et al. Lipoproteins in Drosophila melanogaster—Assembly, Function, and Influence on Tissue Lipid Composition. *PLOS Genet*. 2012;8(7):e1002828. doi:10.1371/journal.pgen.1002828

20. Knobloch M, von Schoultz C, Zurkirchen L, Braun SMG, Vidmar M, Jessberger S. SPOT14-positive neural stem/progenitor cells in the hippocampus respond dynamically to neurogenic regulators. *Stem Cell Rep*. 2014;3(5):735-742. doi:10.1016/j.stemcr.2014.08.013

21. Grammont Muriel, Dastugue B, Couderc JL. The Drosophila toucan (toc) gene is required in germline cells for the somatic cell patterning during oogenesis. *Development*. 1997;124(24):4917-4926. doi:10.1242/dev.124.24.4917

22. Grammont M, Berson G, Dastugue B, Couderc JL. Expression and cellular localization of the Toucan protein during *Drosophila* oogenesis. *Mech Dev*. 2000;90(2):289-292. doi:10.1016/S0925-4773(99)00240-3

23. Cabernard C. Cytokinesis in Drosophila melanogaster. *Cytoskeleton*. 2012;69(10):791-809. doi:10.1002/cm.21060

24. Adams RR, Tavares AAM, Salzberg A, Bellen HJ, Glover DM. pavarotti encodes a kinesin-like protein required to organize the central spindle and contractile ring for cytokinesis. *Genes Dev*. 1998;12(10):1483-1494.

25. Goldstein AYN, Jan YN, Luo L. Function and regulation of Tumbleweed (RacGAP50C) in neuroblast proliferation and neuronal morphogenesis. *Proc Natl Acad Sci U S A*. 2005;102(10):3834-3839. doi:10.1073/pnas.0500748102

26. Piekny A, Werner M, Glotzer M. Cytokinesis: welcome to the Rho zone. *Trends Cell Biol*. 2005;15(12):651-658. doi:10.1016/j.tcb.2005.10.006

27. Debec A, Grammont M, Berson G, Dastugue B, Sullivan W, Couderc JL. Toucan protein is essential for the assembly of syncytial mitotic spindles in Drosophila melanogaster. *genesis*. 2001;31(4):167-175. doi:10.1002/gene.10019

28. Mirouse V, Dastugue B, Couderc JL. The Drosophila Toucan protein is a new mitotic microtubule-associated protein required for spindle microtubule stability. *Genes Cells*. 2005;10(1):37-46. doi:10.1111/j.1365-2443.2004.00813.x

29. Betschinger J, Mechtler K, Knoblich JA. The Par complex directs asymmetric cell division by phosphorylating the cytoskeletal protein Lgl. *Nature*. 2003;422(6929):326-330. doi:10.1038/nature01486

30. Cabernard C, Doe CQ. Apical/basal spindle orientation is required for neuroblast homeostasis and neuronal differentiation in Drosophila. *Dev Cell*. 2009;17(1):134-141. doi:10.1016/j.devcel.2009.06.009

31. Cabernard C, Prehoda KE, Doe CQ. A spindle-independent cleavage furrow positioning pathway. *Nature*. 2010;467(7311):91-94. doi:10.1038/nature09334

32. Siller KH, Cabernard C, Doe CQ. The NuMA-related Mud protein binds Pins and regulates spindle orientation in Drosophila neuroblasts. *Nat Cell Biol*. 2006;8(6):594-600. doi:10.1038/ncb1412

Appendix

Yorkie-Myc interaction regulates nutrient-independent proliferation of the mushroom body neuroblasts (MB NBs) in *Drosophila*

Abstract:

The Hippo signaling pathway is evolutionarily conserved across the animal kingdom and plays a role in regulating cell growth and proliferation in a context dependent manner. We have discovered that Yorkie, the downstream effector molecule of the Hippo signaling pathway, is required for the nutrient-independent proliferation of MB NBs during nutrient restriction. A very similar observation was made for Myc, and we found that there is a growth regulatory feedback interaction between Yorkie and Myc which ensures MB NB proliferation during nutrient withdrawal. Yorkie is a transcriptional coactivator and requires a binding partner for its function. We found that Scalloped, the most well-known Yorkie binding partner, is not required for Yorkie function. We also screened G-protein coupled receptors (GPCRs) as potential candidate molecules upstream of the Hippo signaling pathway that can affect Yorkie function in response to various extrinsic cues. We identified five GPCRs as potential candidate regulators of growth and proliferation in the brain: *Octβ1R, AdoR, Smoothened, 5-HT1B* and *CCHa1-R*.

Introduction:

Neural stem cell (NSC) proliferation is regulated by the interaction between cell extrinsic and intrinsic factors [1–3]. *Drosophila* NSCs, known as neuroblasts (NBs), are a great model system to study the role played by both cell intrinsic and extrinsic factors in controlling this proliferation. The *Drosophila* brain consists of two central brain lobes and a ventral nerve cord. There are approximately 100 NBs in each brain lobe and that

number remains fixed throughout brain development. Most of the NBs enter quiescence at the end of the embryonic stage and their reactivation in the larval brain requires freshly hatched larvae to feed on a complete diet. Cell extrinsic nutrient cues turn on evolutionarily conserved PI3K signaling which in turn promotes growth and proliferation of these quiescent NBs [1]. There is, however, a small subset of NBs known as mushroom body neuroblasts (MB NBs) in each brain hemisphere that do not enter developmental quiescence at the end of the embryonic stage. MB NBs are able to continue their proliferation in a nutrient-independent manner which suggests that MB NBs have transcriptional machinery different from that of the non-MB NBs. A recent study has identified Eyeless (Ey) as one of the factors that allows MB NBs to proliferate in a nutrient-independent manner when larvae are grown in a nutrient withdrawal medium (NWM) consisting of twenty percent sucrose in PBS [1]. Whether there might be other genes/factors/signaling pathways involved in this process is unknown.

Hippo signaling is an evolutionarily conserved signaling pathway well known for its role in cell survival and cell proliferation. The Hippo signaling pathways consist of a core kinase cascade, composed of Warts and Hippo kinase in *Drosophila*, which regulates the activity of a transcriptional coactivator molecule [4–6]. Yorkie (Yki) is the Hippo signaling downstream transcriptional coactivator molecule in *Drosophila*. Yki is phosphorylated by Warts which inhibits Yki localization to the nucleus and keeps Yki cytoplasmic. When Yki is not phosphorylated, it translocate to the nucleus and induces the expression of genes involved in cell growth and proliferation. Hippo signaling was first discovered in *Drosophila* and was shown to regulate normal growth in the eye and wing tissues [7]. However, a

recent study has demonstrated that Hippo signaling does not control normal homeostatic tissue growth in either mouse liver or *Drosophila* imaginal discs; instead, it turns on ectopic growth signaling pathways when YAP/TAZ/Yki is overexpressed [8]. Hippo signaling is known to regulate the maintenance of NB quiescence in the freshly hatched *Drosophila* larval brain [9]. However, it remains unknown whether Hippo signaling plays a role in controlling MB NB nutrient-independent proliferation.

The Hippo signaling pathway is considered to be a master regulator of organ growth. It has the capacity to modulate its activity in response to various cues such as cell shape, cell adhesion and overall tissue integrity [5,7,8]. Here we report that in *Drosophila*, the Hippo signaling pathway controls nutrient-independent proliferation of MB NBs during nutrient restriction. We made a very similar observation when we knocked down or overexpressed Myc in the NBs. We also found a regulatory feedback interaction between Yki and Myc that maintains MB NBs nutrient-independent proliferation. Finally, we evaluated the role of the Yorkie binding partner Sd in controlling MB NB proliferation under conditions of food withdrawal (AFW). We found that Sd is expressed ubiquitously in the *Drosophila* larval brain, but it is not required for the MB NBs nutrient-independent proliferation after 7 days of food withdrawal.

Results:

Yorkie (Yki) is necessary and sufficient for the nutrient-independent proliferation of the MB NBs

Yki is the mediator of the Hippo signaling pathway. We asked whether Yki plays a role in MB NB nutrient-independent proliferation. To test this possibility, we fed freshly hatched larvae for 24 hours and then transferred them to a nutrient withdrawal medium (NWM) consisting of 20 percent sucrose in PBS, for up to 8 days. After 8 days of food withdrawal, only four MB NBs incorporated EdU in the wild type (worniuGAl4 x O R) larval brain **(Fig 5.1 A)**. In contrast, MB NBs stopped incorporating EdU at 8 days AFW when Yki was knocked down in the NBs (*worGAL4 > UAS-yki-RNAi*) **(Fig 5.1 B)**. Next, we asked whether Yki is sufficient for the nutrient-independent proliferation of NBs. We overexpressed Yki in a NB specific manner (*worGAL4 > UASYki*) and then put 24 hours fed larvae in NWM for up to 7 days. At 7 days AFW, non-MB NBs in the Yki overexpressed animals continued to incorporate EdU just as MB NBs **(Fig 5.1 D)**. From these observations, we conclude that Yki is required for MB NBs to proliferate in a nutrient-independent manner and that Yki is also sufficient to keep non-MB NBs proliferating once reactivated from quiescence.

Myc is required for nutrient-independent proliferation of the MB NBs

Myc is well known for its role as a master regulator of cell growth and proliferation in homeostatic and disease conditions [10,11]. We used an antibody against Myc to investigate whether Myc is expressed in the *Drosophila* brain. In the freshly hatched larval

brain, Myc was expressed both in the proliferating MB NBs and quiescent non-MBNBs. At 24 hours ALH, Myc was only expressed in the proliferating MB NBs. Myc was expressed only in the MB NBs when the larvae were raised in a NWM for 7 days, suggesting that Myc might play a role in nutrient-independent proliferation of the MB NBs in the *Drosophila* brain **(Fig 5.2 A)**. To test this hypothesis, we knocked down Myc in all NBs (*worGAL4 > UAS-myc-RNAi*) and fed the freshly hatched larvae for 24 hours on a complete diet before transferring them to a NWM where they were raised for up to 7 days. In the freshly hatched larval brains, all of the four MB NBs in a single brain lobe incorporated EdU when Myc was knocked down. Most of the non-MB NBs achieved reactivation by 24 hours ALH. However, once put in the NWM, non-MB NBs started to exit the cycle gradually and by 5 days AFW only four MB NBs were positive for EdU. By 7 days AFW, there were no EdU positive NBs in the larval brain when Myc was knocked down **(Fig 5.2 B)**. When we fed the 7 days AFW larvae with a complete diet for 24 hours, the NBs started to incorporate EdU again. Taken together, these experiments indicate that Myc is necessary for nutrient-independent proliferation of NBs. Next, we asked whether Myc is sufficient for NBs to proliferate in a nutrient-independent manner. To test this hypothesis, we overexpressed Myc in the NBs (*worGAL4 > UAS-myc*) and again fed the freshly hatched larvae with a complete diet before transferring them to a NWM for up to 7 days. Only four MB NBs were seen incorporating EdU in the freshly hatched larval brain where Myc was overexpressed. By 24 hours ALH, most of the non-MB NBs reactivated from quiescence. We observed non-MB NBs along with the MB NBs continuing to incorporate EdU during 7 days AFW when Myc was overexpressed in the

NBs **(Fig 5.2 C)**. From these observations, we conclude that Myc is both necessary and sufficient for the nutrient-independent proliferation of the NBs in the *Drosophila* brain.

Regulatory feedback between Myc and Yki maintains nutrient-independent proliferation of the MBNBs

Next, we asked whether there is a regulatory feedback mechanism between Myc and Yki that controls nutrient-independent proliferation of the MB NBs. First, we overexpressed Myc in the NBs when Yki was knocked down (*worGAL4; UAS-myc > UAS-yki-RNAi*) and raised the larvae in a NWM for 7 days. Overexpression of Myc was able to rescue MB NB proliferation when Yki was knocked down **(Fig 5.3 A, C)**. Next, we overexpressed Yki in NBs when Myc was knocked down (*worGAL4; UAS-yki > UAS-myc-RNAi)* and raised the larvae in a NWM for 7 days. Yki overexpression was able to rescue MB NB proliferation when Myc was knocked down **(Fig 5.3 B, C)**. We conclude that there is a regulatory feedback mechanism between Yki and Myc which controls the nutrient-independent proliferation of the MB NBs.

Yki binding partner Scalloped (Sd) is expressed at 7 days AFW but not required for nutrient-independent proliferation of the MB NBs

Yki is a transcriptional coactivator that requires a binding partner to exert its regulatory effect on cell growth and proliferation. Scalloped (Sd) is the most well-known Yki binding partner in *Drosophila* across multiple tissues [12,13]. We used an antibody against Sd to study its expression in the freshly hatched, 24-hour fed and 7 days AFW

larval brains. We found Sd to be expressed in the MB NBs during all the aforementioned time points **(Fig 5.4 A)**. Next, we asked whether Yki requires Sd to control nutrient-independent proliferation of the MB NBs. We knocked down Sd in the NBs (*worGAL4 > UAS-sd-RNAi*) and performed a standard nutrient withdrawal study for 7 days. We found that MB NBs still incorporated EdU when Sd was knocked down **(Fig 5.4 B, C)**. This suggests that Sd is not the Yki binding partner in the MB NBs that is required for nutrient-independent proliferation

GPCRs are potential upstream regulators of the Hippo signaling pathway

Studies in mammalian cell lines have shown that G-protein coupled receptors (GPCRs) are able to regulate cell proliferation in response to extrinsic cues by modulating Hippo signaling [14]. It remains to be determined whether GPCRs are able to regulate *Drosophila* MB NB proliferation in varying nutrient conditions via the Hippo signaling pathway. There are over 200 GPCR genes in the *Drosophila* genome and 116 of them are classical seven pass transmembrane proteins [15]. To determine whether any of the classic GPCRs are involved in the regulation of growth and proliferation in the *Drosophila* brain, we knocked down individual GPCRs using the *OK107GAL4* driver. *OK107GAL4* is an eye specific driver and we looked for eye specific phenotypes in the knockdown animals. Out of 116 GPCRs, only five of them when knocked down produced visible eye morphology disruption phenotypes **(Fig 5.5 and Supplementary table)**. We hypothesize that these five GPCRs involved in eye development could potentially be involved in *Drosophila* brain cell growth and proliferation.

Discussion:

We have found that Yorkie and Myc interact with each other to support nutrient-independent proliferation of the MB NBs during nutrient withdrawal. Yorkie is a transcriptional coactivator in the Hippo signaling pathway, which controls organ size and tissue homeostasis by regulating cell proliferation and apoptosis [12]. Myc is a well-known transcription factor that promotes cell growth and proliferation. Yki can directly induce the expression of Myc, enhancing Myc's role in promoting cell growth and proliferation. Myc, in turn, can further amplify the transcriptional activity of Yki by enhancing the expression of Yki target genes. Studies in *Drosophila* have shown that Yki directly regulates Myc expression which promotes tissue growth in imaginal discs [16]. In mammals, YAP (the homolog of Yki) and Myc also interact similarly, with YAP promoting Myc expression and Myc enhancing YAP activity. For instance, studies have shown that YAP can upregulate Myc in liver tissues, contributing to liver size and regeneration [17,18].

Yki interacts with several binding partners to execute its functions. Scalloped (Sd) is the most well-known Yorkie binding partner which is a transcription factor that forms a complex with Yorkie to regulate gene expression [12]. We have found that Sd knockdown does not affect the MB NBs ability to proliferate in a nutrient-independent manner. This suggests that Sd is not the Yki binding partner in the NBs although Sd is ubiquitously expressed in the fly brain. Homothorax is another transcription factor that works with Yorkie to regulate gene expression during development [19]. Yki is also known to interact with Nervous Wreck (Nwk) to regulate synaptic growth and function, linking the Hippo pathway to neural development [20]. *Drosophila* MAD (dMad) is another transcription factor

in the TGF-β signaling pathway which has been reported to interact with Yki to regulate cell growth and proliferation [21]. It will be of interest to determine if any of these transcription factors interact with Yki to regulate nutrient-independent NB proliferation.

Finally, we have identified six GPCRs that are potential upstream regulators of the Hippo signaling pathways. Our future research will investigate the function of these six GPCRs with the goal of linking Hippo signaling pathway activity with extrinsic environmental cues via GPCRs.

Materials and methods:

Fly stocks

Oregon R, WorniuGal4, UAS-YkiRNAi (BDSC), UAS-YkiOE (BDSC), UAS-MycRNAi, UAS-Myc, UAS-SdRNAi (BDSC), UAS-Sd (BDSC), OK107Gal4, 116 classic GPCRs (listed below, all from BDSC).

Nutrient-withdrawal study

Nutrient withdrawal was performed as described elsewhere (Sipe and Siegrist, 2017). Briefly, freshly hatched *Drosophila* larvae were transferred to a complete diet for 24 hours. Next, they were transferred to a nutrient withdrawal media, consisting of 20 percent

sucrose in PBS, for up to 8 days. Larvae were removed from the media and brains were dissected at indicated time points.

EdU labeling

EdU staining was performed to assess proliferation. For EdU labeling, animals were fed 0.1mg/ml EdU mixed in with BL food or into the NWM directly for time periods indicated in the figures. Larval brains were dissected in PBT and fixed in 4% paraformaldehyde/PEM for 20 min, followed by detection of EdU using the Click-iT EdU imaging kit (Molecular Probes, Eugene, OR).

Data quantification

Deadpan staining was used for identifying NBs. Leica images were opened with Fiji and the number of Dpn and EdU positive cells were quantified manually. Graphpad Prism 10 was used for making the graphs. One way ANOVA was performed for verifying statistical significance. Final images were put together using image processing software Adobe Photoshop and Adobe Illustrator.

Figures

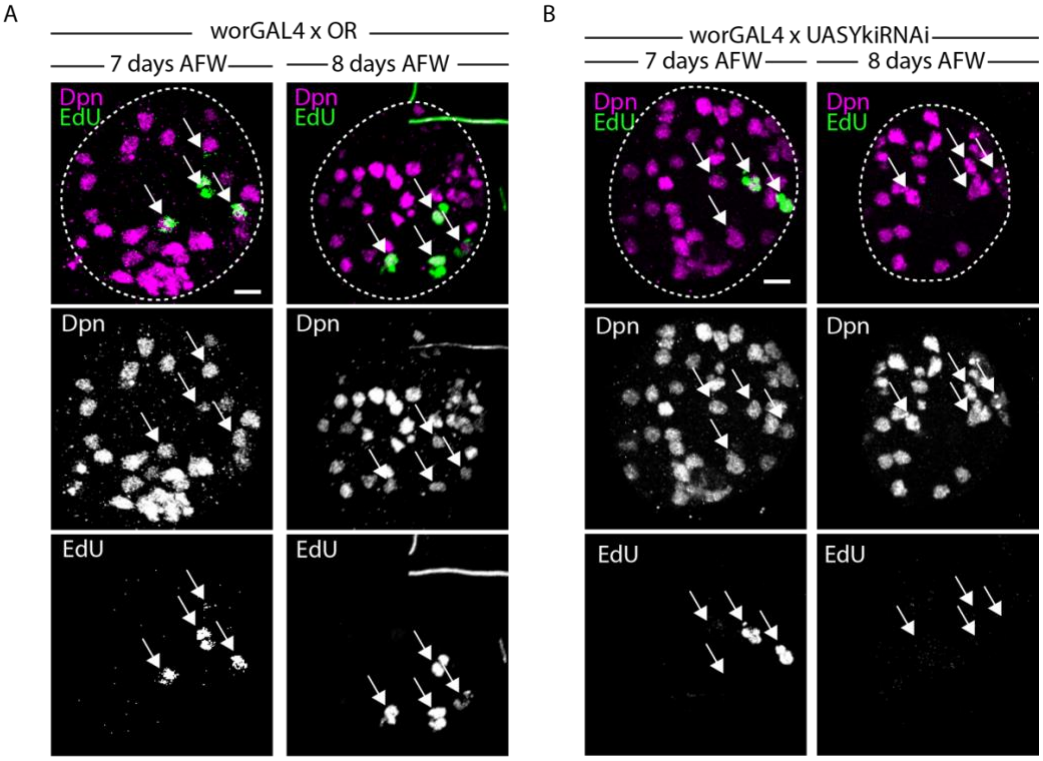
A
worGAL4 x OR
7 days AFW
8 days AFW
Dpn
EdU
B
worGAL4 x UASYkiRNAi
7 days AFW
8 days AFW
Dpn
EdU

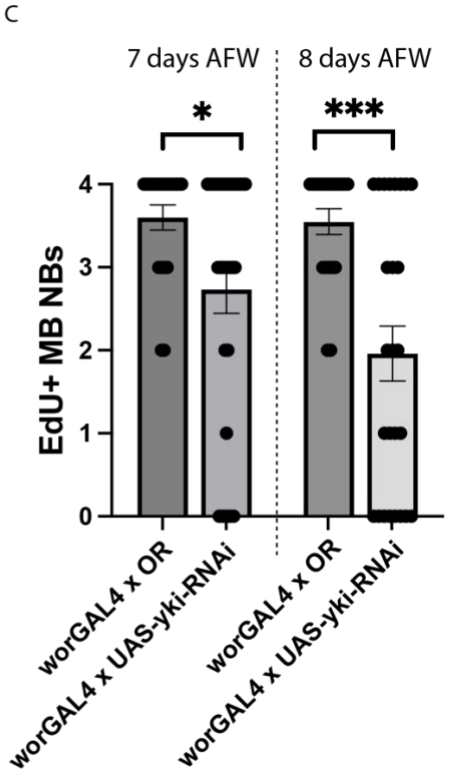
C
7 days AFW
8 days AFW
*
***
EdU+ MB NBs
0
1
2
3
4
worGAL4 x OR
worGAL4 x UAS-yki-RNAi
worGAL4 x OR
worGAL4 x UAS-yki-RNAi

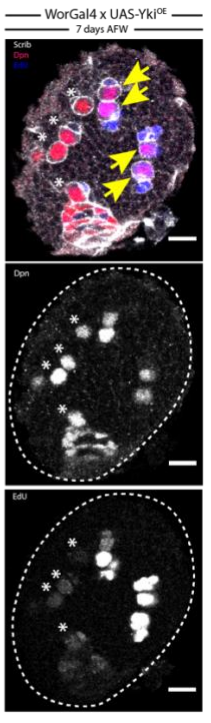
D
WorGal4 x UAS-Yki^OE
7 days AFW
Scrib
Dpn
EdU

Fig 5.1: Yorkie is necessary and sufficient for nutrient-independent proliferation of MB NBs. (A,B,D) Top 15 optical sections of confocal images showing single brain lobes of indicated genotypes at indicated time points. Deadpan marks the NBs and EdU incorporation indicates NB proliferation. White arrows indicate MB NBs. **(A)** In control animals (*worGal4 x OR*), MB NBs continue to incorporate EdU at 7 days and 8 days AFW. **(B)** In Yki knockdown animals (*worGal4 x UASYkiRNAi*), MB NBs gradually exit the cell cycle at 7 and 8 days AFW. **(C)** Quantification of data shown in panel A and B. One way ANOVA was performed for statistical significance. ***** $p < 0.05$, ******* $p < 0.001$. **(D)** In animals in which Yki was overexpressed in NBs, MB NBs continue to proliferate as in control brains (yellow arrows) while non-MB NBs also keep incorporating EdU as indicated by the asterisks. Arrowheads indicate MB NBs. Scale bar is 10 micrometers.

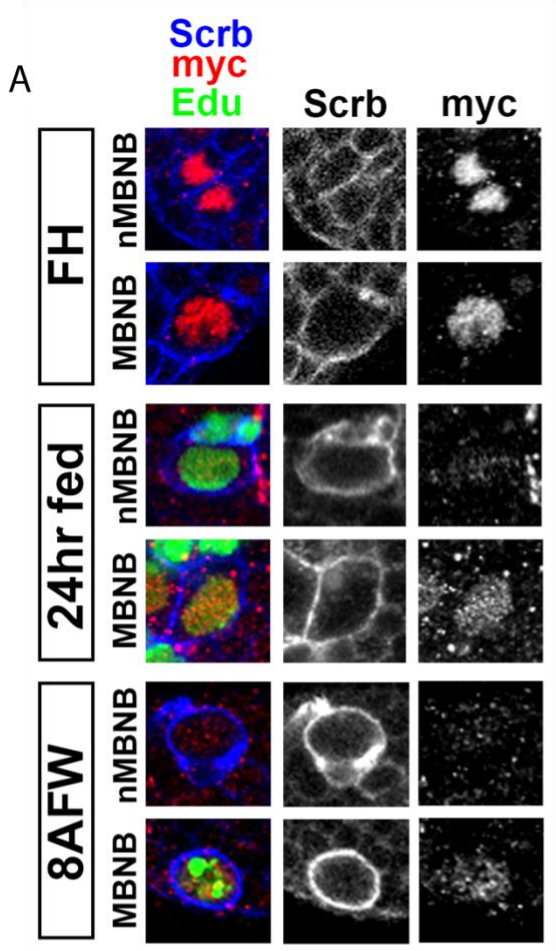
A
Scrb
myc
Edu
Scrb
myc
FH
24hr fed
8AFW
nMBNB
MBNB

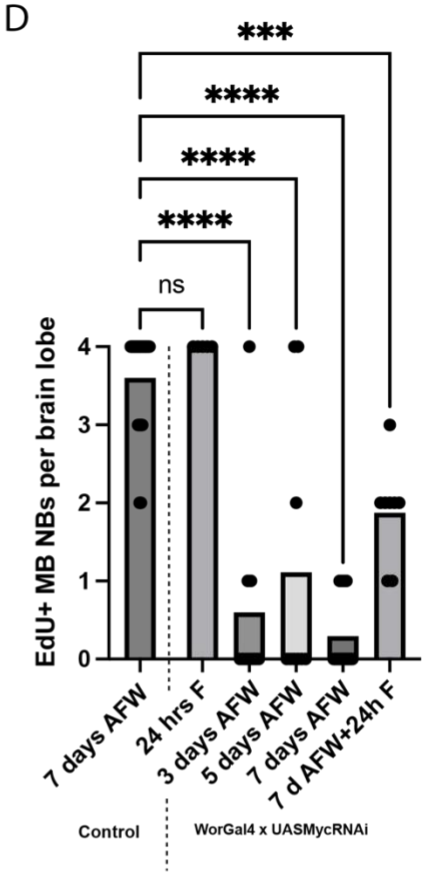
D
***
****
****
****
ns
EdU+ MB NBs per brain lobe
0
1
2
3
4
7 days AFW
24 hrs F
3 days AFW
5 days AFW
7 days AFW
7 d AFW+24h F
Control
WorGal4 x UASMycRNAi

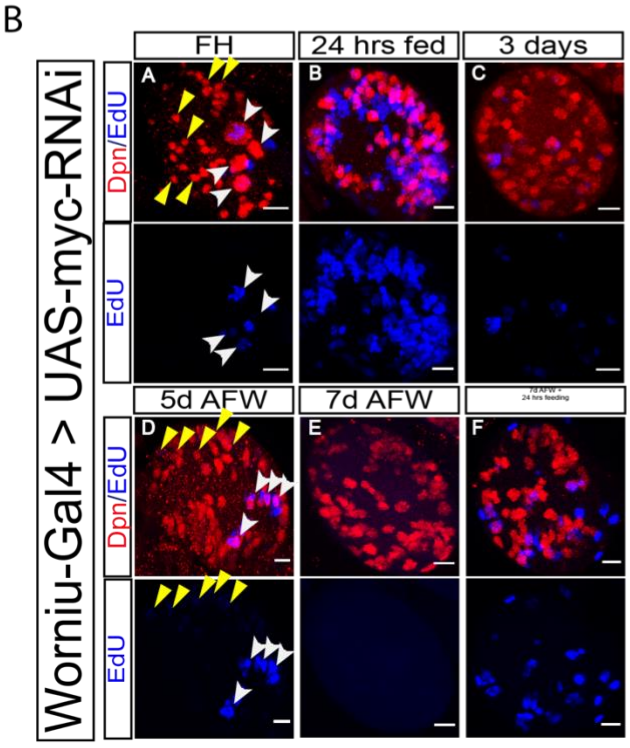
B
Worniu-Gal4 > UAS-myc-RNAi
FH
24 hrs fed
3 days
5d AFW
7d AFW
Dpn/EdU
EdU
A
B
C
D
E
F

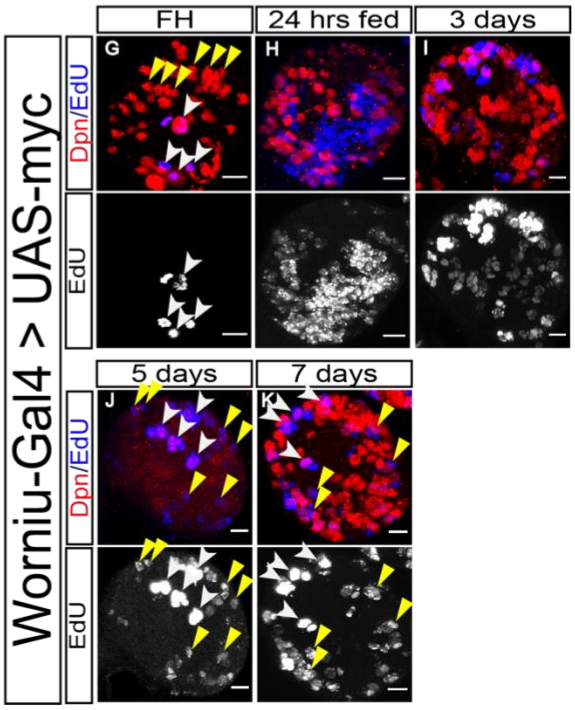
C
Worniu-Gal4 > UAS-myc
FH
24 hrs fed
3 days
5 days
7 days
Dpn/EdU
EdU
G
H
I
J
K

Fig 5.2: Myc is necessary and sufficient for the nutrient-independent proliferation of the MB NBs. (A) Myc is expressed in both MB NBs and non-MB NBs in freshly hatched larval brains. At 24 hours ALH and 8 days AFW, only MB NBs express Myc. **(B-C)** Top 60 optical sections of confocal images showing single brain lobes of indicated genotypes at indicated time points. Deadpan marks the NBs and EdU incorporation indicates NBs proliferation. White arrowheads indicate MB NBs and yellow arrowheads indicate non-MB NBs **(B)** NB specific Myc knockdown causes MB NBs to exit the cell cycle by 7 days AFW. 24 hours of refeeding causes the quiescent NBs to enter cell cycle again. (D) Overexpression of Myc in the NBs causes non-MB NBs to continue to incorporate EdU just as MB NBs during 7 days AFW. **(C)** Quantification of data in panel B. One way ANOVA was performed to test for statistical significance, *** $p < 0.001$, **** $p < 0.0001$. Scale bar is 10 micrometers.

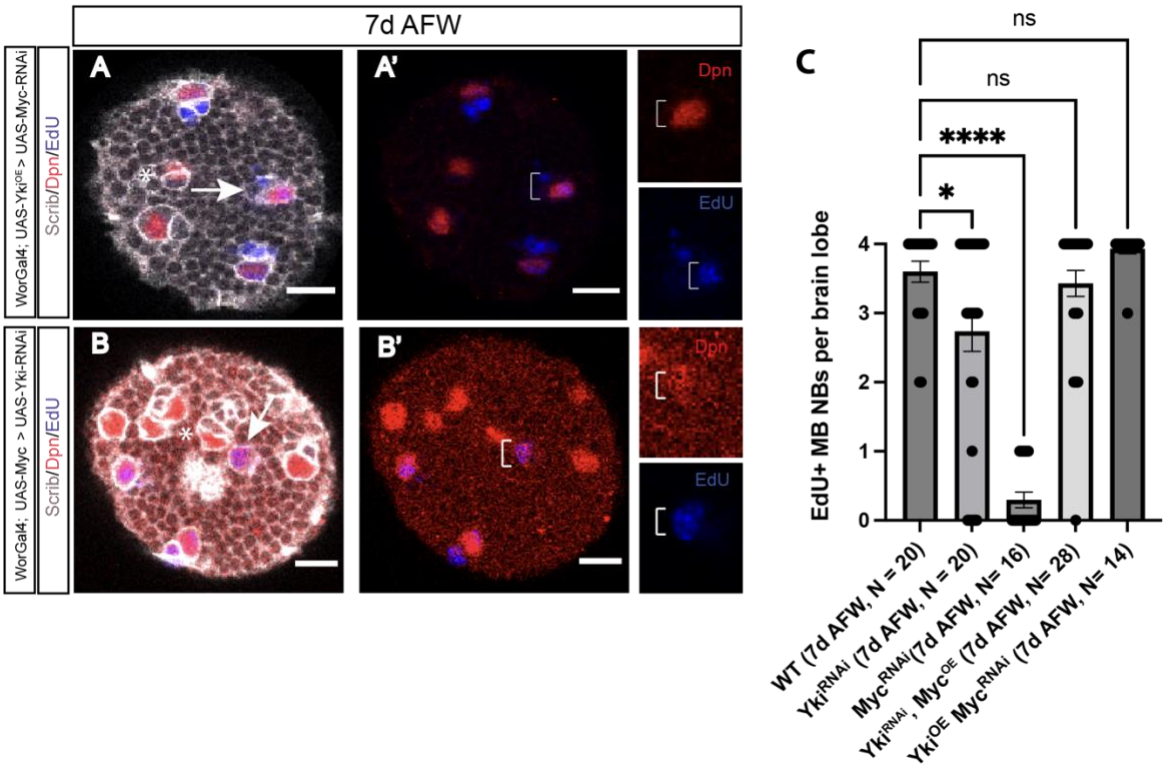

Fig 5.3: Regulatory feedback between Myc and Yorkie maintains nutrient-independent proliferation of the MBNBs. (A,B) Single optical section from the dorsal surface of brain lobes. Deadpan marks the NBs and EdU incorporation indicates NB proliferation. White arrows indicate MB NBs and asterisk marks non-MB NBs **(A-A')** Yki overexpression in Myc knockdown NBs rescues proliferation defects caused by Myc knockdown during 7 days AFW. **(B)** Myc overexpression in Yki knockdown NBs rescues proliferation defects caused by Yki knockdown during 7 days AFW. **(C)** Quantification of data in A and B. Scale bar is 10 micrometers. One way ANOVA was performed to test for statistical significance, * $p < 0.05$, **** $p < 0.0001$

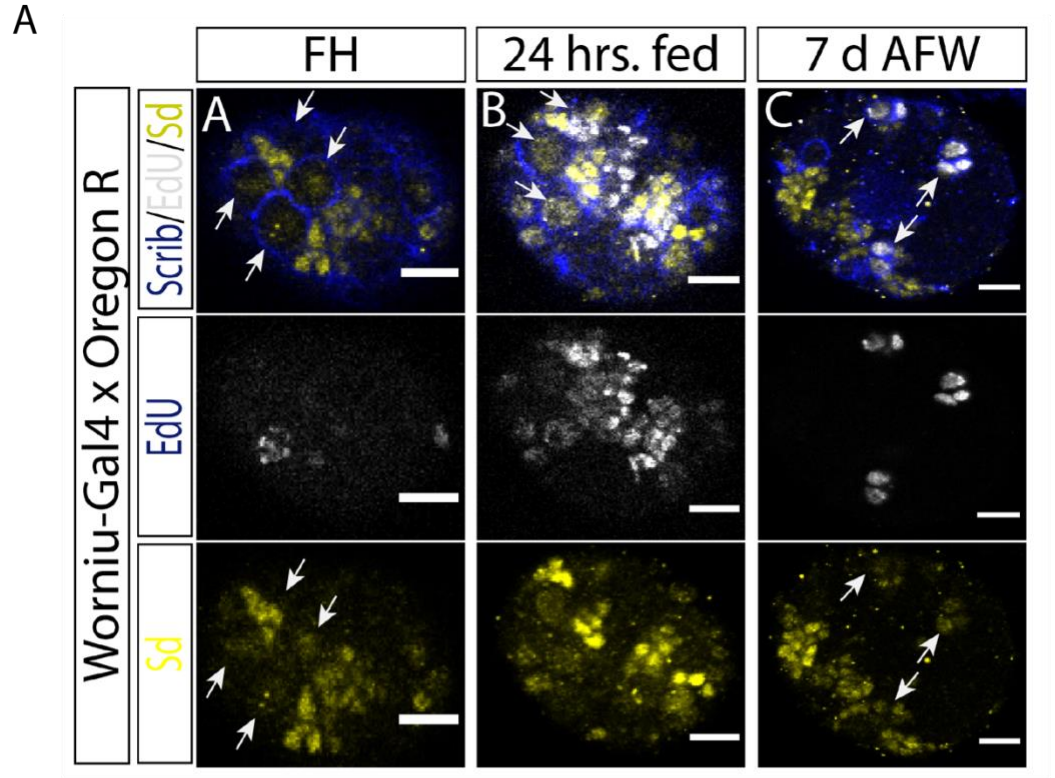
A
FH
24 hrs. fed
7 d AFW
Worniu-Gal4 x Oregon R
Scrib/EdU/Sd
EdU
Sd
A
B
C

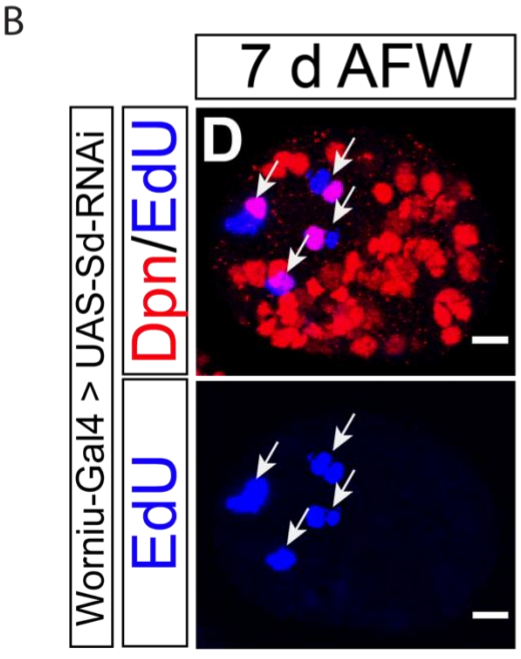
B
7 d AFW
Worniu-Gal4 > UAS-Sd-RNAi
Dpn/EdU
EdU
D

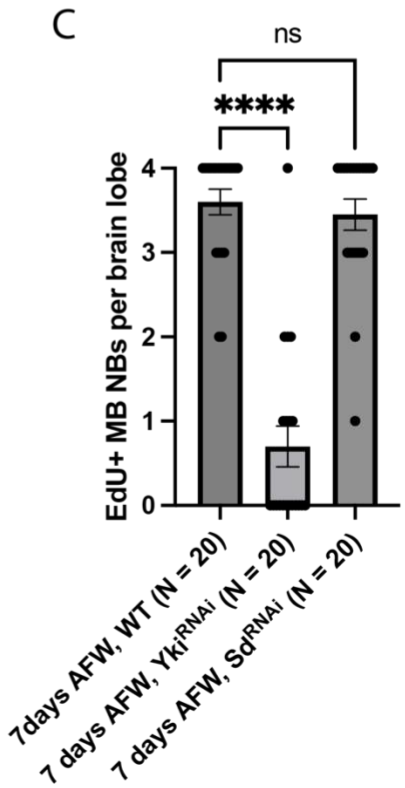
C
ns
****
EdU+ MB NBs per brain lobe
0
1
2
3
4
7days AFW, WT (N = 20)
7 days AFW, Yki^RNAi (N = 20)
7 days AFW, Sd^RNAi (N = 20)

Fig 5.4: Scalloped (Sd) is not required for Yorkie function in MB NBs during nutrient withdrawal. (A) Sd is expressed in all NBs and their progeny in freshly hatched, 24 hours ALH and 7 days AFW brains. White arrows indicate MB NBs **(B)** NB specific knockdown of Sd does not affect MB NBs proliferation at 7 days AFW. White arrows indicate MB NBs **(C)** Quantification of NB proliferation in wild type, *WorGal4>Yki RNAi* and *WorGal4 > Sd RNAi* animals at 7 days AFW. One way ANOVA was performed to test for statistical significance, **** $p < 0.0001$.

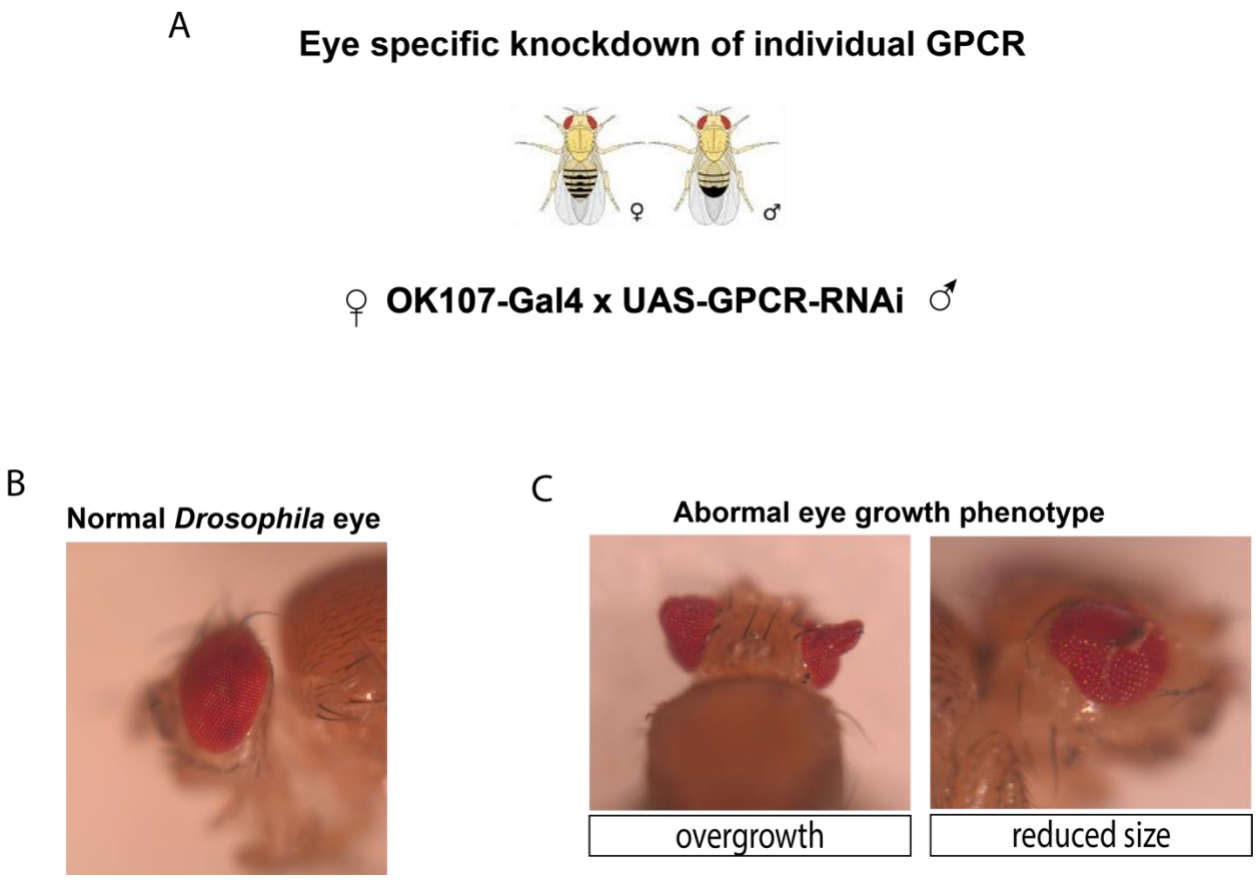

Fig 5.5: Eye specific knockdown of individual GPCRs causes growth defects in the *Drosophila* eye. **(A)** The *Drosophila* eye specific *OK107Gal4* driver was used to knock down individual GPCRs. **(B)** Normal eye morphology in a *Drosophila* Oregon R wild type animal **(C)** Abnormal eye growth was observed, either overgrowth or shrinkage, in specific GPCR knockdown animals.

Supplementary table:

GPCR name	Gene symbol	BDSC ID	Eye Phenotype
5-hydroxytryptamine (serotonin) receptor 1A	5-HT1A	25834	normal eye
5-hydroxytryptamine (serotonin) receptor 1A	5-HT1A	33885	normal eye
Adipokinetic hormone receptor	AkhR	29577	normal eye
Adipokinetic hormone receptor	AkhR	51710	normal eye
Allatostatin A receptor 1	AstA-R1	27280	normal eye
Leucine-rich repeat-containing G protein-coupled receptor 3	Lgr3	28789	normal eye
Leucine-rich repeat-containing G protein-coupled receptor 3	Lgr3	36887	NA
Leucine-rich repeat-containing G protein-coupled receptor 3	Lgr3	55910	normal eye
Pyrokinin 1 receptor	PK1-R	27539	normal eye
short neuropeptide F receptor	sNPF-R	27507	normal eye
Trapped in endoderm 1	Tre1	33718	normal eye
Trapped in endoderm 1	Tre1	38925	NA
Trapped in endoderm 1	Tre1	27672	normal eye
Trapped in endoderm 1	Tre1	34956	normal eye
Diuretic hormone 31 Receptor	Dh31-R	25925	normal eye
Dopamine 2-like receptor	Dop2R	50621	normal eye
Dopamine 2-like receptor	Dop2R	26001	normal eye
starry night	stan	26022	normal eye
starry night	stan	35050	normal eye
frizzled	fz	34321	rough eye
frizzled	fz	31311	slightly bigger eye
frizzled	fz	31036	normal eye
metabotropic GABA-B receptor subtype 1	GABA-B-R1	51817	normal eye
metabotropic GABA-B receptor subtype 1	GABA-B-R1	28353	normal eye
metabotropic Glutamate Receptor	mGluR	41668	normal eye
metabotropic Glutamate Receptor	mGluR	25938	normal eye
methuselah	mth	36823	normal eye

methuselah	mth	67829	normal eye
methuselah-like 1	mthl1	57699	normal eye
methuselah-like 1	mthl1	41930	normal eye
muscarinic Acetylcholine Receptor, A-type	mAChR-A	44469	normal eye
muscarinic Acetylcholine Receptor, A-type	mAChR-A	27571	normal eye
muscarinic Acetylcholine Receptor, B-type	mAChR-B	67775	normal eye
Octopamine receptor in mushroom bodies	Oamb	31233	normal eye
Octopamine receptor in mushroom bodies	Oamb	31171	normal eye
α2-adrenergic-like octopamine receptor	Octα2R	50678	normal eye
Octopamine β1 receptor	Octβ1R	31107	normal eye
Octopamine β1 receptor	Octβ1R	58179	shrunken/missing eye
Octopamine β1 receptor	Octβ1R	50701	normal eye
CG13579	CG13579	51053	normal eye
CG13579	CG13579	28644	normal eye
Adenosine receptor	AdoR	56866	normal eye
Adenosine receptor	AdoR	27536	very small eye
neither inactivation nor afterpotential E	ninaE	31647	normal eye
neither inactivation nor afterpotential E	ninaE	31648	normal eye
Rhodopsin 2	Rh2	77340	normal eye
Rhodopsin 3	Rh3	36885	normal eye
Rhodopsin 3	Rh3	31112	normal eye
Rhodopsin 4	Rh4	77159	normal eye
smoothened	smo	27037	normal eye
smoothened	smo	62987	eye missing
Octopamine-Tyramine receptor	Oct-TyrR	28332	normal eye
Tyramine receptor	TyrR	57496	normal eye
Tyramine receptor	TyrR	25857	normal eye
Tyramine receptor II	TyrRII	27670	normal eye
Tyramine receptor II	TyrRII	64964	normal eye
smog	smog	51705	normal eye
smog	smog	43135	normal eye
CG32447	CG32447	60466	normal eye

5-hydroxytryptamine (serotonin) receptor 1B	5-HT1B	33418	normal eye
5-hydroxytryptamine (serotonin) receptor 1B	5-HT1B	54006	rough eye
5-hydroxytryptamine (serotonin) receptor 1B	5-HT1B	51842	normal eye
bride of sevenless	boss	67317	normal eye
Trissin receptor	TrissinR	60109	normal eye
Trissin receptor	TrissinR	36825	normal eye
Tachykinin-like receptor at 99D	TkR99D	27513	normal eye
Tachykinin-like receptor at 99D	TkR99D	55732	normal eye
Tachykinin-like receptor at 86C	TkR86C	31884	normal eye
Sex peptide receptor	SPR	77389	normal eye
Diuretic hormone 44 receptor 1	Dh44-R1	28780	normal eye
Calcium-independent receptor for α-latrotoxin	Cirl	34821	normal eye
Calcium-independent receptor for α-latrotoxin	Cirl	27524	normal eye
Dopamine 1-like receptor 1	Dop1R1	31765	normal eye
Dopamine 1-like receptor 2	Dop1R2	55239	normal eye
Dopamine 1-like receptor 3	Dop1R3	62193	normal eye
Octopamine β2 receptor	Octβ2R	50580	normal eye
Octopamine β2 receptor	Octβ2R	34673	normal eye
Octopamine β3 receptor	Octβ3R	31108	normal eye
Octopamine β3 receptor	Octβ3R	62283	normal eye
Octopamine-Tyramine receptor	Oct-TyrR	28332	normal eye
5-hydroxytryptamine (serotonin) receptor 2A	5-HT2A	31882	normal
5-hydroxytryptamine (serotonin) receptor 2A	5-HT2A	56870	normal
5-hydroxytryptamine (serotonin) receptor 2B	5-HT2B	25874	normal
5-hydroxytryptamine (serotonin) receptor 2B	5-HT2B	60488	normal
5-hydroxytryptamine (serotonin) receptor 7	5-HT7	27273	NA
5-hydroxytryptamine (serotonin) receptor 7	5-HT7	32471	normal

Allatostatin A receptor 2	AstA-R2	67864	normal
Allatostatin A receptor 2	AstA-R2	25935	normal
Allatostatin C receptor 1	AstC-R1	27506	normal
Allatostatin C receptor 1	AstC-R1	62372	normal
Diuretic hormone 44 receptor 2	Dh44-R2	29610	normal
Diuretic hormone 44 receptor 2	Dh44-R2	67862	normal
CG11318	CG11318	51792	normal
CG15556	CG15556	44574	normal
Dopamine/Ecdysteroid receptor	DopEcR	31981	normal
frizzled 2	fz2	31390	normal
frizzled 2	fz2	67863	normal
frizzled 2	fz2	31312	normal
metabotropic GABA-B receptor subtype 2	GABA-B-R2	27699	normal
metabotropic GABA-B receptor subtype 2	GABA-B-R2	50608	normal
mangetout	mtt	44076	rough eye (females)
mangetout	mtt	32376	normal
Allatostatin C receptor 2	AstC-R2	25940	reorder
Allatostatin C receptor 2	AstC-R2	36888	normal eye
Capability receptor	CapaR	27275	normal eye
Crustacean cardioactive peptide receptor	CCAP-R	31490	normal eye
CCHamide-1 receptor	CCHa1-R	27669	normal eye
CCHamide-1 receptor	CCHa1-R	51168	rough, small eyes
CCHamide-2 receptor	CCHa2-R	25855	normal eye
Cholecystokinin-like receptor at 17D1	CCKLR-17D1	67865	normal eye
Cholecystokinin-like receptor at 17D1	CCKLR-17D1	27494	NA
Cholecystokinin-like receptor at 17D3	CCKLR-17D3	67866	normal eye
Cholecystokinin-like receptor at 17D3	CCKLR-17D3	28333	normal eye
hector	hec	29623	reorder
Pigment-dispersing factor receptor	Pdfr	42508	normal eye
Pigment-dispersing factor receptor	Pdfr	38347	normal eye

frizzled 3	fz3	44468	normal eye
frizzled 3	fz3	66951	NA
frizzled 4	fz4	64990	normal eye
metabotropic GABA-B receptor subtype 3	GABA-B-R3	50622	normal eye
metabotropic GABA-B receptor subtype 3	GABA-B-R3	42752	NA
methuselah-like 2	mthl2	65041	NA
methuselah-like 3	mthl3	36822	normal eye
methuselah-like 3	mthl3	62496	normal eye
methuselah-like 4	mthl4	55244	normal eye
methuselah-like 5	mthl5	65073	normal eye
methuselah-like 5	mthl5	36884	normal eye
muscarinic Acetylcholine Receptor, C-type	mAChR-C	61306	normal eye
muscarinic Acetylcholine Receptor, C-type	mAChR-C	29612	normal eye
Rhodopsin 5	Rh5	67971	normal eye
Rhodopsin 6	Rh6	56029	NA
Rhodopsin 7	Rh7	62176	normal eye
rickets	rk	31958	normal eye
RYamide receptor	RYa-R	25944	normal eye
SIFamide receptor	SIFaR	34947	normal eye
SIFamide receptor	SIFaR	25831	normal eye
SIFamide receptor	SIFaR	44068	NA
Proctolin receptor	Proc-R	29414	normal eye
Pyrokinin 2 receptor 3	PK2-R2	28781	NA
Pyrokinin 2 receptor 1	PK2-R1	29624	NA
Neuropeptide F receptor	NPFR	25939	normal eye
Myosuppressin receptor 2	MsR2	67869	normal eye
Myosuppressin receptor 3	MsR2	25832	NA
Myosuppressin receptor 1	MsR1	27529	NA
moody	moody	66326	normal eye
Leucokinin receptor	Lkr	65934	normal eye
Leucokinin receptor	Lkr	25936	normal eye
Leucine-rich repeat-containing G protein-coupled receptor 4	mthl6	28655	normal eye

Leucine-rich repeat-containing G protein-coupled receptor 1	Lgr1	51465	normal eye
Leucine-rich repeat-containing G protein-coupled receptor 1	Lgr1	27509	normal eye
FMRFamide Receptor	FMRFaR	25858	normal eye
ETHR	ETHR	28783	NA
ETHR	ETHR	51828	normal eye
Corazonin receptor	CrzR	42751	normal eye
Corazonin receptor	CrzR	26017	normal eye
methuselah-like 6	mthl6	44497	normal eye
methuselah-like 7	mthl7	44498	normal eye
methuselah-like 8	mthl8	60373	normal eye
methuselah-like 9	mthl9	51695	normal eye
methuselah-like 9	mthl9	62896	normal eye
methuselah-like 10	mthl10	51753	normal eye
methuselah-like 10	mthl10	62315	normal eye
CG4313	CG4313	32960	normal eye
CG12290	CG12290	42520	NA
CG12290	CG12290	31873	normal eye
CG13229	CG13229	29419	NA
CG13575	CG13575	25827	normal eye
CG13995	CG13995	26733	normal eye
CG30340	CG30340	67867	normal eye
CG30340	CG30340	28652	NA
CG32547	CG32547	67868	normal eye
CG32547	CG32547	28621	normal eye
CG33639	CG33639	28614	normal eye
CNMamide Receptor	CNMaR	28380	normal eye
CNMamide Receptor	CNMaR	57859	normal eye
methuselah-like 11	mthl11	62008	normal eye
methuselah-like 11	mthl11	64481	normal eye
methuselah-like 12	mthl12	44516	normal eye
methuselah-like 13	mthl13	65203	normal eye

methuselah-like 14	mthl14	67342	normal eye
methuselah-like 15	mthl15	28017	normal eye
methuselah-like 15	mthl15	42515	normal eye
CG12290	CG12290	42520	normal eye
CG13229	CG13229	29419	normal eye
Leucine-rich repeat-containing G protein-coupled receptor 4	Lgr4	28655	normal eye
Leucine-rich repeat-containing G protein-coupled receptor 3	Lgr3	36887	normal eye
Trapped in endoderm 1	Tre1	38925	normal eye
Octopamine-Tyramine receptor	Oct-TyrR	28332	NA
Allatostatin C receptor 2	AstC-R2	25940	normal eye
hector	hec	29623	normal eye
frizzled 3	fz3	66951	normal eye
metabotropic GABA-B receptor subtype 3	GABA-B-R3	42752	NA
CG30340	CG30340	28652	normal eye
Octopamine-Tyramine receptor	Oct-TyrR	28332	NA
Octopamine β1 receptor	Octβ1R	58179	NA
Adenosine receptor	AdoR	27536	normal eye
Cholecystokinin-like receptor at 17D1	CCKLR-17D1	27494	normal eye
Rhodopsin 6	Rh6	56029	normal eye
SIFamide receptor	SIFaR	44068	normal eye
Pyrokinin 2 receptor 3	PK2-R2	28781	normal eye
Pyrokinin 2 receptor 1	PK2-R1	29624	NA
Myosuppressin receptor 3	MsR2	25832	normal eye
Myosuppressin receptor 1	MsR1	27529	normal eye
ETHR	ETHR	28783	normal eye

References:

1. Sipe CW, Siegrist SE. Eyeless uncouples mushroom body neuroblast proliferation from dietary amino acids in Drosophila. *eLife*. 6:e26343. doi:10.7554/eLife.26343

2. Britton JS, Edgar BA. Environmental control of the cell cycle in Drosophila: nutrition activates mitotic and endoreplicative cells by distinct mechanisms. *Dev Camb Engl*. 1998;125(11):2149-2158. doi:10.1242/dev.125.11.2149

3. Sousa-Nunes R, Yee LL, Gould AP. Fat cells reactivate quiescent neuroblasts via TOR and glial insulin relays in Drosophila. *Nature*. 2011;471(7339):508-512. doi:10.1038/nature09867

4. Poon CLC, Mitchell KA, Kondo S, Cheng LY, Harvey KF. The Hippo Pathway Regulates Neuroblasts and Brain Size in Drosophila melanogaster. *Curr Biol CB*. 2016;26(8):1034-1042. doi:10.1016/j.cub.2016.02.009

5. Snigdha K, Gangwani KS, Lapalikar GV, Singh A, Kango-Singh M. Hippo Signaling in Cancer: Lessons From Drosophila Models. *Front Cell Dev Biol*. 2019;7. doi:10.3389/fcell.2019.00085

6. Fu M, Hu Y, Lan T, Guan KL, Luo T, Luo M. The Hippo signalling pathway and its implications in human health and diseases. *Signal Transduct Target Ther*. 2022;7(1):1-20. doi:10.1038/s41392-022-01191-9

7. Pan D. The Hippo Signaling Pathway in Development and Cancer. *Dev Cell*. 2010;19(4):491-505. doi:10.1016/j.devcel.2010.09.011

8. Kowalczyk W, Romanelli L, Atkins M, et al. Hippo signaling instructs ectopic but not normal organ growth. *Science*. 2022;378(6621):eabg3679. doi:10.1126/science.abg3679

9. Ding R, Weynans K, Bossing T, Barros CS, Berger C. The Hippo signalling pathway maintains quiescence in Drosophila neural stem cells. *Nat Commun*. 2016;7(1):10510. doi:10.1038/ncomms10510

10. Dang CV. *MYC* on the Path to Cancer. *Cell*. 2012;149(1):22-35. doi:10.1016/j.cell.2012.03.003

11. Elend M, Eilers M. Cell growth: Downstream of Myc – to grow or to cycle? *Curr Biol*. 1999;9(24):R936-R938. doi:10.1016/S0960-9822(00)80109-8

12. Goulev Y, Fauny JD, Gonzalez-Marti B, Flagiello D, Silber J, Zider A. SCALLOPED interacts with YORKIE, the nuclear effector of the hippo tumor-suppressor pathway in Drosophila. *Curr Biol CB*. 2008;18(6):435-441. doi:10.1016/j.cub.2008.02.034

13. Guo T, Lu Y, Li P, et al. A novel partner of Scalloped regulates Hippo signaling via antagonizing Scalloped-Yorkie activity. *Cell Res*. 2013;23(10):1201-1214. doi:10.1038/cr.2013.120

14. Yu FX, Zhao B, Panupinthu N, et al. Regulation of the Hippo-YAP pathway by G-protein-coupled receptor signaling. *Cell*. 2012;150(4):780-791. doi:10.1016/j.cell.2012.06.037

15. Hanlon CD, Andrew DJ. Outside-in signaling – a brief review of GPCR signaling with a focus on the Drosophila GPCR family. *J Cell Sci*. 2015;128(19):3533-3542. doi:10.1242/jcs.175158

16. Neto-Silva RM, Beco S de, Johnston LA. Evidence for a Growth-Stabilizing Regulatory Feedback Mechanism between Myc and Yorkie, the Drosophila Homolog of Yap. *Dev Cell*. 2010;19(4):507-520. doi:10.1016/j.devcel.2010.09.009

17. Pibiri M, Simbula G. Role of the Hippo pathway in liver regeneration and repair: recent advances. *Inflamm Regen*. 2022;42(1):59. doi:10.1186/s41232-022-00235-5

18. Fan S, Gao Y, Qu A, et al. YAP-TEAD mediates PPAR α–induced hepatomegaly and liver regeneration in mice. *Hepatol Baltim Md*. 2022;75(1):74-88. doi:10.1002/hep.32105

19. Peng HW, Slattery M, Mann RS. Transcription factor choice in the Hippo signaling pathway: homothorax and yorkie regulation of the microRNA bantam in the progenitor domain of the Drosophila eye imaginal disc. *Genes Dev*. 2009;23(19):2307-2319. doi:10.1101/gad.1820009

20. Emoto K, Parrish JZ, Jan LY, Jan YN. The tumour suppressor Hippo acts with the NDR kinases in dendritic tiling and maintenance. *Nature*. 2006;443(7108):210-213. doi:10.1038/nature05090

21. Oh H, Irvine KD. In vivo regulation of Yorkie phosphorylation and localization. *Dev Camb Engl*. 2008;135(6):1081-1088. doi:10.1242/dev.015255

References

1. Hippenmeyer S. Principles of neural stem cell lineage progression: Insights from developing cerebral cortex. *Curr Opin Neurobiol*. 2023;79:102695. doi:10.1016/j.conb.2023.102695

2. Liszewska E, Jaworski J. Neural Stem Cell Dysfunction in Human Brain Disorders. *Results Probl Cell Differ*. 2018;66:283-305. doi:10.1007/978-3-319-93485-3_13

3. Homem CCF, Repic M, Knoblich JA. Proliferation control in neural stem and progenitor cells. *Nat Rev Neurosci*. 2015;16(11):647-659. doi:10.1038/nrn4021

4. Ossola C, Kalebic N. Roots of the Malformations of Cortical Development in the Cell Biology of Neural Progenitor Cells. *Front Neurosci*. 2022;15:817218. doi:10.3389/fnins.2021.817218

5. Hazlett HC, Poe MD, Gerig G, et al. Early brain overgrowth in autism associated with an increase in cortical surface area before age 2 years. *Arch Gen Psychiatry*. 2011;68(5):467-476. doi:10.1001/archgenpsychiatry.2011.39

6. Richards GS, Rentzsch F. Transgenic analysis of a SoxB gene reveals neural progenitor cells in the cnidarian Nematostella vectensis. *Dev Camb Engl*. 2014;141(24):4681-4689. doi:10.1242/dev.112029

7. Cunningham D, Casey ES. Spatiotemporal development of the embryonic nervous system of Saccoglossus kowalevskii. *Dev Biol*. 2014;386(1):252-263. doi:10.1016/j.ydbio.2013.12.001

8. Adameyko I. Evolutionary origin of the neural tube in basal deuterostomes. *Curr Biol*. 2023;33(8):R319-R331. doi:10.1016/j.cub.2023.03.045

9. Arefin B, Parvin F, Bahrampour S, Stadler CB, Thor S. Drosophila Neuroblast Selection Is Gated by Notch, Snail, SoxB, and EMT Gene Interplay. *Cell Rep*. 2019;29(11):3636-3651.e3. doi:10.1016/j.celrep.2019.11.038

10. Hartenstein V, Stollewerk A. The Evolution of Early Neurogenesis. *Dev Cell*. 2015;32(4):390-407. doi:10.1016/j.devcel.2015.02.004

11. Doe CQ. Neural stem cells: balancing self-renewal with differentiation. *Dev Camb Engl*. 2008;135(9):1575-1587. doi:10.1242/dev.014977

12. Homem CCF, Knoblich JA. Drosophila neuroblasts: a model for stem cell biology. *Dev Camb Engl*. 2012;139(23):4297-4310. doi:10.1242/dev.080515

13. Gage FH. Mammalian neural stem cells. *Science*. 2000;287(5457):1433-1438. doi:10.1126/science.287.5457.1433

14. Sasai Y. Roles of Sox factors in neural determination: conserved signaling in evolution? *Int J Dev Biol*. 2001;45(1):321-326.

15. Bylund M, Andersson E, Novitch BG, Muhr J. Vertebrate neurogenesis is counteracted by Sox1-3 activity. *Nat Neurosci*. 2003;6(11):1162-1168. doi:10.1038/nn1131

16. Elkouris M, Balaskas N, Poulou M, et al. Sox1 maintains the undifferentiated state of cortical neural progenitor cells via the suppression of Prox1-mediated cell cycle exit and neurogenesis. *Stem Cells Dayt Ohio*. 2011;29(1):89-98. doi:10.1002/stem.554

17. Mizuseki K, Kishi M, Shiota K, Nakanishi S, Sasai Y. SoxD: an essential mediator of induction of anterior neural tissues in Xenopus embryos. *Neuron*. 1998;21(1):77-85. doi:10.1016/s0896-6273(00)80516-4

18. Niehrs C. On growth and form: a Cartesian coordinate system of Wnt and BMP signaling specifies bilaterian body axes. *Dev Camb Engl*. 2010;137(6):845-857. doi:10.1242/dev.039651

19. Beatus P, Lendahl U. Notch and neurogenesis. *J Neurosci Res*. 1998;54(2):125-136. doi:10.1002/(SICI)1097-4547(19981015)54:2<125::AID-JNR1>3.0.CO;2-G

20. Kageyama R, Ohtsuka T, Kobayashi T. Roles of Hes genes in neural development. *Dev Growth Differ*. 2008;50 Suppl 1:S97-103. doi:10.1111/j.1440-169X.2008.00993.x

21. Stigloher C, Chapouton P, Adolf B, Bally-Cuif L. Identification of neural progenitor pools by E(Spl) factors in the embryonic and adult brain. *Brain Res Bull*. 2008;75(2-4):266-273. doi:10.1016/j.brainresbull.2007.10.032

22. Zhang R, Quan H, Wang Y, Luo F. Neurogenesis in primates versus rodents and the value of non-human primate models. *Natl Sci Rev*. 2023;10(11):nwad248. doi:10.1093/nsr/nwad248

23. Huttner WB, Kosodo Y. Symmetric versus asymmetric cell division during neurogenesis in the developing vertebrate central nervous system. *Curr Opin Cell Biol*. 2005;17(6):648-657. doi:10.1016/j.ceb.2005.10.005

24. Wang X, Tsai JW, LaMonica B, Kriegstein AR. A new subtype of progenitor cell in the mouse embryonic neocortex. *Nat Neurosci*. 2011;14(5):555-561. doi:10.1038/nn.2807

25 Martínez-Cerdeño V, Cunningham CL, Camacho J, et al. Comparative analysis of the subventricular zone in rat, ferret and macaque: evidence for an outer subventricular zone in rodents. *PloS One*. 2012;7(1):e30178. doi:10.1371/journal.pone.0030178

26. Kriegstein A, Alvarez-Buylla A. The Glial Nature of Embryonic and Adult Neural Stem Cells. *Annu Rev Neurosci*. 2009;32:149-184. doi:10.1146/annurev.neuro.051508.135600

27. Mori T, Buffo A, Götz M. The novel roles of glial cells revisited: the contribution of radial glia and astrocytes to neurogenesis. *Curr Top Dev Biol*. 2005;69:67-99. doi:10.1016/S0070-2153(05)69004-7

28. Hansen DV, Lui JH, Parker PRL, Kriegstein AR. Neurogenic radial glia in the outer subventricular zone of human neocortex. *Nature*. 2010;464(7288):554-561. doi:10.1038/nature08845

29. Haubensak W, Attardo A, Denk W, Huttner WB. Neurons arise in the basal neuroepithelium of the early mammalian telencephalon: a major site of neurogenesis. *Proc Natl Acad Sci U S A*. 2004;101(9):3196-3201. doi:10.1073/pnas.0308600100

30. Noctor SC, Martínez-Cerdeño V, Ivic L, Kriegstein AR. Cortical neurons arise in symmetric and asymmetric division zones and migrate through specific phases. *Nat Neurosci*. 2004;7(2):136-144. doi:10.1038/nn1172

31. Kriegstein A, Noctor S, Martínez-Cerdeño V. Patterns of neural stem and progenitor cell division may underlie evolutionary cortical expansion. *Nat Rev Neurosci*. 2006;7(11):883-890. doi:10.1038/nrn2008

32. Betizeau M, Cortay V, Patti D, et al. Precursor diversity and complexity of lineage relationships in the outer subventricular zone of the primate. *Neuron*. 2013;80(2):442-457. doi:10.1016/j.neuron.2013.09.032

33. Lui JH, Hansen DV, Kriegstein AR. Development and evolution of the human neocortex. *Cell*. 2011;146(1):18-36. doi:10.1016/j.cell.2011.06.030

34. Shitamukai A, Konno D, Matsuzaki F. Oblique radial glial divisions in the developing mouse neocortex induce self-renewing progenitors outside the germinal zone that resemble primate outer subventricular zone progenitors. *J Neurosci Off J Soc Neurosci*. 2011;31(10):3683-3695. doi:10.1523/JNEUROSCI.4773-10.2011

35. Ponti G, Obernier K, Guinto C, Jose L, Bonfanti L, Alvarez-Buylla A. Cell cycle and lineage progression of neural progenitors in the ventricular-subventricular zones of adult mice. *Proc Natl Acad Sci U S A*. 2013;110(11):E1045-1054. doi:10.1073/pnas.1219563110

36. Doetsch F, Caillé I, Lim DA, García-Verdugo JM, Alvarez-Buylla A. Subventricular zone astrocytes are neural stem cells in the adult mammalian brain. *Cell*. 1999;97(6):703-716. doi:10.1016/s0092-8674(00)80783-7

37. Seri B, García-Verdugo JM, McEwen BS, Alvarez-Buylla A. Astrocytes give rise to new neurons in the adult mammalian hippocampus. *J Neurosci Off J Soc Neurosci*. 2001;21(18):7153-7160. doi:10.1523/JNEUROSCI.21-18-07153.2001

38. Otsuki L, Brand AH. Quiescent Neural Stem Cells for Brain Repair and Regeneration: Lessons from Model Systems. *Trends Neurosci*. 2020;43(4):213-226. doi:10.1016/j.tins.2020.02.002

39. Reeve RL, Yammine SZ, Morshead CM, van der Kooy D. Quiescent Oct4+ Neural Stem Cells (NSCs) Repopulate Ablated Glial Fibrillary Acidic Protein+ NSCs in the Adult Mouse Brain. *Stem Cells Dayt Ohio*. 2017;35(9):2071-2082. doi:10.1002/stem.2662

40. Bouchard-Cannon P, Lowden C, Trinh D, Cheng HYM. Dexras1 is a homeostatic regulator of exercise-dependent proliferation and cell survival in the hippocampal neurogenic niche. *Sci Rep*. 2018;8(1):5294. doi:10.1038/s41598-018-23673-z

41. Cayre M, Malaterre J, Scotto-Lomassese S, Strambi C, Strambi A. The common properties of neurogenesis in the adult brain: from invertebrates to vertebrates. *Comp Biochem Physiol Part B*. 2002;132(1):1-15. doi:10.1016/S1096-4959(01)00525-5

42. Mira H, Morante J. Neurogenesis From Embryo to Adult – Lessons From Flies and Mice. *Front Cell Dev Biol*. 2020;8. doi:10.3389/fcell.2020.00533

43. Boldrini M, Fulmore CA, Tartt AN, et al. Human Hippocampal Neurogenesis Persists throughout Aging. *Cell Stem Cell*. 2018;22(4):589-599.e5. doi:10.1016/j.stem.2018.03.015

44. Sorrells SF, Paredes MF, Cebrian-Silla A, et al. Human hippocampal neurogenesis drops sharply in children to undetectable levels in adults. *Nature*. 2018;555(7696):377-381. doi:10.1038/nature25975

45. Hartenstein V, Campos-Ortega JA. Early neurogenesis in wild-typeDrosophila melanogaster. *Wilhelm Rouxs Arch Dev Biol*. 1984;193(5):308-325. doi:10.1007/BF00848159

46. Hartenstein V, Wodarz A. Initial neurogenesis in Drosophila. *Wiley Interdiscip Rev Dev Biol*. 2013;2(5):701-721. doi:10.1002/wdev.111

47. Doe CQ. Molecular markers for identified neuroblasts and ganglion mother cells in the Drosophila central nervous system. *Dev Camb Engl*. 1992;116(4):855-863. doi:10.1242/dev.116.4.855

48. San-Juán BP, Baonza A. The bHLH factor deadpan is a direct target of Notch signaling and regulates neuroblast self-renewal in Drosophila. *Dev Biol*. 2011;352(1):70-82. doi:10.1016/j.ydbio.2011.01.019

49. Jussen D, von Hilchen J, Urbach R. Genetic regulation and function of epidermal growth factor receptor signalling in patterning of the embryonic Drosophila brain. *Open Biol*. 2016;6(12):160202. doi:10.1098/rsob.160202

50. Skeath JB. The Drosophila EGF receptor controls the formation and specification of neuroblasts along the dorsal-ventral axis of the Drosophila embryo. *Dev Camb Engl*. 1998;125(17):3301-3312. doi:10.1242/dev.125.17.3301

51. Urbach R, Technau GM. Segment polarity and DV patterning gene expression reveals segmental organization of the Drosophila brain. *Dev Camb Engl*. 2003;130(16):3607-3620. doi:10.1242/dev.00532

52. Urbach R, Technau GM. Neuroblast formation and patterning during early brain development in Drosophila. *BioEssays News Rev Mol Cell Dev Biol*. 2004;26(7):739-751. doi:10.1002/bies.20062

53. Isshiki T, Pearson B, Holbrook S, Doe CQ. Drosophila neuroblasts sequentially express transcription factors which specify the temporal identity of their neuronal progeny. *Cell*. 2001;106(4):511-521. doi:10.1016/s0092-8674(01)00465-2

54. Bahrampour S, Gunnar E, Jonsson C, Ekman H, Thor S. Neural Lineage Progression Controlled by a Temporal Proliferation Program. *Dev Cell*. 2017;43(3):332-348.e4. doi:10.1016/j.devcel.2017.10.004

55. Kambadur R, Koizumi K, Stivers C, Nagle J, Poole SJ, Odenwald WF. Regulation of POU genes by castor and hunchback establishes layered compartments in the Drosophila CNS. *Genes Dev*. 1998;12(2):246-260.

56. Kao CF, Yu HH, He Y, Kao JC, Lee T. Hierarchical Deployment of Factors Regulating Temporal Fate in a Diverse Neuronal Lineage of the *Drosophila* Central Brain. *Neuron*. 2012;73(4):677-684. doi:10.1016/j.neuron.2011.12.018

57. Truman JW, Bate M. Spatial and temporal patterns of neurogenesis in the central nervous system of Drosophila melanogaster. *Dev Biol*. 1988;125(1):145-157. doi:10.1016/0012-1606(88)90067-x

58. Sousa-Nunes R, Cheng LY, Gould AP. Regulating neural proliferation in the Drosophila CNS. *Curr Opin Neurobiol*. 2010;20(1):50-57. doi:10.1016/j.conb.2009.12.005

59. Bello BC, Hirth F, Gould AP. A pulse of the Drosophila Hox protein Abdominal-A schedules the end of neural proliferation via neuroblast apoptosis. *Neuron*. 2003;37(2):209-219. doi:10.1016/s0896-6273(02)01181-9

60. Ito K, Hotta Y. Proliferation pattern of postembryonic neuroblasts in the brain of Drosophila melanogaster. *Dev Biol*. 1992;149(1):134-148. doi:10.1016/0012-1606(92)90270-q

61. Tsuji T, Hasegawa E, Isshiki T. Neuroblast entry into quiescence is regulated intrinsically by the combined action of spatial Hox proteins and temporal identity factors. *Development*. 2008;135(23):3859-3869. doi:10.1242/dev.025189

62. Sipe CW, Siegrist SE. Eyeless uncouples mushroom body neuroblast proliferation from dietary amino acids in Drosophila. *eLife*. 6:e26343. doi:10.7554/eLife.26343

63. Britton JS, Edgar BA. Environmental control of the cell cycle in Drosophila: nutrition activates mitotic and endoreplicative cells by distinct mechanisms. *Dev Camb Engl*. 1998;125(11):2149-2158. doi:10.1242/dev.125.11.2149

64. Otsuki L, Brand AH. Dorsal-Ventral Differences in Neural Stem Cell Quiescence Are Induced by p57KIP2/Dacapo. *Dev Cell*. 2019;49(2):293-300.e3. doi:10.1016/j.devcel.2019.02.015

65. Lai SL, Doe CQ. Transient nuclear Prospero induces neural progenitor quiescence. Brand A, ed. *eLife*. 2014;3:e03363. doi:10.7554/eLife.03363

66. Ding R, Weynans K, Bossing T, Barros CS, Berger C. The Hippo signalling pathway maintains quiescence in Drosophila neural stem cells. *Nat Commun*. 2016;7(1):10510. doi:10.1038/ncomms10510

67. Poon CLC, Mitchell KA, Kondo S, Cheng LY, Harvey KF. The Hippo Pathway Regulates Neuroblasts and Brain Size in Drosophila melanogaster. *Curr Biol CB*. 2016;26(8):1034-1042. doi:10.1016/j.cub.2016.02.009

68. Ebens AJ, Garren H, Cheyette BNR, Zipursky SL. The Drosophila *anachronism* locus: A glycoprotein secreted by glia inhibits neuroblast proliferation. *Cell*. 1993;74(1):15-27. doi:10.1016/0092-8674(93)90291-W

69. Sousa-Nunes R, Yee LL, Gould AP. Fat cells reactivate quiescent neuroblasts via TOR and glial insulin relays in Drosophila. *Nature*. 2011;471(7339):508-512. doi:10.1038/nature09867

70. Chell JM, Brand AH. Nutrition-responsive glia control exit of neural stem cells from quiescence. *Cell*. 2010;143(7):1161-1173. doi:10.1016/j.cell.2010.12.007

71. Yuan X, Sipe CW, Suzawa M, Bland ML, Siegrist SE. Dilp-2–mediated PI3-kinase activation coordinates reactivation of quiescent neuroblasts with growth of their glial stem cell niche. *PLoS Biol*. 2020;18(5):e3000721. doi:10.1371/journal.pbio.3000721

72. Kanai MI, Kim MJ, Akiyama T, et al. Regulation of neuroblast proliferation by surface glia in the Drosophila larval brain. *Sci Rep*. 2018;8:3730. doi:10.1038/s41598-018-22028-y

73. Park Y, Rangel C, Reynolds MM, et al. Drosophila perlecan modulates FGF and hedgehog signals to activate neural stem cell division. *Dev Biol*. 2003;253(2):247-257. doi:10.1016/s0012-1606(02)00019-2

74. Voigt A, Pflanz R, Schäfer U, Jäckle H. Perlecan participates in proliferation activation of quiescent Drosophila neuroblasts. *Dev Dyn Off Publ Am Assoc Anat*. 2002;224(4):403-412. doi:10.1002/dvdy.10120

75. Datta S. Control of proliferation activation in quiescent neuroblasts of the Drosophila central nervous system. *Dev Camb Engl*. 1995;121(4):1173-1182. doi:10.1242/dev.121.4.1173

76. Puig O, Tjian R. Transcriptional feedback control of insulin receptor by dFOXO/FOXO1. *Genes Dev*. 2005;19(20):2435-2446. doi:10.1101/gad.1340505

77. Puig O, Marr MT, Ruhf ML, Tjian R. Control of cell number by Drosophila FOXO: downstream and feedback regulation of the insulin receptor pathway. *Genes Dev*. 2003;17(16):2006-2020. doi:10.1101/gad.1098703

78. Siegrist SE, Haque NS, Chen CH, Hay BA, Hariharan IK. Inactivation of both Foxo and reaper promotes long-term adult neurogenesis in Drosophila. *Curr Biol CB*. 2010;20(7):643-648. doi:10.1016/j.cub.2010.01.060

79. Li S, Koe CT, Tay ST, et al. An intrinsic mechanism controls reactivation of neural stem cells by spindle matrix proteins. *Nat Commun*. 2017;8(1):122. doi:10.1038/s41467-017-00172-9

80. Ly PT, Tan YS, Koe CT, et al. CRL4Mahj E3 ubiquitin ligase promotes neural stem cell reactivation. *PLOS Biol*. 2019;17(6):e3000276. doi:10.1371/journal.pbio.3000276

81. Gil-Ranedo J, Gonzaga E, Jaworek KJ, Berger C, Bossing T, Barros CS. STRIPAK Members Orchestrate Hippo and Insulin Receptor Signaling to Promote Neural Stem Cell Reactivation. *Cell Rep*. 2019;27(10):2921-2933.e5. doi:10.1016/j.celrep.2019.05.023

82. Sood C, Justis VT, Doyle SE, Siegrist SE. Notch signaling regulates neural stem cell quiescence entry and exit in *Drosophila*. *Development*. 2022;149(4):dev200275. doi:10.1242/dev.200275

83. Gallaud E, Pham T, Cabernard C. Drosophila melanogaster Neuroblasts: A Model for Asymmetric Stem Cell Divisions. In: Tassan JP, Kubiak JZ, eds. *Asymmetric Cell Division in Development, Differentiation and Cancer*. Results and Problems in Cell Differentiation. Springer International Publishing; 2017:183-210. doi:10.1007/978-3-319-53150-2_8

84. Boone JQ, Doe CQ. Identification of Drosophila type II neuroblast lineages containing transit amplifying ganglion mother cells. *Dev Neurobiol*. 2008;68(9):1185-1195. doi:10.1002/dneu.20648

85. Urbach R, Technau GM. Molecular markers for identified neuroblasts in the developing brain of Drosophila. *Dev Camb Engl*. 2003;130(16):3621-3637. doi:10.1242/dev.00533

86. Bello BC, Izergina N, Caussinus E, Reichert H. Amplification of neural stem cell proliferation by intermediate progenitor cells in Drosophila brain development. *Neural Develop*. 2008;3:5. doi:10.1186/1749-8104-3-5

87. Wirtz-Peitz F, Nishimura T, Knoblich JA. Linking Cell Cycle to Asymmetric Division: Aurora-A Phosphorylates the Par Complex to Regulate Numb Localization. *Cell*. 2008;135(1):161-173. doi:10.1016/j.cell.2008.07.049

88. Shen CP, Jan LY, Jan YN. Miranda Is Required for the Asymmetric Localization of Prospero during Mitosis in Drosophila. *Cell*. 1997;90(3):449-458. doi:10.1016/S0092-8674(00)80505-X

89. Shen CP, Knoblich JA, Chan YM, Jiang MM, Jan LY, Jan YN. Miranda as a multidomain adapter linking apically localized Inscuteable and basally localized Staufen and Prospero during asymmetric cell division in Drosophila. *Genes Dev*. 1998;12(12):1837-1846.

90. Doe CQ, Chu-LaGraff Q, Wright DM, Scott MP. The prospero gene specifies cell fates in the Drosophila central nervous system. *Cell*. 1991;65(3):451-464. doi:10.1016/0092-8674(91)90463-9

91. Rhyu MS, Jan LY, Jan YN. Asymmetric distribution of numb protein during division of the sensory organ precursor cell confers distinct fates to daughter cells. *Cell*. 1994;76(3):477-491. doi:10.1016/0092-8674(94)90112-0

92. Erben V, Waldhuber M, Langer D, Fetka I, Jansen RP, Petritsch C. Asymmetric localization of the adaptor protein Miranda in neuroblasts is achieved by diffusion and sequential interaction of Myosin II and VI. *J Cell Sci*. 2008;121(Pt 9):1403-1414. doi:10.1242/jcs.020024

93. Sousa-Nunes R, Chia W, Somers WG. Protein Phosphatase 4 mediates localization of the Miranda complex during Drosophila neuroblast asymmetric divisions. *Genes Dev*. 2009;23(3):359-372. doi:10.1101/gad.1723609

94. Smith CA, Lau KM, Rahmani Z, et al. aPKC-mediated phosphorylation regulates asymmetric membrane localization of the cell fate determinant Numb. *EMBO J*. 2007;26(2):468-480. doi:10.1038/sj.emboj.7601495

95. Lu B, Rothenberg M, Jan LY, Jan YN. Partner of Numb Colocalizes with Numb during Mitosis and Directs Numb Asymmetric Localization in *Drosophila* Neural and Muscle Progenitors. *Cell*. 1998;95(2):225-235. doi:10.1016/S0092-8674(00)81753-5

96. Wang H, Ouyang Y, Somers WG, Chia W, Lu B. Polo inhibits progenitor self-renewal and regulates Numb asymmetry by phosphorylating Pon. *Nature*. 2007;449(7158):96-100. doi:10.1038/nature06056

97. Cabernard C, Doe CQ. Apical/basal spindle orientation is required for neuroblast homeostasis and neuronal differentiation in Drosophila. *Dev Cell*. 2009;17(1):134-141. doi:10.1016/j.devcel.2009.06.009

98. Cabernard C, Prehoda KE, Doe CQ. A spindle-independent cleavage furrow positioning pathway. *Nature*. 2010;467(7311):91-94. doi:10.1038/nature09334

99. Wodarz A, Ramrath A, Kuchinke U, Knust E. Bazooka provides an apical cue for Inscuteable localization in Drosophila neuroblasts. *Nature*. 1999;402(6761):544-547. doi:10.1038/990128

100. Yu F, Morin X, Cai Y, Yang X, Chia W. Analysis of partner of inscuteable, a Novel Player of Drosophila Asymmetric Divisions, Reveals Two Distinct Steps in Inscuteable Apical Localization. *Cell*. 2000;100(4):399-409. doi:10.1016/S0092-8674(00)80676-5

101. Schaefer M, Shevchenko A, Shevchenko A, Knoblich JA. A protein complex containing Inscuteable and the Galpha-binding protein Pins orients asymmetric cell divisions in Drosophila. *Curr Biol CB*. 2000;10(7):353-362. doi:10.1016/s0960-9822(00)00401-2

102. Siller KH, Cabernard C, Doe CQ. The NuMA-related Mud protein binds Pins and regulates spindle orientation in Drosophila neuroblasts. *Nat Cell Biol*. 2006;8(6):594-600. doi:10.1038/ncb1412

103. Siegrist SE, Doe CQ. Microtubule-Induced Pins/Gαi Cortical Polarity in Drosophila Neuroblasts. *Cell*. 2005;123(7):1323-1335. doi:10.1016/j.cell.2005.09.043

104. Cabernard C. Cytokinesis in Drosophila melanogaster. *Cytoskeleton*. 2012;69(10):791-809. doi:10.1002/cm.21060

105. Giansanti MG, Bonaccorsi S, Bucciarelli E, Gatti M. Drosophila male meiosis as a model system for the study of cytokinesis in animal cells. *Cell Struct Funct*. 2001;26(6):609-617. doi:10.1247/csf.26.609

106. Somma MP, Fasulo B, Cenci G, Cundari E, Gatti M. Molecular dissection of cytokinesis by RNA interference in Drosophila cultured cells. *Mol Biol Cell*. 2002;13(7):2448-2460. doi:10.1091/mbc.01-12-0589

107. Echard A, Hickson GRX, Foley E, O'Farrell PH. Terminal cytokinesis events uncovered after an RNAi screen. *Curr Biol CB*. 2004;14(18):1685-1693. doi:10.1016/j.cub.2004.08.063

108. Prokopenko SN, Brumby A, O'Keefe L, et al. A putative exchange factor for Rho1 GTPase is required for initiation of cytokinesis in Drosophila. *Genes Dev*. 1999;13(17):2301-2314.

109. O'Keefe L, Somers WG, Harley A, Saint R. The pebble GTP exchange factor and the control of cytokinesis. *Cell Struct Funct*. 2001;26(6):619-626. doi:10.1247/csf.26.619

110. Somers WG, Saint R. A RhoGEF and Rho family GTPase-activating protein complex links the contractile ring to cortical microtubules at the onset of cytokinesis. *Dev Cell*. 2003;4(1):29-39. doi:10.1016/s1534-5807(02)00402-1

111. Lehner CF. The pebble gene is required for cytokinesis in Drosophila. *J Cell Sci*. 1992;103 (Pt 4):1021-1030. doi:10.1242/jcs.103.4.1021

112. Adams RR, Tavares AAM, Salzberg A, Bellen HJ, Glover DM. pavarotti encodes a kinesin-like protein required to organize the central spindle and contractile ring for cytokinesis. *Genes Dev*. 1998;12(10):1483-1494.

113. Inoue YH, Savoian MS, Suzuki T, Máthé E, Yamamoto MT, Glover DM. Mutations in orbit/mast reveal that the central spindle is comprised of two microtubule populations, those that initiate cleavage and those that propagate furrow ingression. *J Cell Biol*. 2004;166(1):49-60. doi:10.1083/jcb.200402052

114. Basto R, Gomes R, Karess RE. Rough deal and Zw10 are required for the metaphase checkpoint in Drosophila. *Nat Cell Biol*. 2000;2(12):939-943. doi:10.1038/35046592

115. Bowman SK, Neumüller RA, Novatchkova M, Du Q, Knoblich JA. The Drosophila NuMA Homolog Mud regulates spindle orientation in asymmetric cell division. *Dev Cell*. 2006;10(6):731-742. doi:10.1016/j.devcel.2006.05.005

116. Tsankova A, Pham TT, Garcia DS, Otte F, Cabernard C. Cell Polarity Regulates Biased Myosin Activity and Dynamics during Asymmetric Cell Division via Drosophila Rho Kinase and Protein Kinase N. *Dev Cell*. 2017;42(2):143-155.e5. doi:10.1016/j.devcel.2017.06.012

117. Ou G, Stuurman N, D'Ambrosio M, Vale RD. Polarized myosin produces unequal-size daughters during asymmetric cell division. *Science*. 2010;330(6004):677-680. doi:10.1126/science.1196112

118. Connell M, Cabernard C, Ricketson D, Doe CQ, Prehoda KE. Asymmetric cortical extension shifts cleavage furrow position in Drosophila neuroblasts. *Mol Biol Cell*. 2011;22(22):4220-4226. doi:10.1091/mbc.E11-02-0173

119. Piekny A, Werner M, Glotzer M. Cytokinesis: welcome to the Rho zone. *Trends Cell Biol*. 2005;15(12):651-658. doi:10.1016/j.tcb.2005.10.006

120. Straight AF, Field CM, Mitchison TJ. Anillin binds nonmuscle myosin II and regulates the contractile ring. *Mol Biol Cell*. 2005;16(1):193-201. doi:10.1091/mbc.e04-08-0758

121. D'Avino PP, Takeda T, Capalbo L, et al. Interaction between Anillin and RacGAP50C connects the actomyosin contractile ring with spindle microtubules at the cell division site. *J Cell Sci*. 2008;121(Pt 8):1151-1158. doi:10.1242/jcs.026716

122. Rodal AA, Kozubowski L, Goode BL, Drubin DG, Hartwig JH. Actin and Septin Ultrastructures at the Budding Yeast Cell Cortex. *Mol Biol Cell*. 2005;16(1):372-384. doi:10.1091/mbc.E04-08-0734

123. Knobloch M, Braun SMG, Zurkirchen L, et al. Metabolic control of adult neural stem cell activity by Fasn-dependent lipogenesis. *Nature*. 2013;493(7431):226-230. doi:10.1038/nature11689

124. Knobloch M, von Schoultz C, Zurkirchen L, Braun SMG, Vidmar M, Jessberger S. SPOT14-positive neural stem/progenitor cells in the hippocampus respond dynamically to neurogenic regulators. *Stem Cell Rep*. 2014;3(5):735-742. doi:10.1016/j.stemcr.2014.08.013

125. Bowers M, Liang T, Gonzalez-Bohorquez D, et al. FASN-Dependent Lipid Metabolism Links Neurogenic Stem/Progenitor Cell Activity to Learning and Memory Deficits. *Cell Stem Cell*. 2020;27(1):98-109.e11. doi:10.1016/j.stem.2020.04.002

126. Stoll EA, Makin R, Sweet IR, et al. Neural Stem Cells in the Adult Subventricular Zone Oxidize Fatty Acids to Produce Energy and Support Neurogenic Activity. *Stem Cells Dayt Ohio*. 2015;33(7):2306-2319. doi:10.1002/stem.2042

127. Knobloch M, Pilz GA, Ghesquière B, et al. A Fatty Acid Oxidation-Dependent Metabolic Shift Regulates Adult Neural Stem Cell Activity. *Cell Rep*. 2017;20(9):2144-2155. doi:10.1016/j.celrep.2017.08.029

128. Madsen S, Ramosaj M, Knobloch M. Lipid metabolism in focus: how the build-up and breakdown of lipids affects stem cells. *Development*. 2021;148(10):dev191924. doi:10.1242/dev.191924

129. Petrelli F, Scandella V, Montessuit S, Zamboni N, Martinou JC, Knobloch M. Mitochondrial pyruvate metabolism regulates the activation of quiescent adult neural stem cells. *Sci Adv*. 2023;9(9):eadd5220. doi:10.1126/sciadv.add5220

130. Olzmann JA, Carvalho P. Dynamics and functions of lipid droplets. *Nat Rev Mol Cell Biol*. 2019;20(3):137-155. doi:10.1038/s41580-018-0085-z

131. Murphy DJ. The dynamic roles of intracellular lipid droplets: from archaea to mammals. *Protoplasma*. 2012;249(3):541-585. doi:10.1007/s00709-011-0329-7

132. Ralhan I, Chang CL, Lippincott-Schwartz J, Ioannou MS. Lipid droplets in the nervous system. *J Cell Biol*. 2021;220(7):e202102136. doi:10.1083/jcb.202102136

133. Ramosaj M, Madsen S, Maillard V, et al. Lipid droplet availability affects neural stem/progenitor cell metabolism and proliferation. *Nat Commun*. 2021;12(1):7362. doi:10.1038/s41467-021-27365-7

134. Hamilton LK, Dufresne M, Joppé SE, et al. Aberrant Lipid Metabolism in the Forebrain Niche Suppresses Adult Neural Stem Cell Proliferation in an Animal Model of Alzheimer's Disease. *Cell Stem Cell*. 2015;17(4):397-411. doi:10.1016/j.stem.2015.08.001

135. Liu L, Zhang K, Sandoval H, et al. Glial lipid droplets and ROS induced by mitochondrial defects promote neurodegeneration. *Cell*. 2015;160(1-2):177-190. doi:10.1016/j.cell.2014.12.019

136. Bailey AP, Koster G, Guillermier C, et al. Antioxidant Role for Lipid Droplets in a Stem Cell Niche of Drosophila. *Cell*. 2015;163(2):340-353. doi:10.1016/j.cell.2015.09.020

137. Yi M, Li J, Chen S, et al. Emerging role of lipid metabolism alterations in Cancer stem cells. *J Exp Clin Cancer Res*. 2018;37(1):118. doi:10.1186/s13046-018-0784-5

138. Nakamura-Ishizu A, Ito K, Suda T. Hematopoietic Stem Cell Metabolism during Development and Aging. *Dev Cell*. 2020;54(2):239-255. doi:10.1016/j.devcel.2020.06.029

139. Alonso S, Yilmaz ÖH. Nutritional Regulation of Intestinal Stem Cells. *Annu Rev Nutr*. 2018;38(Volume 38, 2018):273-301. doi:10.1146/annurev-nutr-082117-051644

140. Ito K, Bonora M, Ito K. Metabolism as master of hematopoietic stem cell fate. *Int J Hematol*. 2019;109(1):18-27. doi:10.1007/s12185-018-2534-z

141. Baulies A, Angelis N, Li VSW. Hallmarks of intestinal stem cells. *Dev Camb Engl*. 2020;147(15):dev182675. doi:10.1242/dev.182675

142. Ito K, Carracedo A, Weiss D, et al. A PML–PPAR-δ pathway for fatty acid oxidation regulates hematopoietic stem cell maintenance. *Nat Med*. 2012;18(9):1350-1358. doi:10.1038/nm.2882

143. Tiwari SK, Toshniwal AG, Mandal S, Mandal L. Fatty acid β-oxidation is required for the differentiation of larval hematopoietic progenitors in Drosophila. VijayRaghavan K, Yamashita YM, eds. *eLife*. 2020;9:e53247. doi:10.7554/eLife.53247

144. Yasumoto Y, Miyazaki H, Vaidyan LK, et al. Inhibition of Fatty Acid Synthase Decreases Expression of Stemness Markers in Glioma Stem Cells. *PLOS ONE*. 2016;11(1):e0147717. doi:10.1371/journal.pone.0147717

145. Li H, Feng Z, He ML. Lipid metabolism alteration contributes to and maintains the properties of cancer stem cells. *Theranostics*. 2020;10(16):7053-7069. doi:10.7150/thno.41388

146. Welte MA. As the fat flies: The dynamic lipid droplets of Drosophila embryos. *Biochim Biophys Acta BBA - Mol Cell Biol Lipids*. 2015;1851(9):1156-1185. doi:10.1016/j.bbalip.2015.04.002

147. Kilwein MD, Dao TK, Welte MA. Drosophila embryos allocate lipid droplets to specific lineages to ensure punctual development and redox homeostasis. *PLoS Genet*. 2023;19(8):e1010875. doi:10.1371/journal.pgen.1010875

148. Heier C, Kühnlein RP. Triacylglycerol Metabolism in Drosophila melanogaster. *Genetics*. 2018;210(4):1163-1184. doi:10.1534/genetics.118.301583

149. Parvy JP, Napal L, Rubin T, et al. Drosophila melanogaster Acetyl-CoA-Carboxylase Sustains a Fatty Acid–Dependent Remote Signal to Waterproof the Respiratory System. *PLOS Genet*. 2012;8(8):e1002925. doi:10.1371/journal.pgen.1002925

150. Garrido D, Rubin T, Poidevin M, et al. Fatty Acid Synthase Cooperates with Glyoxalase 1 to Protect against Sugar Toxicity. *PLOS Genet*. 2015;11(2):e1004995. doi:10.1371/journal.pgen.1004995

151. Dobrosotskaya IY, Seegmiller AC, Brown MS, Goldstein JL, Rawson RB. Regulation of SREBP Processing and Membrane Lipid Production by Phospholipids in Drosophila. *Science*. 2002;296(5569):879-883. doi:10.1126/science.1071124

152. Walker AK, Jacobs RL, Watts JL, et al. A Conserved SREBP-1/Phosphatidylcholine Feedback Circuit Regulates Lipogenesis in Metazoans. *Cell*. 2011;147(4):840-852. doi:10.1016/j.cell.2011.09.045

153. Osborne TF, Espenshade PJ. Evolutionary conservation and adaptation in the mechanism that regulates SREBP action: what a long, strange tRIP it's been. *Genes Dev*. 2009;23(22):2578-2591. doi:10.1101/gad.1854309

154. Reiff T, Jacobson J, Cognigni P, et al. Endocrine remodelling of the adult intestine sustains reproduction in Drosophila. Freeman M, ed. *eLife*. 2015;4:e06930. doi:10.7554/eLife.06930

155. Song W, Veenstra JA, Perrimon N. Control of Lipid Metabolism by Tachykinin in *Drosophila*. *Cell Rep*. 2014;9(1):40-47. doi:10.1016/j.celrep.2014.08.060

156. Krycer JR, Sharpe LJ, Luu W, Brown AJ. The Akt–SREBP nexus: cell signaling meets lipid metabolism. *Trends Endocrinol Metab*. 2010;21(5):268-276. doi:10.1016/j.tem.2010.01.001

157. Sieber MH, Thummel CS. The DHR96 Nuclear Receptor Controls Triacylglycerol Homeostasis in *Drosophila*. *Cell Metab*. 2009;10(6):481-490. doi:10.1016/j.cmet.2009.10.010

158. Horne I, Haritos VS, Oakeshott JG. Comparative and functional genomics of lipases in holometabolous insects. *Insect Biochem Mol Biol*. 2009;39(8):547-567. doi:10.1016/j.ibmb.2009.06.002

159. Palm W, Sampaio JL, Brankatschk M, et al. Lipoproteins in Drosophila melanogaster—Assembly, Function, and Influence on Tissue Lipid Composition. *PLOS Genet*. 2012;8(7):e1002828. doi:10.1371/journal.pgen.1002828

160. Carvalho M, Sampaio JL, Palm W, Brankatschk M, Eaton S, Shevchenko A. Effects of diet and development on the Drosophila lipidome. *Mol Syst Biol*. 2012;8(1):600. doi:10.1038/msb.2012.29

161. Rodríguez-Vázquez M, Vaquero D, Parra-Peralbo E, Mejía-Morales JE, Culi J. Drosophila Lipophorin Receptors Recruit the Lipoprotein LTP to the Plasma Membrane to Mediate Lipid Uptake. *PLOS Genet*. 2015;11(6):e1005356. doi:10.1371/journal.pgen.1005356

162. Parra-Peralbo E, Culi J. Drosophila Lipophorin Receptors Mediate the Uptake of Neutral Lipids in Oocytes and Imaginal Disc Cells by an Endocytosis-Independent Mechanism. *PLOS Genet*. 2011;7(2):e1001297. doi:10.1371/journal.pgen.1001297

163. Li Z, Thiel K, Thul PJ, Beller M, Kühnlein RP, Welte MA. Lipid droplets control the maternal histone supply of Drosophila embryos. *Curr Biol CB*. 2012;22(22):2104-2113. doi:10.1016/j.cub.2012.09.018

164. Buszczak M, Lu X, Segraves WA, Chang TY, Cooley L. Mutations in the midway gene disrupt a Drosophila acyl coenzyme A: diacylglycerol acyltransferase. *Genetics*. 2002;160(4):1511-1518. doi:10.1093/genetics/160.4.1511

165. Schüpbach T, Wieschaus E. Female sterile mutations on the second chromosome of Drosophila melanogaster. II. Mutations blocking oogenesis or altering egg morphology. *Genetics*. 1991;129(4):1119-1136. doi:10.1093/genetics/129.4.1119

166. Bi J, Wang W, Liu Z, et al. Seipin Promotes Adipose Tissue Fat Storage through the ER Ca2+-ATPase SERCA. *Cell Metab*. 2014;19(5):861-871. doi:10.1016/j.cmet.2014.03.028

167. Baumbach J, Hummel P, Bickmeyer I, et al. A *Drosophila* In Vivo Screen Identifies Store-Operated Calcium Entry as a Key Regulator of Adiposity. *Cell Metab*. 2014;19(2):331-343. doi:10.1016/j.cmet.2013.12.004

168. Gutierrez E, Wiggins D, Fielding B, Gould AP. Specialized hepatocyte-like cells regulate Drosophila lipid metabolism. *Nature*. 2007;445(7125):275-280. doi:10.1038/nature05382

169. Thiel K, Heier C, Haberl V, et al. The evolutionarily conserved protein CG9186 is associated with lipid droplets, required for their positioning and for fat storage. *J Cell Sci*. 2013;126(10):2198-2212. doi:10.1242/jcs.120493

170. Welte MA. Expanding Roles for Lipid Droplets. *Curr Biol*. 2015;25(11):R470-R481. doi:10.1016/j.cub.2015.04.004

171. Walther TC, Chung J, Jr RVF. Lipid Droplet Biogenesis. *Annu Rev Cell Dev Biol*. 2017;33(Volume 33, 2017):491-510. doi:10.1146/annurev-cellbio-100616-060608

172. Grönke S, Mildner A, Fellert S, et al. Brummer lipase is an evolutionary conserved fat storage regulator in Drosophila. *Cell Metab*. 2005;1(5):323-330. doi:10.1016/j.cmet.2005.04.003

173. Haemmerle G, Zimmermann R, Hayn M, et al. Hormone-sensitive Lipase Deficiency in Mice Causes Diglyceride Accumulation in Adipose Tissue, Muscle, and Testis*. *J Biol Chem*. 2002;277(7):4806-4815. doi:10.1074/jbc.M110355200

174. Bi J, Xiang Y, Chen H, et al. Opposite and redundant roles of the two Drosophila perilipins in lipid mobilization. *J Cell Sci*. 2012;125(Pt 15):3568-3577. doi:10.1242/jcs.101329

175. Bickel PE, Tansey JT, Welte MA. PAT proteins, an ancient family of lipid droplet proteins that regulate cellular lipid stores. *Biochim Biophys Acta BBA - Mol Cell Biol Lipids*. 2009;1791(6):419-440. doi:10.1016/j.bbalip.2009.04.002

176. Grönke S, Beller M, Fellert S, Ramakrishnan H, Jäckle H, Kühnlein RP. Control of Fat Storage by a *Drosophila* PAT Domain Protein. *Curr Biol*. 2003;13(7):603-606. doi:10.1016/S0960-9822(03)00175-1

177. Wang B, Moya N, Niessen S, et al. A Hormone-Dependent Module Regulating Energy Balance. *Cell*. 2011;145(4):596-606. doi:10.1016/j.cell.2011.04.013

178. Choi S, Lim DS, Chung J. Feeding and Fasting Signals Converge on the LKB1-SIK3 Pathway to Regulate Lipid Metabolism in Drosophila. *PLOS Genet*. 2015;11(5):e1005263. doi:10.1371/journal.pgen.1005263

179. Kis V, Barti B, Lippai M, Sass M. Specialized Cortex Glial Cells Accumulate Lipid Droplets in Drosophila melanogaster. Roman G, ed. *PLOS ONE*. 2015;10(7):e0131250. doi:10.1371/journal.pone.0131250

180. Dong Q, Zavortink M, Froldi F, Golenkina S, Lam T, Cheng LY. Glial Hedgehog signalling and lipid metabolism regulate neural stem cell proliferation in Drosophila. *EMBO Rep*. 2021;22(5):e52130. doi:10.15252/embr.202052130

181. Liu L, MacKenzie KR, Putluri N, Maletić-Savatić M, Bellen HJ. The Glia-Neuron Lactate Shuttle and Elevated ROS Promote Lipid Synthesis in Neurons and Lipid Droplet Accumulation in Glia via APOE/D. *Cell Metab*. 2017;26(5):719-737.e6. doi:10.1016/j.cmet.2017.08.024

182. Schulz JG, Laranjeira A, Van Huffel L, et al. Glial β-Oxidation regulates Drosophila Energy Metabolism. *Sci Rep*. 2015;5(1):7805. doi:10.1038/srep07805